DOE/FE/60181-225

CHEMCOAL PROCESS RECYCLE TEST/INDIAN HEAD LIGNITE

Clifford R. Porter

Carbon Resources, Inc.
4891 Independence Street, Suite 130
Wheat Ridge, Colorado 80033

and

Melanie D. Hetland, Curtis L. Knudson, John R. Rindt, and Warrack G. Willson

University of North Dakota Energy Research Center
Box 8213, University Station
Grand Forks, North Dakota 58202

Work Performed Under Contract No. DE-FC21-83FE60181
For
U. S. Department of Energy
Office of Fossil Energy
Morgantown Energy Technology Center
Grand Forks Project Office
Grand Forks, North Dakota

and

Electric Power Research Institute Contract No. 2655-3
Palo Alto, California

For Presentation at the
Fourteenth Biennial Lignite Symposium on the
Technology and Utilization of Low-Rank Coals
Dallas, Texas
May 18-21, 1987

DISCLAIMER

PATENT STATUS

TECHNICAL STATUS

CHEMCOAL PROCESS RECYCLE TEST/INDIAN HEAD LIGNITE

by

C. R. Porter
Carbon Resources, Inc.
M. D. Hetland, C. L. Knudson, J. R. Rindt, and W. G. Willson
University of North Dakota Energy Research Center

ABSTRACT

This report details work at the University of North Dakota Energy Research Center (UNDERC) demonstrating the ChemCoal Process as applied to Indian Head lignite in a full solvent recycle to lined-out, steady-state operation. The ChemCoal Process uses chemical methods to transform coal into clean solid and liquid products. The process features low-severity conversion (temperatures less than 340°C; pressures less than 12.4 MPa (1800 psig)) of coal in a phenolic solvent, with an alkali promoter and carbon monoxide reductant. The work presented in this report was funded by the United States Department of Energy (DOE) through UND/DOE Cooperative Agreement DE-FC21-83FE60181, the Electric Power Research Institute (EPRI) Contract 2655-3, the University of North Dakota (UND), and Carbon Resources Inc. (CRI).

A successful CPU recycle test to solvent lineout was achieved. Operation was maintained for 39 theoretical passes and was concluded voluntarily. The recycle test was primarily aimed at resolving potential process flaws identified in a 1985 report by Bechtel Group, Inc., "ChemCoal Process Evaluation Study." The recycle results showed:

- ChemCoal Process conversion averaged over 80% of MAF coal and remained relatively constant.
- No loss in conversion occurred as process-derived solvent replaced start-up solvent in multiple recycles.
- Excess solvent (113%) was generated under all conditions.
- Reductant consumption was below 2.0 wt% of the MAF coal as hydrogen gas.

INTRODUCTION

The ChemCoal Process originated in 1975 as a result of work performed to catalytically desulfurize coal. In early 1982, it was found that, under proper conditions, a process-derived polar solvent in the presence of aqueous alkali and carbon monoxide reacted to produce high yields of high-quality hydrocarbon products under unexpectedly mild processing conditions.

Thus, the ChemCoal Process uses a chemical method to separate ash and sulfur compounds from the organic matrix of coal. This chemical method consists of an ionic reaction between the coal, a phenolic solvent, alkali, and a reductant such as carbon monoxide. The combination of phenolics and alkali provide a good physical solvation medium for the organics in the coal. When heated to temperatures of 325°-340°C at pressures below 12.4 MPa (1800 psig), the organic matrix of the coal is broken down by the reaction of the phenolics, alkali and carbon monoxide to produce lower molecular weight material. This material is soluble in the organic solvent, while the ash and mineral matter from the coal remain as suspended solids. These solid inorganic impurities are removed by centrifugation and/or filtration, leaving an organic liquid which is low in ash and sulfur. The fine-particulate solid product is precipitated, and low-temperature distillation is used to recover recycle solvent and the precipitating solvent (1,2,3,4).

Between 1981 and 1984, more than 300 experiments were performed by Carbon Resources in batch, semi-batch, and continuous process unit (CPU) systems in their laboratory near Boulder, Colorado. The experimental portion of the ChemCoal Process development program was moved to the University of North Dakota Energy Research Center (UNDERC) in 1985. The development program at UNDERC involved a series of shakedown tests, equipment development, and process operations evaluations. The five-step ChemCoal Process which evolved from the work at UNDERC is shown in Figure 1.

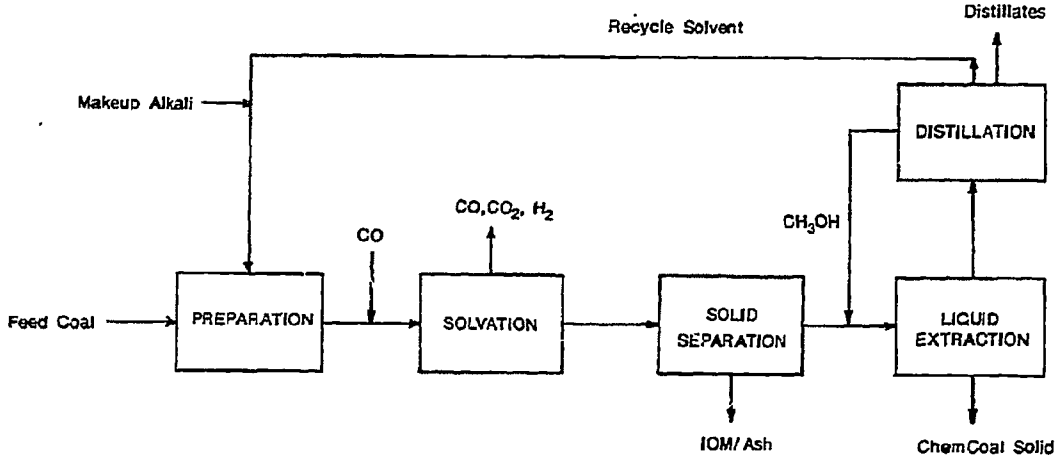

Figure 1. Five-Step ChemCoal Process

The work performed at UNDERC between May 1, 1985, and April 1, 1986, on the ChemCoal Process culminated in a continuous solvent recycle test (5). The goal was to validate the chemistry of the entire process, including both the conversion and downstream separations loops. To do this, it was necessary to operate until functional lineout of the solvent was achieved. The subject of this paper is CPU Run 123, which was a continuous process run whose primary purposes were an assessment of recycle solvent quality and quantity, and process yields at functional lineout. These objectives were considered to be more important than reactor design, studies of residence time or system parameters, or the on-line production of ChemCoal solids.

EQUIPMENT AND MATERIALS

Equipment

The original research plan called for operation of the UNDERC continuous processing unit as it was configured for the liquefaction of low-rank coal (LRC) using bottoms recycle and classical, high-boiling solvent systems. In this configuration, the CPU had been operated successfully to functional solvent lineout during many previous runs, which were under DOE contract (6). Due to this past operational record, as well as the behavior of the test equipment operated independently by CRI, it was presumed that little difficulty would be encountered in the reactor loop and that most problems would arise during the integration of the downstream separations loop.

However, numerous operating problems were encountered with the existing reactor configuration when used in the ChemCoal processing mode. Solids loading in the reactor increased over the course of the run, eventually forcing shutdown.

As a result of numerous equipment design modifications, it was discovered that essentially all problems resulted from solvent vaporization and its subsequent stripping from the reactor system, leaving the coal behind to settle in the reactor. Figure 2 is a diagram of the resulting reactor configuration which addressed the problems of solvent vaporization. This reactor configuration, which was used during Run 123, included a 17-foot long, upflow, co-current tubular preheater and two 2-gallon continuously stirred tank reactors (CSTRs). The first CSTR functioned as a preheater and the second as a reactor. Each CSTR was equipped with a knock-back condenser to enable retention of enough solvent to effectively slurry the coal. This system, depending on reactor residence time, was capable of operating with a throughput of up to 10 pounds of slurry feed per hour.

CPU Operations

During the run, the feed slurry was pumped through the tubular preheater with a high-pressure positive displacement metering pump. After leaving the tubular preheater, the feed slurry entered the CSTR preheater. This preheater was kept half full through the use of a dip tube that extended up from the bottom of the vessel. In an effort to reduce the load on the knock-back condenser, the upper half of the preheater was not heated.

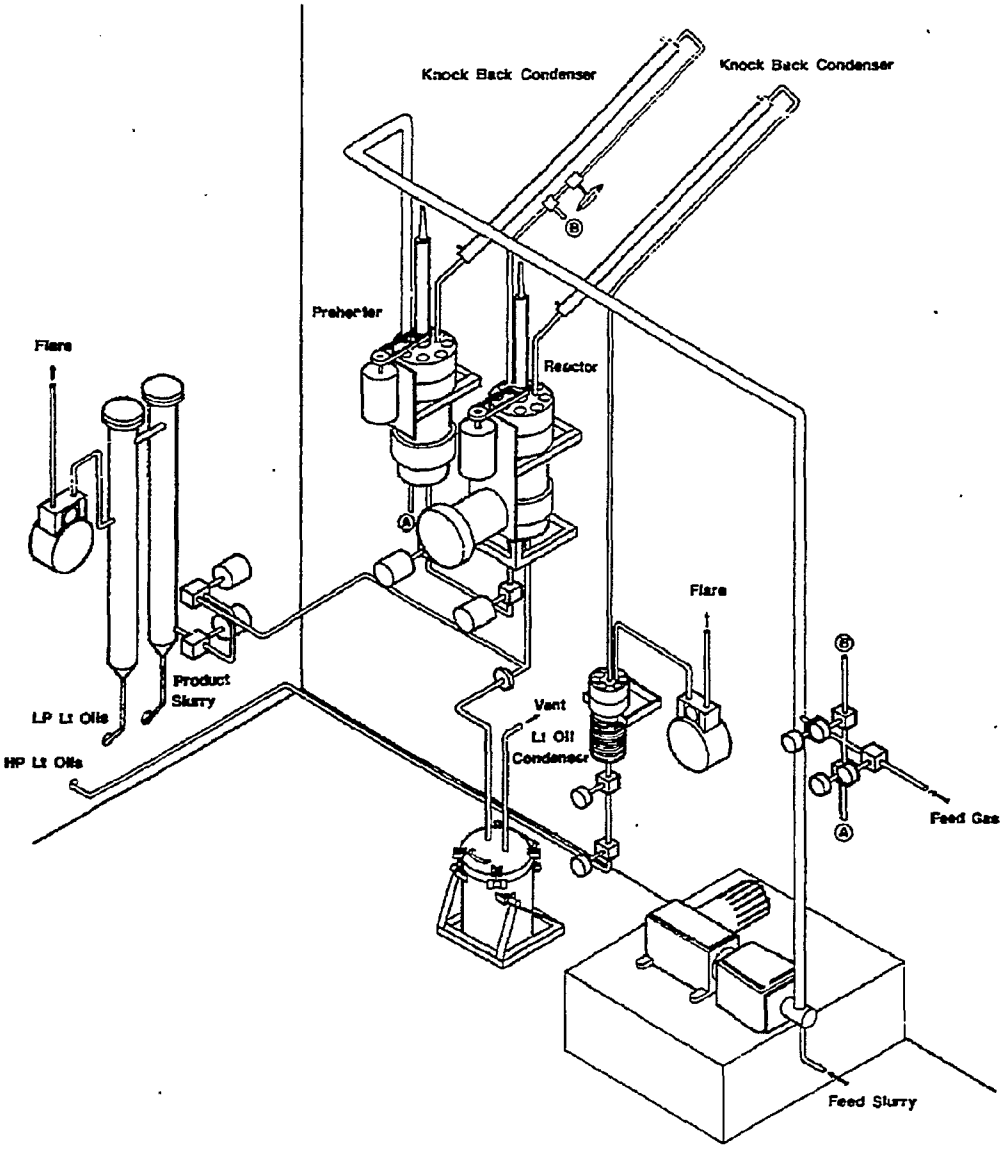

Figure 2. Continuous Process Unit ChemCoal Configuration, Run 123

The slurry was transferred batchwise every 30 seconds into the reactor through the use of a pressure differential caused by injection of reductant gas into the CSTR preheater. After the slurry transfer, fresh reductant was injected into the CSTR reactor through the transfer line. This method of slurry transfer resulted in minimal accumulation of solids in the line due to settling. The reactor was also kept half full, and slurry was introduced into the reactor near the top of the liquid level. This ensured that the slurry crossed the entire length of the reactor so that the longest possible residence time, and therefore the greatest conversion, would occur. The liquid level was monitored by a nuclear level indicator which permitted tracking of inventory changes within the reactor. The product slurry was depressurized, collected and transferred to a stirred surge tank.

Introduction of reducing gas into the CPU was handled by a sequential lockhopper letdown system. Cold reducing gas entered the tubular preheater at the same location as the feed slurry. Both the pre eated gas and slurry were injected into the CSTR preheater where additional reducing gas was added. After passing through a condenser, the gas from the stirred preheater was injected into the reactor. Additional fresh reductant was also injected into the bottom of the CSTR reactor. Gas from the reactor was cooled in a high-pressure knock-out pot to remove any readily condensible organics. It was then metered, analyzed by on-line GC, and flared.

All CPU operations--including slurry and gas transfers, slurry and gas letdowns, and reductant gas injection--were computer controlled to maintain accurate flow rates and simplify data acquisition. Mass flow rates and balances were available within 15 minutes after the end of each 4-hour run period.

Downstream Separations Operation

A flowsheet of the separations loop is presented as Figure 3. The loop included a centrifuge, precipitation tank and a distillation unit, and could be operated in either Mode 1 or 2. In Mode 1, following temporary storage in the stirred surge tank, the product slurry was transferred to a precipitation tank. In this tank, methanol was added to effect the precipitation of the ChemCoal solid. The precipitated slurry, which contained solvent, ChemCoal solids, ash, and IOM, was centrifuged to remove the solids. The liquid stream was then distilled to separate the methanol from the phenolic recycle solvent. The phenolic solvent was then recycled to the system. This mode of operation was used for simplicity to reach solvent lineout. In Mode 2, the methanol was added to the product slurry after the ash and IOM were removed by centrifugation in order to quantify ChemCoal solids yield and quality. The ChemCoal solid was then collected on a filtration unit that had been integrated into the distillation unit. These two modes of operation provided the flexibility necessary to handle the changes that would be expected to occur during the long-term unit operations necessary to achieve solvent lineout.

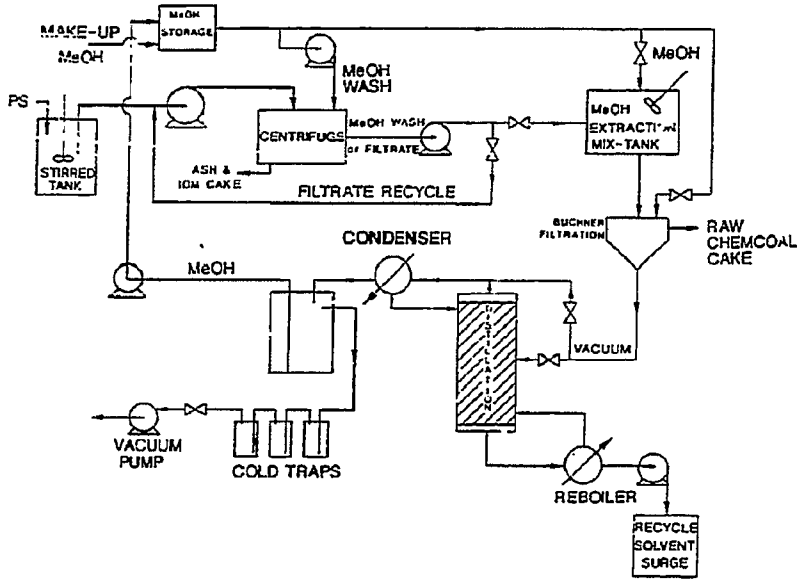

Figure 3. ChemCoal Downstream Processing Loop

CONTINUOUS PROCESS UNIT RUN 123 CONDITIONS

For this run, the reductant gas, CO, was fed at 3 scfh per pound of Indian Head lignite slurry fed. The system pressure was maintained at 1700 to 1800 psig. As the feed slurry was passed through the tubular preheater, the slurry temperature was raised to 100°C in the first six feet and to 200°C in the remaining eleven feet. After exiting the tubular preheater, the feed slurry entered the CSTR preheater. The temperature of the slurry in the CSTR preheater was maintained at 250°C. The liquid temperature in the reactor was kept at 340°C. The slurry feed rate for passes 1 through 20 was 2.5 lbs/hr; for passes 21 through 39, the slurry feed rate was 1.25 lbs/hr.

A change in downstream processing resulted in the decrease in the slurry feed rate from pass 21 through the end of the run. This change was required because too much phenolic solvent had been removed from the system during the centrifugation and distillation steps. The lack of phenolic solvent in the system eventually led to reduced effectiveness of precipitation of the ChemCoal product and plugging of the centrifuge.

To rectify the situation, the ratio of methanol to feed slurry was increased in the precipitation tank from 1:1 to 3:1. This change resulted in an easier centrifugation step in which less phenolics were retained in the cake. To further retain the recycle solvent in the system, the temperature in the distillation column was lowered from 110° to 80°C. This virtually eliminated the removal of any phenolics with the methanol fraction, as well as leaving some methanol in the recycle solvent. In addition, the phenolic solvent was extracted from the ChemCoal-IOM-ash centrifuge cake and replaced in the system.

The result of the changes made to maintain recycle solvent increased the load on the distillation column to the point where it was unable to keep up with the throughput. Therefore, the slurry feed rate of 2.5 lbs/hr was changed to 1.25 lbs/hr for passes 21 through 39. The gas feed rate was adjusted to maintain the required ratio with the feed slurry.

RESULTS AND DISCUSSION

Mass Yield Summary

The global mass balances for Run 123 averaged 96.7%. Because the mass balances were so high, the mass flow rates used in yield calculations discussed in this section were not normalized. Figure 4 is an example of the mass balance summary sheets which were used to track on-line data stream processing during the run. The balance sheets contain the mass flow rate in grams per hour for all streams and an estimated conversion value based upon tetrahydrofuran insoluble (THFI) analysis. They also supply per-pass mass balances. Combined with the routine analyses, these balances form the basis for all calculations and yield determinations used.

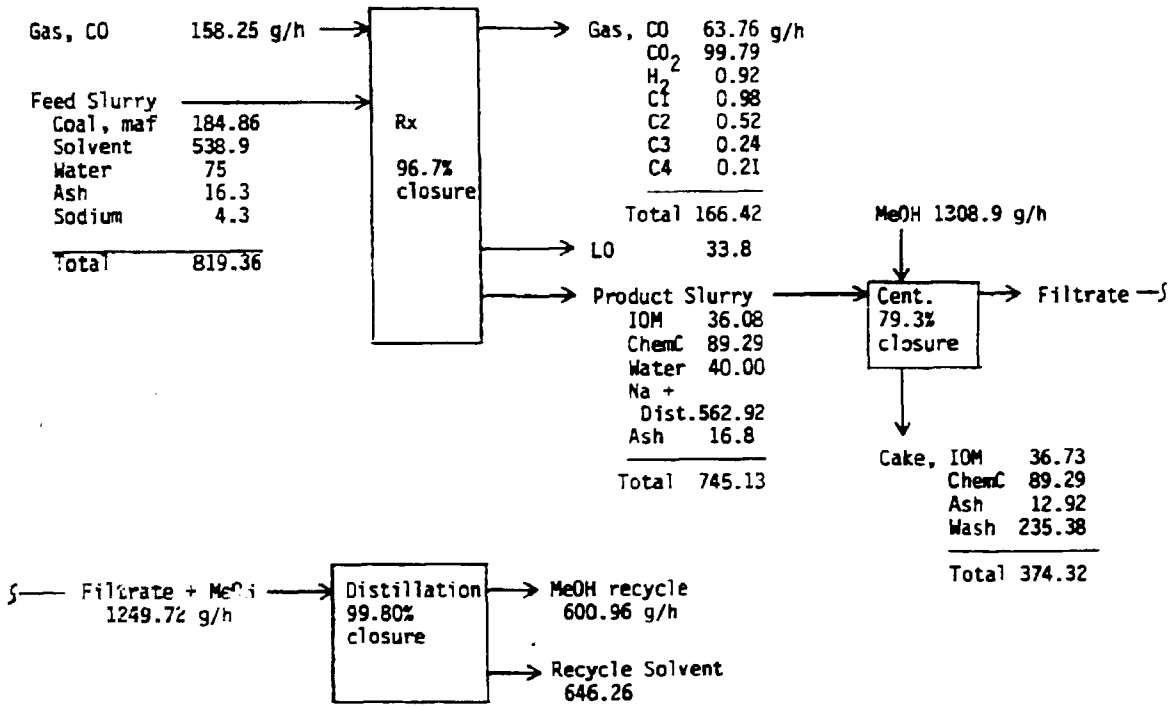

Figure 4. Mass Balance Summary Sheet

Average Yield Summary

Figure 5 summarizes the yields obtained during this run. During Run 123, 80.5% of the coal, on an MAF basis, was converted to product. The product distribution was as follows; 48.3% of the moisture and ash free coal (MAF) fed was ChemCoal solid, 30.2% of the MAF fed was methanol-soluble distillate, and 2.0% of the MAF was gas product. It should be noted that the ChemCoal solid product yields remained relatively constant throughout the run. Apparently the basic conversion mechanism remained constant, even as the solvent composition changed to include more complex phenolics.

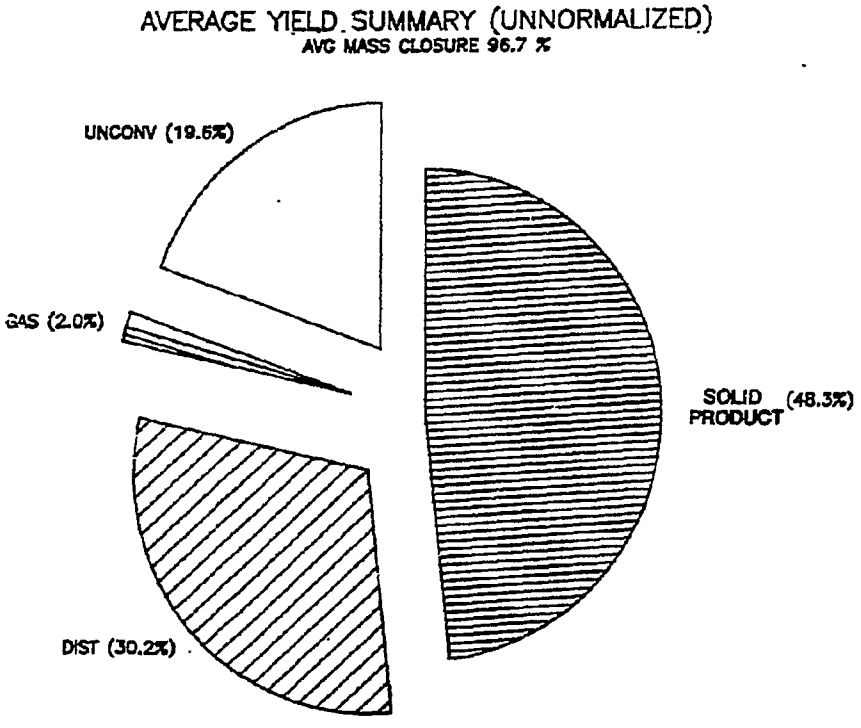

Figure 5. Average Yield Summary (unnormalized), CPU Run 123

Table 1 compares the elemental analyses of the ChemCoal solid with Indian Head lignite. As the table clearly shows, the ChemCoal Process reduced the moisture, ash, sulfur, oxygen, sodium, calcium, and titanium contents of the lignite. By reducing the sulfur and oxygen contents, the percent carbon, hydrogen, and nitrogen contents increased. The volatile matter, fixed carbon and heating values were also increased.

TABLE 1

COAL AND CHEMCOAL SOLID DATA

Form of Material	Lignite[a] -60 Mesh	UNDERC Solid[a] Powder
Proximate, wt% AR:		
Moisture	25.3	2.0
VM	30.8	44.0
FC	36.0	52.0
Ash	7.5	0.5-1.0
Ultimate, wt% maf:		
C	71.6	81.0
H	4.41	6.4
N	0.66	0.8
O (diff)	22.39	11.5
S	0.95	0.3
Heating Value, Btu/lb	6,000-8,000	14,800
Specific Gravity	1.4	>1.0
Na, ppm mf	1,900	22
Ca, ppm mf	8,300	115
Ti, ppm mf	300	45

[a] An analysis of an Indian Head lignite (ZAP2C) used and ChemCoal solid product produced at UNDERC.

Gas Yields

Average gas consumption and production during Run 123 produced molar ratios of CO, H_2O, H_2 and CO_2 as follows:

$$\underset{1.4}{CO} + \underset{1.8}{H_2O} \longrightarrow \underset{0.4}{H_2} + \underset{1.6}{CO_2}$$

The results of the water-gas shift reaction as it occurred in this system show a net consumption of shift reaction H_2 (4). The net wt% H_2 consumption came to 2% of the MAF fed. Hydrocarbon gas production was minimal at only 1% of the MAF.

Distillate Yields

The distillate yield was largely dependent upon two key downstream process variables: 1) variability of the operational temperature of the distillation unit; and 2) the effectivness of the solvent recovery from the centrifuge

cakes. Because operation of the distillation unit was different during the first 20 passes of the run than during the last 19, varied yield structures were produced for the overall process. As a result of the processing changes, the distillate yield increased from an average of 27% (MAF basis) prior to pass 20 to an average of 35.5% after pass 21.

Operational Solvent Balance

Figure 6 shows that the operational solvent balance prior to run pass 20, provided little leeway for losses in mixing and transfer. After pass 21, however, the processing modifications improved solvent balance to a comfortable excess. The intentional replacement of previously processed phenolics into the system, coupled with the changes which occurred in the downstream processing loops after pass 21, resulted in improved solvent recovery.

Solvent Characterization

Throughout Run 123, the phenolic start-up solvent was removed and replaced by a coal-derived recycle solvent characteristic of both the coal and the process. The start-up solvent was a commercial mixture of m- and p-cresols. As the distillate solvent was recycled from pass to pass, the m- and p-cresols were diluted with both phenolics formed from the coal and by methanol from the precipitation step. The replacement of start-up solvent by the system is a natural result of processing, but during this run was accelerated by selective retention of phenolic solvent in the centrifuge cake. Figure 7 illustrates the removal of phenolic solvent that occurred in the system during the course of the run.

Capillary GC/MS was used to identify many of the components in the process streams; these chromatograms are pictured in Figure 8. The analyses showed that a variety of coal-derived phenolics were formed during the reaction of the lignite. Early in the run, during pass 6, the solvent was composed primarily of the two cresols and their methylethers, as shown in Figure 8. Later in the run, as is also shown in Figure 8, a variety of other phenolic compounds from the coal were also present. Some of the components analyzed are labelled on the figure. Nine of the 26 components analyzed, in addition to m- and p-cresols, were present in significant quantities.

CONCLUSIONS AND RECOMMENDATIONS

Conclusions

CPU Run 123 demonstrated that the ChemCoal Process can be run successfully to lineout with solvent recycle. During this run, it was demonstrated that excess solvent was generated under all conditions and that reductant consumption as hydrogen gas and/or hydrogen equivalents was below 2.0 wt% of the MAF. ChemCoal Process conversion averaged over 80% of the MAF fed. This conversion remained relatively constant, with no loss in conversion occurring as process-derived solvent replaced start-up solvent in multiple recycles.

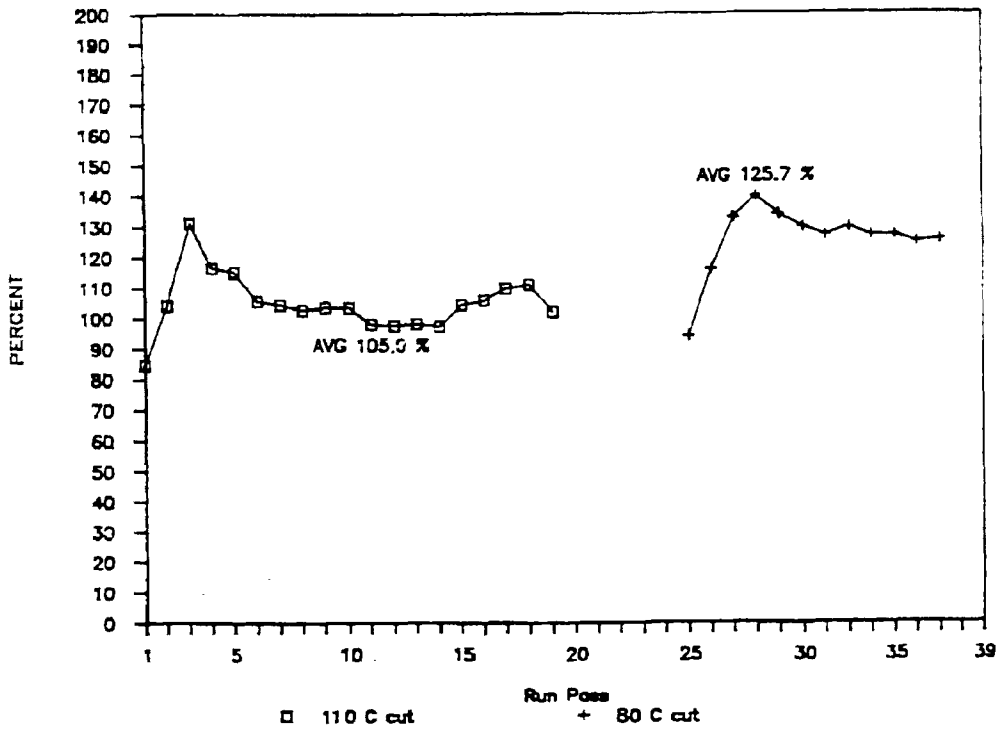

Figure 6. Operational Solvent Balance, Run 123

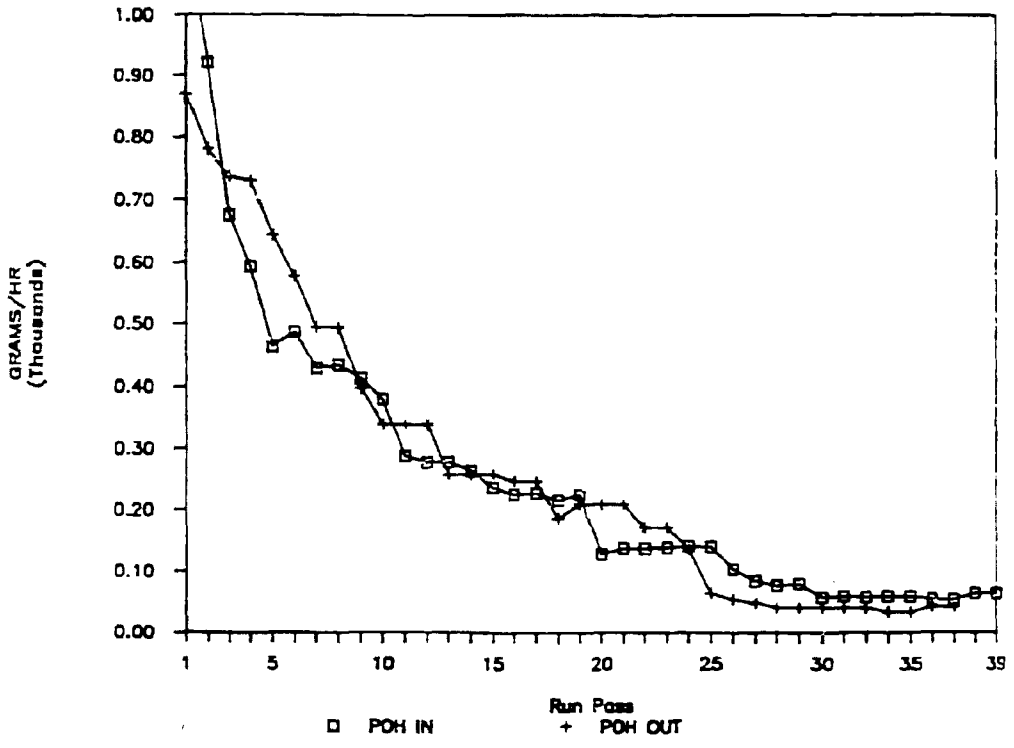

Figure 7. Phenolic Solvent Balance, Run 123

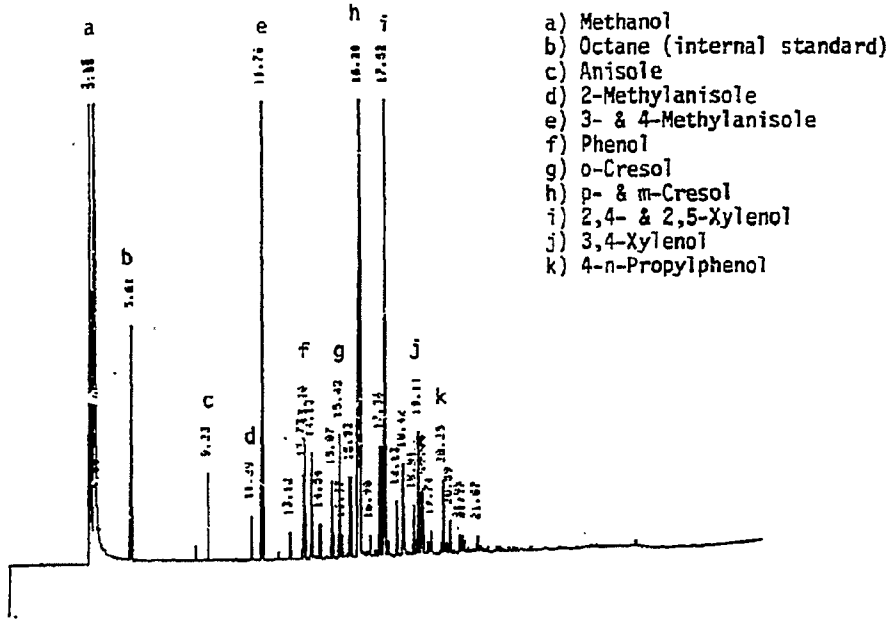

a) Pass 36, 5% of the total was seen by the GC but not quantified; 31.6% was non-volatile material

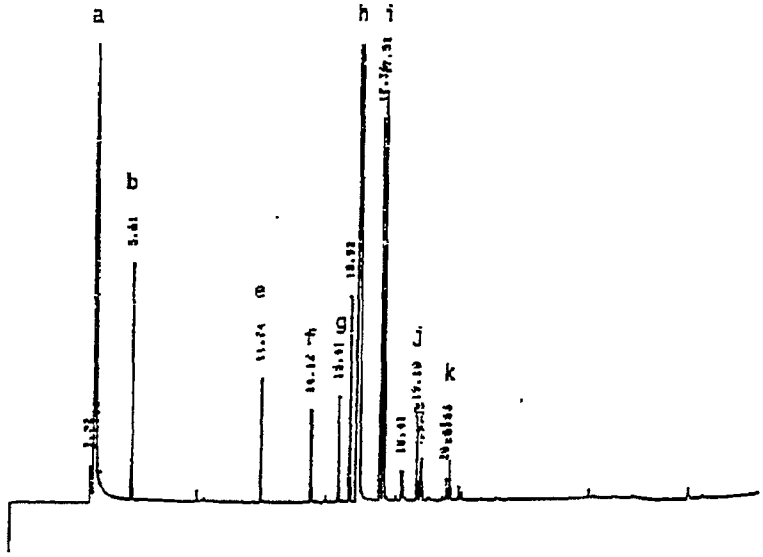

b) Pass 6, 1.89% of the total was seen by the GC but not quantified; 27.2% was non-volatile material

Figure 8. Capillary GC Charges in Phenolic Distillate Solvent in CPU Run 123, Pass 6 and 36

Recommendations

Significant developments and process improvements have been made since development research was undertaken at UNDERC, leading to new patent applications. More development is needed, including the following areas:

- Production of quantities of solid ChemCoal product for testing in end-use applications. This should be produced with the improved downstream processing developed resulting from the experience obtained during CPU Run 123 in which solvent lineout was achieved. To achieve successful processing operations with the ChemCoal Process, it is necessary to limit the loss of phenolic solvent during downstream processing. This includes the following:

  1. There should be virtually no loss of phenolics with the centrifuge cake. The addition of a pyrolysis unit after the centrifuge would recover any phenolics carried out of the stream with the centrifuge cake, as well as producing additional volatiles from the unconverted coal.

  2. The ChemCoal solids cake should be washed thoroughly to remove as many phenolics as is possible.

- The recycle test using Indian Head lignite should be repeated to determine reproducibility and to produce ChemCoal product for combustion testing.

- Other coals should be evaluated as ChemCoal feeds in the ERC CPU.

- A reactor design study should be undertaken.

- Residence time/temperature requirements with the condenser-reactor configuration used during Run 123 should be determined.

- The process economics should be updated to include new reactor concepts and product separation and recovery techniques.

- Proof of concept should be provided in a process demonstration unit.

ACKNOWLEDGEMENTS

The authors acknowledge the assistance of USDOE, EPRI, UNDERC, and CRI for funding of this work and the members of these organizations who contributed their time, effort and suggestions.

REFERENCES

1. Knudson, C.L. and S.A. Farnum, "Subbituminous Coal Characterization." Proceedings of the Tenth Annual EPRI Contractors' Conference on Clean Liquid and Solid Fuels, Palo Alto, CA, April 23-25, 1985.

2. Porter, C.R. and H.D. Kaesz, "The ChemCoal Process for the Chemical Transformation of Low-Rank Coal." Proceedings of the Thirteenth Biennial Lignite Symposium, Bismarck, ND, May 21-23, 1985.

3. Knudson, C.L., S.A. Farnum, and J.R. Rindt, "Bench-Scale Data on the ChemCoal Process." Proceedings of the Eleventh Annual EPRI Contractors' Conference on Clean Liquid and Solid Fuels, Palo Alto, CA, May 7-9, 1986.

4. Porter, C.R., C.L. Knudson, and J.R. Rindt, "The ChemCoal Process for Low-Temperature Conversion." ACS Div. Fuel Chem. Preprints, 31, 4, 70, 1986.

5. Willson, W.G., C.L. Knudson, S.A. Farnum, S. Cisney, R. Ness, J.R. Rindt, C.R. Porter, and H.J. Brolick, "ChemCoal Process CPU Recycle Development Program With Indian Head Lignite." Final Report, June 27, 1986, DOE/FF/60181.

6. Wiltsee, G.A., Low-Rank Coal Research Quarterly Technical Progress Reports, June 1983-December 1985.

ISOTOPIC CONSTRAINTS ON THE EFFICIENCY OF LIQUEFACTION OF LOW-RANKED COAL

by
J. Steer, K. Muehlenbachs
Geology Department, University of Alberta
Edmonton, Alberta, Canada
and
T. Ohuchi, D. Carson, B. Doherty, B. Ignasiak
Coal Research Department, Alberta Research Council, Devon,Alberta, Canada.

ABSTRACT

The influence of subbituminous Vesta coal upon the processing of stripped Athabasca bitumen(-350°C distillate fraction removed) was investigated in a series of 1 litre stirred autoclave runs in which coal concentration was systematically increased from 0 to 27 wt%. The inherent difference in $^{13}C/^{12}C$ ratio existing between Vesta coal and stripped bitumen (3.94 parts per thousand) was utilized as a natural isotopic tracer to monitor coal and bitumen incorporation into each synthetic liquid fraction. Comparision of isotopically determined coal-derived product yields indicate that; coal incorporation into distillate, toluene soluble and toluene insoluble fractions progressively increases with increasing coal concentration; and that a change in coal concentration from 15 to 26 wt% results in a three fold increase in toluene insoluble product. Relative incorporation of bitumen-derived carbon into synthetic liquid fractions changes as a function of coal concentration. Comparision of product yields obtained for hydrotreatment of bitumen with those isotopically determined from co-processing runs indicates that, for coal concentrations of 4 to 8 wt% a 14 to 17% increase in distillate yield is observed with a congruent 32 to 49% decrease in toluene soluble yields. Coal concentrations of 15 to 26 wt% result in no appreciable increase in distillate yield over co-processing of bitumen alone, while bitumen derived carbon in the toluene insoluble fraction increases from 0.9 to 5.0%. The results suggest that co-processing of coal-bitumen mixtures comprising of 5 to 10 wt% coal can enhance generation distillate derived from bitumen.

ISOTOPIC CONSTRAINTS ON THE EFFICIENCY OF LIQUEFACTION OF LOW-RANKED COAL

by
J. Steer, K. Muehlenbachs
Geology Department, University of Alberta
Edmonton, Alberta, Canada
and
T. Ohuchi, D. Carson, B. Doherty, B. Ignasiak
Coal Research Department, Alberta Research Council, Devon,Alberta, Canada.

ABSTRACT

The influence of subbituminous Vesta coal upon the processing of stripped Athabasca bitumen(-350°C distillate fraction removed) was investigated in a series of 1 litre stirred autoclave runs in which coal concentration was systematically increased from 0 to 27 wt%. The inherent difference in $^{13}C/^{12}C$ ratio existing between Vesta coal and stripped bitumen (3.94 parts per thousand) was utilized as a natural isotopic tracer to monitor coal and bitumen incorporation into each synthetic liquid fraction. Comparision of isotopically determined coal-derived product yields indicate that; coal incorporation into distillate, toluene soluble and toluene insoluble fractions progressively increases with increasing coal concentration; and that a change in coal concentration from 15 to 26 wt% results in a three fold increase in toluene insoluble product. Relative incorporation of bitumen-derived carbon into synthetic liquid fractions changes as a function of coal concentration. Comparision of product yields obtained for hydrotreatment of bitumen with those isotopically determined from co-processing runs indicates that, for coal concentrations of 4 to 8 wt% a 14 to 17% increase in distillate yield is observed with a congruent 32 to 49% decrease in toluene soluble yields. Coal concentrations of 15 to 26 wt% result in no appreciable increase in distillate yield over co-processing of bitumen alone, while bitumen derived carbon in the toluene insoluble fraction increases from 0.9 to 5.0%. The results suggest that co-processing of coal-bitumen mixtures comprising of 5 to 10 wt% coal can enhance generation distillate derived from bitumen.

INTRODUCTION

Future energy self sufficiency is an objective pursued by both the provincial and federal goverments of Canada. As a consequence the Alberta Research Council (A.R.C.) has initiated experimentation into the efficient generation of transportation fuels from Alberta's two greatest energy resources- subbituminous coal and bituminous oils. It would be economically desirable in heavy oil upgrading to supplement bituminous oils with inexpensive coal, provided a high conversion to distillate could be achieved. An important process variable in co-processing would be then the proportion of coal to bitumen in the slurry. The efficiency of distillate synthesis, as well as coal solubilization, was examined in a series of 1 litre autoclave experiments in which 0,8,15,30,60 grams of subbituminous Vesta coal were processed with 125 grams of stripped bitumen.

The standard method of evaluating process efficiency, coal conversion, underestimates the conversion of coal due to a component of the insoluble matter being bitumen-derived. We have found from carbon isotpoe studies that 0.5 to 5.0% of the total carbon in bitumen was incorporated into the toluene insoluble fraction. This results in an error of approximately 15% when calculating "coal conversion". The amount of either coal or bitumen incorporated into any synthetic product derived from co-processing can be quantitatively evaluated by stable isotope mass balance calculations[1]. In nature there exist an innate difference in $^{13}C/^{12}C$ between marine and terrestrial plants. This distinction in $^{13}C/^{12}C$ is preserved after burial and catagenesis. As a result, coal (primarily terrestrial in origin) and bitumen (primarily marine in origin) have different carbon isotope signatures. Measured $^{13}C/^{12}C$ values of stripped Athabasca bitumen and Vesta subbituminous coal differ by 3.94 ppt. (parts per thousand) which is the order of 70 times the experimental error in isotopic ratio measurements. Utilizing the inherent difference as an isotopic tracer it is possible to model the carbon budget during liquifaction as the mass balance between two end members[1]. Precise determination of the $^{13}C/^{12}C$ ratio of a synthetic liquid fraction allows for calculation of the relative proportion of coal derived carbon incorporated into that fraction.

METHODS

The coal-bitumen co-processing scheme examined in these experiments was a single stage process for solubilizing subbituminous coal using stripped bitumen as solvent.

A one litre Magne-Drive stirred (750 rpm) stainless steel autoclave was charged with 125 grams of Athabasca stripped bitumen atmospheric residue (-350°C fraction removed by distillation) and 0,8,15,30, or 60 grams of vacuum dried Vesta subbituminous coal ground to 100 mesh. The autoclave was pressurized by hydrogen to 8.6 MPa. at ambient temperature and heated at a rate of 8°C per minute with continual stirring until an operational temperture of 430°C was attained. Conditions were maintained for 45 minutes. The autoclave was subsequently cooled to 200°C and the naphta fraction directly removed from the autoclave. Product gases were collected, their volume measured, and analyzed by gas chromatography. Reaction mixture was transferred to glassware and distilled under reduced pressure to isolate a fraction distillable to less than 524°C (distillate). Residue after distillation was extracted by n-pentane and toluene successively in a Soxhlet extractor to isolate the pentane and toluene soluble fractions. The residue was collected as the toluene insoluble fraction. Each product fraction was analyzed for yield by weight, elemental analysis, and $^{13}C/^{12}C$ ratio. Dumas-Schöniger combustion was used as before to quantitatively convert the hydrocarbons products to CO_2 (1). The gas was purified to remove N_2 and waters of combustion and the $^{13}C/^{12}C$ ratio of the CO_2 gas measured by mass spectrometery. Most analysis were done in duplicate. The $\delta^{13}C$ was calculated from the measured $^{13}C/^{12}C$ ratio according to the following equation(1).

$$(1)\quad \delta^{13}C = \frac{(^{13}C/^{12}C)_{sample} - (^{13}C/^{12}C)_{ref}}{(^{13}C/^{12}C)_{ref}} \times 10^3 \text{ ppt.}$$

Values for $\delta^{13}C$ are presented with respect to the internationally accepted PDB scale(2). For duplicated autoclave runs, the error of measurement in $\delta^{13}C$ between simular product types was ±.07 ppt. By comparision, ±.03 ppt. represents the analytic limit of repeated measurement of $^{13}C/^{12}C$ in one CO_2 sample by the mass spectrometer.

RESULTS AND DISCUSSION

Contrast in $^{13}C/^{12}C$ ratio between Vesta coal and stripped Athabasca bitumen may be utilized as a natural isotopic tracer in order to monitor coal or bitumen incorporation into synthetic product fractions. When two isotopically distinct substances intereact in a closed system the products will have an isotopic signature intermediate between the parental sources reflecting relative amounts of each component utilized. Algebraically the relation can be derived from a simple two end member mixing model(1). Coal (or bitumen) contribution in a product is then:

$$(2)\ \%COAl\text{-}C = \left[1 - \frac{\delta^{13}C_{prod} - \delta^{13}C_{coal}}{\delta^{13}C_{bit} - \delta^{13}C_{coal}}\right] X100\%$$

The validity of the model depends upon two assumptions: that major chemical components of a reservoir must be isotopically uniform, for prefered reaction of one isotopically distinct fraction will bias the calculation; and that any isotopic partitioning caused by the process be known and compensated for.

We have analyzed the major components of our starting materials to test for intrasample isotopic variation. Given the greater variation in nature of $\delta^{13}C$ value for petroluems (-15 to -30 ppt. (3)) as compared to coals (-20 to -25 (4)), a larger selection of bitumen product fraction were analyzed, table(2) . The $\delta^{13}C$ value for pyridine extract of another subbituminous coal and acid treated Vesta coal were also determined. Measured $\delta^{13}C$ values of the isolated fractions lie within experimental error of the composite materials, indicating that the major chemical fractions of stripped

TABLE 1a Elemental Composition of Vesta Coal and Stripped Bitumen

Fraction	Coal	Bitumen
Carbon	71.6	82.4
Hydrogen	5.0	10.1
Nitrogen	1.7	0.5
Sulphur	1.0	4.9
Ash	17.0	0.7
Moisture	0.7	0.0

TABLE 1b Composition of feed and run products of Athabasca stripped bitumen

Fraction	Bitumen Feed wt%	Processed Bitumen Carbon in Grams
Distillate	14.6	49.9
Pentane Soluble	61.5	24.1
Toluene Soluble	23.9	24.7
Toluene Insoluble	0.0	0.9
Evolved Gases	-	4.4
% Recovery	-	101.7

Table 2 Reservoir Uniformity

Bitumen and Coal Fractions	$\delta^{13}C$ ppt.
Athabasca Stripped Bitumen	-29.22
Suncor Bitumen	-29.22
Toluene Soluble	-29.10
Pentane Soluble	-29.29
Middle Distillate 350-524 °C	-29.24
524 °C Distillate	-29.19
Highvale Coal	-25.54
Highvale Coal Pyridine Extract	-25.64
Vesta Coal	-25.28
Vesta Coal Treated with HCl	-25.26
Vesta Coal Treated with HF	-25.29

TABLE 3 Evolved gas fractions (carbon in grams)

Run #	DC-1	DC-2	DC-3	DC-51	DC-45	DC-5
Amount of coal (in grams)	60	60	30	15	8	0
Methane to Pentane	4.83	4.83	4.44	3.32	3.82	4.10
CO_2	1.41	1.07	0.53	0.26	0.23	0.19
CO	0.28	0.27	0.21	0.16	0.12	0.12
TOTAL	6.52	6.17	5.18	3.74	4.17	4.41

Athabasca bitumen and Vesta coal are uniform in $^{13}C/^{12}C$.

The second assumption in the mass balance calculation is that any isotopic partioning caused by the process be known and compensated for. During the co-processing of coal-bitumen thermally activated bond severing results in the evolution of low ^{13}C hydrocarbon gases, carbon monoxide, and ^{13}C-enriched carbon dioxide.

Vacuum pyrolysis experiments have been performed on a varity of subbituminous coals [5,6,7] and model compounds [9]. In general methane evolved from subbituminous coal over the temperature range of 400-500°C enriches the residue in ^{13}C by 2 to 8 ppt.[5,6,7], while the liberation of CO_2 depletes the source material of ^{13}C by about 3 ppt.. At present, data for the isotopic shifts induced by CO liberation in coal pyrolysis in the temperature range 400-500°C are contradictory. Sacket and Chung [5] have reported a ^{13}C depletion in the gas occurs between evolved CO and the source material, whereas Gaveau et. al. [7] observed that evolved CO was enriched in ^{13}C with respect to the source. Isotopic shifts due to reverse reaction of the evolved gases with the source material to "scramble" the isotopic signature of the evolved gas has been demonstrated to be insignificant. Experimental evidence indicates that heating at 500°C for over 180 hours results in no ^{13}C exchange among methane, carbon dioxide, and carbon monoxide [8].

Comparision of the quantity and composition of the gas phases evolved during coal-bitumen co-processing and a bitumen-only blank run allow for a first order calculation by difference, of the type and quantity of gas evolved solely from coal. Isotopic shift in coal due to gas evolution is estimated to be about +0.06 ppt. or about the same as the experimental error of measurement.

In analogous fashion isotopic depletion or enrichment in ^{13}C for crack gas liberation in bitumen hydrotreatment can be estimated from isotopic shifts measured in pyrolysis of bitumen and model compounds [9,10]. Utilizing the isotopic shifts reported in liturature, crack gas evolution is expected to enrich the residue approxiamatly +0.4 [1]. Generation of ^{12}C enriched gases must be taken into account for bitumen when calculating the quantity of parential material utilized in generation of a product fraction. Failure to account for the gas results in the mass balance of coal-derived carbon being erroneously high due to the isotopic ratio of bitumen's residue

becoming more coal like.

To correct for the enrichment of ^{13}C in bitumen the $^{13}C/^{12}C$ ratio of the synthetic liquids derived from a bitumen-only blank run were determined in order to provide an indication of bitumen's responce to processing. In equation (2) the gas effect is compensated for by replacement of $\delta^{13}C_{bit}$ with the $\delta^{13}C$ value obtained for a blank run product when calculcating coal incorporation for the same product type.

After isotopic correction for crack gas evolution, the amount of coal (or bitumen) calculated to be present should equal its weight in the experimental charge. The amount of bitumen as calculated from the corrected equation 2, ranged from 98 to 102% of the actual experimental charge, appendix(1). For coal 93 to 127% of the experimental charge was acounted for. In run DC-3 the excess yields calculated for the carbon budget of bitumen and coal 102, 108% respectively, are in part artifacts of the excess yield of product recovered from the autoclave, 103% by weight. A more serious discrepancy is observed experiments DC-45 and DC-51 between the isotopically calculated amount of coal derived carbon and the intial charge of coal in the autoclave (127,123% excess yield respectively).

Both excess yield experiments had a net decrease in C_1 to C_5 hydrocarbon gas evolution (7,19% respectively) relative to the bitumen-only blank run, table(3). As well the naphta fraction (-200°C) of each exhibited a 0.5 ppt. enrichment in ^{12}C relative to bitumen. The observed decrease in light hydrocarbon (C_1 to C_5) with the addition of 4 to 8 wt% coal may influence the ^{12}C depletion of bitumen due to processing. A precise measurement of the $^{13}C/^{12}C$ ratio of the crack gases liberated via co-processing is required in order to more accurately estimate coal incorporation. Progress is now under way for the analysis of $^{13}C/^{12}C$ ratios in light hydrocarbon gases, CO_2, and CO liberated during co-processing.

With the addition of coal and it's subsequent solubilization a portion of each synthetic product will be coal derived. Any relative change of coals incorporation in a product fraction directly monitors process efficiency. Increasing coal content in the reaction slurry, illustrated in figure(1), results in greater coal incorporation into every product fraction. Calculated yields of distillate (-524°C) solely derived from coal are observed to increase in a near linear fashion with coal concentration, figure(1).

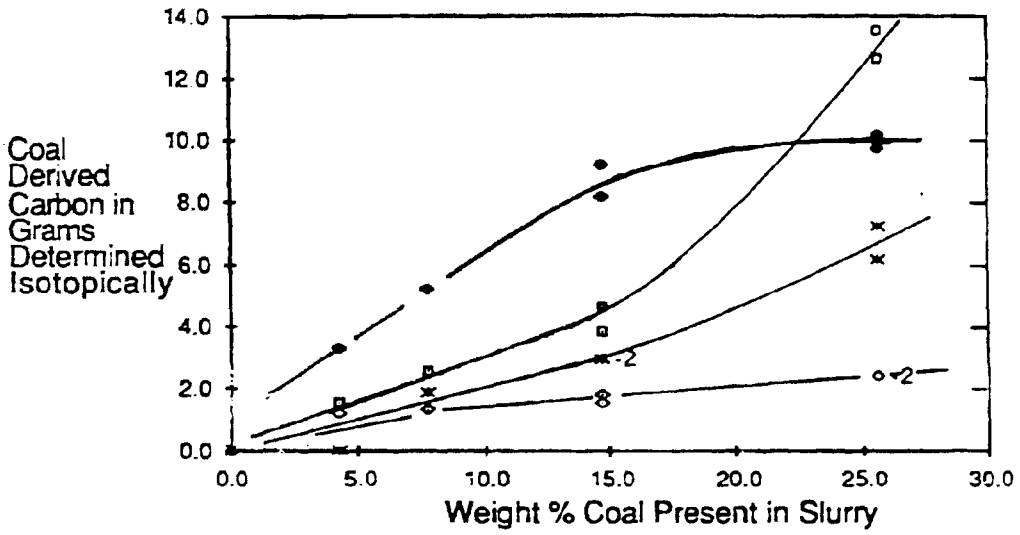

Figure 1 Variation in the isotopically determined amount of coal derived carbon incorporated into each synthetic liquid. Symbols ⁎- Distillate; ○- Pentane Soluble; ●- Toluene Soluble; ▫- Toluene Insoluble.

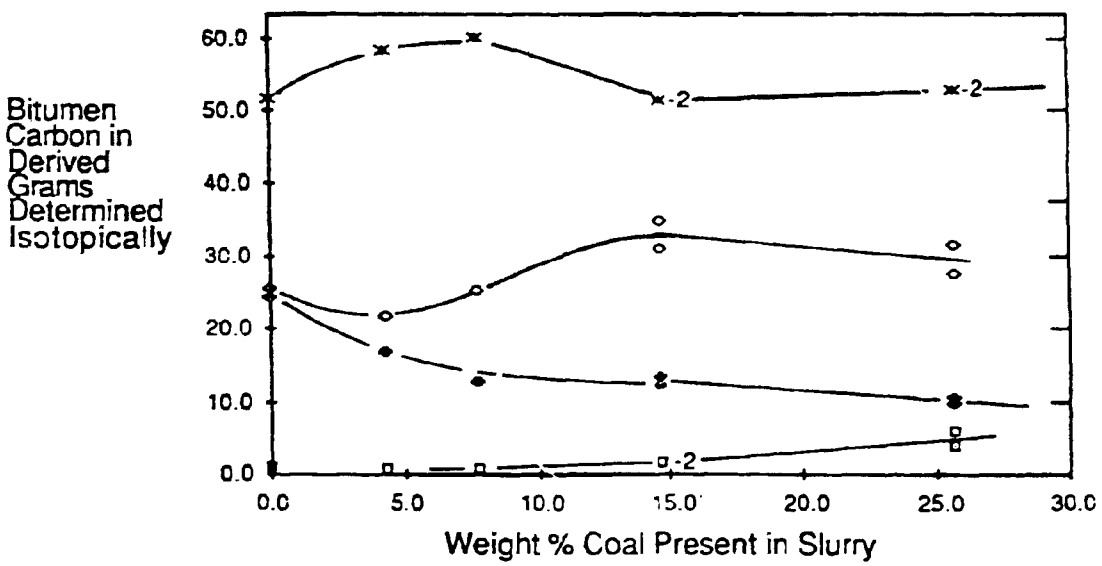

Figure 2 Variation in the isotopically determined amount of bitumen derived carbon incorporated into each synthetic liquid as a function of coal concentration in the slurry. Symbols; ⁎- Distillate; ○- Pentane Soluble; ●- Toluene Soluble; ▫- Toluene Insoluble.

Incorporation of coal-derived material in the pentane soluble fraction appears to be largely independent of coal concentration. Yields of coal-derived pentane soluble fraction are similar for autoclave runs in which 4 and 15 wt% coal were added, 1.2 and 1.7 grams repectively (appendix 1), inspite of the three fold increase in coal concentration. A "break in slope" is observed in the plot of the coal derived toluene insoluble material versus coal concentration, figure(1). Coal derived insoluble yields increase gradually (figure(1)) over the concentration range of 0 to 15 wt%. In contrast a sharp increase in toluene insoluble yield for coal concentrations in excess of 15 wt% was observed, 4.1 grams for 15 wt% coal rising to 13.1 grams for coal concentrations of 26 wt% (appendix 1). Another "break in slope" is observed in the plot of coal derived toluene soluble material versus coal concentration. For coal concentrations of 0 to 15 wt% a large relative increase in the amount of coal derived toluene soluble material exists. Beyond coal concentrations of 15 wt% the curve denoting toluene solublility appears to "level off". At coal concentrations in excess of 15 wt% a diminished capacity for bitumen's solubilization of coal-derived toluene soluble matter appears to exist. Results suggest that bitumen and coal fragments of high molecular weight generated during thermolysis may repolymerize to stable compounds (toluene insoluble material) prior to hydrogen capping when coal concentration is in excess of 15 wt%. For siurry ratios of 0 to 15 wt% coal a linear relationship appears to exist between coal concentration and the incorporation of coal-derived carbon into each product fraction.

In analogous fashion the incorporation of bitumen-derived carbon into the synthetic liquids can be evaluated, figure(2). Several discernible trends are apparent from the isotopically calculated yields of bitumen-derived carbon. Most notable is an increase in distillate yield (14 to 17%) with the addition of 4 to 8 wt% coal, over distillate yields obtained in the hydrotreatment of bitumen alone. Graphically there appears to be antithetic correllation between bitumen-derived distillate and pentane soluble yields. From the distillate and pentane soluble curves, figure(2), a general trend of increased distillate yield corresponds with a decrease in the bitumen-derived pentane soluble fraction. For coal concentrations greater than 8 wt% the bitumen-derived carbon component (yields ranging from 25.3

to 33.2 grams) of the pentane soluble fraction are in excess of the yield obtained from the processing of bitumen alone (24.1 grams, table1b).

The excess bitumen derived carbon in the distillate and pentane soluble fractions seems to be derived at the expense of the toluene soluble fraction. As coal concentration increases, bitumen derived component of the toluene soluble material decreases from 24.7 grams (bitumen only) to 10.2 grams (26 wt% coal). The effect is more pronounced at low coal concentrations decreasing from 24.7 grams in the bitumen-only experiment to 16.9 grams for coal concentrations of 4 wt%, a 32% decrease. By comparision the decrease in bitumen-derived toluene soluble product yields over the concentration range of 8 to 26 wt% is only from 12.1 to 10.2 grams, a 16% reduction. Isotopically determined bitumen-derived carbon yields of the three fractions, distillate, pentane soluble, and toluene soluble suggest that the increased distillate yield observed for coal concentrations of 4 to 8 wt% are derived via thermal degradation of pentane soluble and toluene soluble material.

The proportion of distillate derived solely from bitumen shows no appreciable change in yield for coal concentrations in excess of 15 wt%, (51.4 grams-26 wt%; 52.9 grams-15 wt%; 51.4 grams-0 wt%). For bitumen-coal slurry ratios in excess of 15 wt% the amount of bitumen-derived carbon present in the toluene insoluble fraction increases from 1.3 to 5.1 grams. This increase parallels a measured increase in toluene insoluble product yields for coal-derived carbon (4.1 to 13.1 grams, appendix 1). The sharp increase in insoluble yields is in part due to polymeriaztion reactions, (as evidenced by the increase in bitumen-derived component of the toluene insoluble product), and in part by coal saturation in the slurry (as evidenced by the three fold increase in coal-derived insoluble matter). Coal concentration in excess of 15 wt% appears to enhance the conversion of the toluene soluble fraction inherent in bitumen into pentane soluble and toluene insoluble products. No appreciable change in the bitumen-derived component of the distillate is observed at this concentration range.

CONCLUSIONS

A stable isotope mass balance techinque was used to investigate the efficiency of single stage coal-bitumen co-processing for the solubilization of coal. Stable isotope mass balance calculations indicate that changes in coal concentration in bitumen co-processing evoke differing effects in coal liquefaction and bitumen upgrading. At coal concentrations of 0-10 wt% a 14 to17% increase yield is observed in the bitumen-derived component of the distillate fraction. Concordently the bitumen derived component of the toluene soluble fraction decreases from 32 to 49% with respect to yields obtained for the hydrotreatment of bitumen alone. Excess distillate yields appear to have been primarily generated from the conversion of the toluene soluble fraction and pentane soluble fraction of bitumen. With futher addition of coal, 15 to 26 wt%, no appreciable change in the amount of bitumen incorporated into distillate fraction occurs. Yields of bitumen-derived pentane soluble material are in excess of those obtained for the processing of bitumen alone. Yields in the bitumen-derived toluene soluble fraction are observed to decrease by 17% as coal concentration increases from 15 to 26 wt%. Over the same concentration range nearly a four fold increase in toluene insoluble yield occurs. Calculated coal-derived product yields indicate that a limit may exist for the solubility of coal-derived toluene soluble product in bitumen and that at higher coal concentrations a dramatic increase in the insoluble product (unreacted coal) occurs. The results suggest that co-processing of coal-bitumen mixtures consisting of 5 to 10 wt% coal will generate a synthetic liquid low in toluene insoluble material and result in distillate yields in excess of those obtained from the hydrotreatment of bitumen.

ACKNOWLEDGMENTS

Laboratory work was supported by a grant from the Alberta Energy and Natural Resources: Office of Coal Research Technology. The autoclave runs and chemical analysis were preformed at the Alberta Research Council, Coal Department.

REFERENCES

1 J.G. Steer, T. Ohuchi and K. Muehlenbachs, Efficacy of coal-bitumen co-processing as determined by isotopic mass balance calculation, Fuel Proc. Tech., Vol.15, (1987), pp.429-438.

2 H. Craig, Isotopic standards for carbon and oxygen and correction factor for mass-spectrometric analysis of carbon dioxide, Geochim. Cosmochim. Acta., Vol.12, (1957),pp133-149.

3 S.R. Silverman, and S. Epstein, Carbon isotopic compositions of petroleums and other sedimentary organic materials, Bull. Amer. Assoc. Pet. Geol., Vol. 42, (1958), pp.998-1012.

4 J.W. Smith, Gould K.W. and Rigby D., The stable isotope geochemistry of Australian coals, Org. Geochem., Vol. 3, (1982), pp.111-131.

5 H.M. Chung, and W.M. Sackett, Use of stable carbon isotope composition of pyrolytically derived methane as maturity indices for carbonaceous materials, Geocim. Cosmochim. Acta, Vol. 43, (1979), pp.1979-1988.

6 H.U. Friedrich and H. Juntgen, Some measurements of the $^{13}C/^{12}C$-ratio in methane or ethane desorbed from hard coal or released by pyrolysis, Advances in Organic Geochemistry, Pergamon press, Oxford, (1972), pp.639-646.

7 B. Gaveau, R. Letolle and M. Monthioux, Evaluation of kinetic parameters from ^{13}C isotope effect during coal pyrolysis, Fuel, Vol. 66, (1987), pp.228-231.

8 W. M. Sackett and H.M. Chung, Experimental confirmation of the lack of carbon isotope exchange between methane and carbon oxides at high temperatures, Geocim. Cosmochim. Acta, Vol. 42, (1978), pp.273-276.

9 W. M. Sackett, Carbon and hydrogen isotope effects during the thermocatalytic production of hydrocarbons in laboratory simulation experiments, Geocim. Cosmochim. Acta, Vol. 42, (1978), pp.571-580.

10 K.N. Jha, J. Gray and O.P. Strausz, The isotopic compostion of carbon in the Alberta oil sands, Geocim. Cosmochim. Acta, Vol. 43, (1979), pp.1571-1573.

APPENDIX 1a Coal and bitumen incorporation into synthetic products

Run DC-1: 60 grams Vesta coal (35.4 grams carbon)
125 grams Athabasca stripped bitumen (102.3 grams carbon)

Product Type	%COAL-C	Total Carbon	Coal Derived Carbon	Bitumen Derived Carbon
Distillate	12.2	60.2	7.3	52.9
Pentane Soluble	8.1	30.2	2.4	27.8
Toluene Soluble	50.4	19.2	9.7	9.5
Toluene Insoluble	70.2	19.3	13.5	5.8
Total Carbon in Products		128.9	32.9	96.0
Carbon in Evolved Gases		6.5	2.1	4.4
Total Carbon Budget in Grams		135.4	35.0	100.4
% Recovery		98.3	98.9	98.1

APPENDIX 1b Coal and bitumen incorporation into synthetic products

Run DC-2: 60 grams Vesta coal (35.4 grams carbon)
125 grams Athabasca stripped bitumen (102.3 grams carbon)

Product Type	%COAL-C	Total Carbon	Coal Derived Carbon	Bitumen Derived Carbon
Distillate	10.3	59.0	6.1	52.9
Pentane Soluble	6.7	34.3	2.3	32.0
Toluene Soluble	48.5	21.1	10.2	10.9
Toluene Insoluble	74.5	16.9	12.6	4.3
Total Carbon in Products		131.3	31.2	100.1
Carbon in Evolved Gases		6.2	1.8	4.4
Total Carbon Budget in Grams		137.5	33.0	104.5
% Recovery		99.9	93.2	102.2

APPENDIX 1c Coal and bitumen incorporation into synthetic products

Run DC-3: 30 grams Vesta coal (17.7 grams carbon)
125 grams Athabasca stripped bitumen (102.3 grams carbon)

Product Type	%COAL-C	Total Carbon	Coal Derived Carbon	Bitumen Derived Carbon
Distillate	5.3	54.3	2.9	51.4
Pentane Soluble	5.0	36.9	1.9	35.0
Toluene Soluble	43.3	21.2	9.2	12.0
Toluene Insoluble	75.9	5.6	4.6	1.3
Total Carbon in Products		118.0	18.3	99.7
Carbon in Evolved Gases		5.2	0.8	4.4
Total Carbon Budget in Grams		123.3	19.1	104.1
% Recovery		102.7	107.9	101.8

APPENDIX 1d Coal and bitumen incorporation into synthetic products

Run DC-4: 30 grams Vesta coal (17.7grams carbon)
125 grams Athabasca stripped bitumen (102.3 grams carbon)

Product Type	%COAL-C	Total Carbon	Coal Derived Carbon	Bitumen Derived Carbon
Condensate	5.3	54.5	2.9	51.6
Pentane Soluble	4.5	32.9	1.5	31.4
Toluene Soluble	38.3	21.3	8.2	13.1
Toluene Insoluble	77.0	5.1	3.9	1.2
Total Carbon in Products		113.8	16.5	97.3
Carbon in Evolved Gases		5.2	0.8	4.4
Total Carbon Budget in Grams		119.0	17.3	101.7
% Recovery		99.2	97.7	99.4

APPENDIX 1e Coal and bitumen incorporation into synthetic products

Run DC-51: 15 grams Vesta coal (8.9 grams carbon)
127.3 grams Athabasca stripped bitumen (104.1 grams carbon)

Product Type	%COAL-C	Total Carbon	Coal Derived Carbon	Bitumen Derived Carbon
Condensate	0.0	6.2	0.0	6.2
Gas Oil	3.4	55.7	1.9	53.8
Pentane Soluble	5.0	26.6	1.3	25.3
Toluene Soluble	29.2	17.7	5.2	12.6
Toluene Insoluble	81.2	3.1	2.5	0.6
Total Carbon in Products		109.3	10.9	98.5
Carbon in Evolved Gases		3.7	0.0	3.7
Total Carbon Budget in Grams		113.0	10.9	102.2
% Recovery		100.0	122.5	98.2

APPENDIX 1f Coal and bitumen incorporation into synthetic products

Run DC-45: 8 grams Vesta coal (4.7 grams carbon)
126.3 grams Athabasca stripped bitumen (103.3 grams carbon)

Product Type	%COAL-C	Total Carbon	Coal Derived Carbon	Bitumen Derived Carbon
Condensate	0.0	4.7	0.0	4.7
Gas Oil	0.0	53.6	0.0	53.6
Pentane Soluble	5.3	23.0	1.2	21.8
Toluene Soluble	16.3	20.2	3.3	16.9
Toluene Insoluble	74.1	2.1	1.5	0.5
Total Carbon in Products		103.6	6.0	97.5
Carbon in Evolved Gases		4.2	0.0	4.2
Total Carbon Budget in Grams		107.8	6.0	101.7
% Recovery		99.8	127.7	98.5

THE STUDY OF VARIABILITY IN THE DISTRIBUTION OF CHEMICAL SPECIES IN COAL CONVERSION PRODUCTS USING SIZE EXCLUSION CHROMATOGRAPHY - GAS CHROMATOGRAPHY - MASS SPECTROMETRY (SEC-GC-MS)

C. V. Philip and R. G. Anthony

Kinetic, Catalysis and Reaction Engineering Laboratory
Department of Chemical Engineering, Texas A&M University
College Station, Texas 77843 - (409)845-3376

ABSTRACT

The low rank coals used in the liquefaction experiments were Texas Big Brown lignite from the Wilcox formation, Zap-2 Indian Head lignite and Beulah lignite from North Dakota and Wyodak coal from Wyoming. Mini reactors (6.3 and 20 mℓ) used mostly Autoclave high pressure fittings. The liquefaction solvents included anthracene oil, four recycle solvents from the coal liquefaction pilot plant at the University of North Dakota Energy Research Center (UNDERC) and water under supercritical conditions. Hydrogen, carbon monoxide and hydrogen sulphide were the reactive gases which were used in varying proportions. The samples of liquid products from selected experimental conditions were used for the detailed analysis.

The product slurry as well as the recycle solvents were extracted with tetrahydrofuran (THF) and the solubles were used as samples for the analysis. The technique for the analysis is based on the integrated use of three instruments - a size exclusion chromatograph (SEC) with a 100Å SEC column, a high resolution gas chromatograph with a bonded phase wide bore fused silica column and an Ion Trap Detector (ITD, Finnigan), a mass spectrometer for capillary chromatograph. A sample injected into the SEC was separated based on linear molecular size and the fractions of effluents were collected at preprogramed time intervals. The separation of each fraction is continued on the capillary column and the components were detected by the mass spectrometer (ITD). The mass spectral fragmentation data were stored on a 10 megabyte hard disk and were later analyzed by the library search using National Bureau of Standards (NBS) mass spectral data base which has fragmentation patterns of about 40,000 organic compounds. The library search was used to identify the general formula as well as probable functional groups of most major components in coal liquids. The identification of each species was achieved by using several factors including SEC retention volume (linear molecular size), GC retention time (boiling point, molecular weight) and mass spectral fragmentation pattern.

The SEC-GC-MS analysis data on low rank coal derived liquids which were produced under varying liquefaction conditions were used tc identify probable chemical reactions responsible for converting coal to liquid products. We have observed a striking similarity in the identity of chemical species in anthracene oil (A04), recycle solvents and the low rank coal derived liquids. The aromatic species which are characteristic of coking oven products from coal, such as anthracene oil and creosote oil were found in all low rank coal derived liquids from the liquefaction experiments, including the one using water under super critical conditions. However there were variations in the concentrations. The hydroxy aromatics, also known as alkylated phenols, which are produced under lignite liquefaction experiments, are not major components in anthracene oil. The straight chain hydrocarbons, mainly alkanes which are found in any coal liquid and are observed as sharp peaks are substituted with a "hump" of GC. It appears that the pyrolytic conditions used in coking oven are destroying or converting most of the straight-chain alkane species and producing numerous isomeric hydrocarbons as evidenced by the MS fragmentation patterns of the GC "hump". The paper will present analysis data on specific samples to demonstrate the basic trends in liquefaction reactions as well as the instrumentation and analysis techniques.

INTRODUCTION

The major stumbling block in any coal liquefaction study is the time required for analysis of the coal-derived liquids. Most liquefaction studies used only simple routine tests to evaluate the degree of conversion. These tests were based on viscosity of the liquids produced, and on the amounts of residues, distillates, and non-volatiles in the product slurry. Occasionally, more time-consuming analytical tests were alsc performed to estimate the asphaltene and oil content of the product slurry. Rarely, coal liquids (most of the time only certain fraction were used) were also extensively analyzed by sophisticated instrument such as gas chromatography - mass spectrometry (GC-MS), nuclear magnetic resonance (NMR), Fourier Transform Infrared (FTIR) spectrometry and high performance liquid chromatographic separations (HPLC).

Size exclusion chromatography - gas chromatography - mass spectrometry (SEC-GC-MS) is a unique technique which we have developed during the project period for coal liquid analysis. Size exclusion chromatography (SEC) separates molecules based on size in a short analysis time. Unlike other chromatographic techniques, SEC does not retain sample species on the column, the analysis time is fixed, and everything loaded onto the column elutes within a fixed time frame. The application of SEC is limited only by the solubility of the sample in a solvent. Since tetrahydrofuran (THF) is a good solvent for coal liquids, the separation of coal liquids by SEC is easily achieved with appropriate columns.

Although size exclusion chromatography (SEC) has been used primarily for the separation and characterization of polymers based on molecular size or molecular weight, its use can be extended to the separation of smaller size molecules.[1-4] Since coal-derived mixtures have several components of similar sizes, the use of SEC alone does not resolve them for the purpose of identification. The gel columns packed with 5μm polymer particles have about 50,000 theoretical plates per meter, a five-fold increase over that of 10 μm columns; thus, an increase in separation effi-

ciency is achieved. Because sample sizes can be increased with a minimal loss of the number of theoretical plates and still remain reasonably good resolution, a column 60 cm in length can separate a relatively large sample in a time as short as 25 minutes. SEC is used as a preliminary separation technique. Other analytical techniques such as gas chromatography (GC) and gas chromatography-mass spectroscopy (GC-MS) are used to analyze the SEC fractions.

Coal liquids, petroleum crudes, and their distillation cuts have been separated into four or five fractions by SEC. These SEC fractions were analyzed by use of GC.[6,7,8] The fraction collection procedure was performed manually, which was inefficient, and susceptible to human error. A preferred technique is to use a computer controlled fraction collection and subsequent GC-MS analysis technique. The automated fraction collection followed by injection of the fraction into the GC reduces analysis time, and offers an option for the collection of the desired number of fractions at predetermined time intervals. The manual collection of up to 10 one-ml fractions is also used in order to varify the effectiveness of the automated technique.

The flame ionization detector (FID) is used for the detection and quantitative estimation of components separated by the GC. Identifications of major species is achieved by a mass spectrometer which cannot be used for quantitative analysis of complex mixtures such as coal liquids.

Mass spectrometers used to be expensive and complex for routine use as a GC detector. The Ion Trap Detector (ITD, Finnigan) is a low priced mass spectrometer (MS) for capillary chromatography. Three analytical tools - SEC, GC, and ITD - are incorporated into a powerful analytical system for the analysis of complex mixtures such as coal liquids, recyle solvent and anthracene oils. The instrumentation was developed as a part of this DOE project. The SEC-GC-MS analysis of Wyodak recycle solvent is used to illustrate the speed and effectiveness of the technique.

EXPERIMENTAL

Coal Liquid Samples

Coal liquids used for the analysis included recycle solvents which were obtained from the University of North Dakota Energy Research Center (UNDERC). Anthracene oil distillates were used to liquefy low-rank coals and the resulting product slurries were recycled as liquefaction solvents for approximately twenty times before the recycle solvents were produced. The recycle solvent contained a substantial amount of original anthracene oil and its decomposition products along with low-rank coal-derived products. The recycle solvent represents a very complex synthetic crude sample with questionable hydrogen donor capability. Four recycle solvents produced from Wyodak subbituminous coal, two North Dakota lignites (ZAP-2 and Beulah), and Texas Big Brown lignite were used for mini-reactor liquefaction experiments on some coals at Texas A&M University. Some liquefaction experiments were performed using other solvents such as plain anthracene oil and water under supercritical conditions. Temperature pressure and feed gas compositions were varied to produce chemical liquids with different chemical compositions, from low-rank coals. The slurry from the reactor was extracted with THF by sonicating in an ultrasonic bath for 15 minutes. These extracts were also analyzed. A 25% solution of the sample was prepared in tetrahydrofuran (THF) and filtered through 0.45 μm disposable HPLC filters (Supelco) and 100 μls of the filtered solution were used for each SEC separation.

SEC-GC-MS Instrumentation

A schematic of the SEC-GC-MS instrumentation is shown in Figure 1. The system consists of the following: a liquid chromatograph (LC, Waters ALC/SEC Model 202) equipped with a 60 cm, 5 μm, 100 A PL-gel column (Polymer Laboratories) and a refractive index detector (Waters Model R 401); a bonded phase fused silica capillary column manufactured by Scientific Glass Engineering, Inc. (SGE); an autosampler (Varian 8000); a flame ionization detector (FID); a nitrogen specific detector (Thermionic Ion Specific - TSD); and a microcomputer system (IBM CS 9000) with 1000K bytes RAM and dual 8" floppy disk drives for collecting raw chromatographic data.

A Finnigan Ion Trap Detector (ITD), a small mass spectrometer for capillary chromatography, is the third detector interfaced with the gas chromatograph. Finnigan introduced the ITD during the first year of the DOE project and one of the first ones was purchased and installed during the second year of the project. The control of the ITD, the data collection, and the identification of species by a library search with a NBS Mass Spectral Data Base stored on a 10 megabyte hard disk, are performed by an IBM PC XT microcomputer. Since the software from Finnigan did not allow the operation of the ITD in a run programmed mode, it was necessary to run each GC separation manually and reset the ITD between GC runs. A new software for ITD was obtained during the last year of the project, which allows uninterrupted analysis of several samples in an automated mode. It was also a practice to collect samples on the loops of valve V_3 (Figure 2) and to concentrate it before manually injecting the sample (0.2-0.5 μl) with a Scientific Glass Engineering (SGE) on-column injector in order to better identify the minor components.

SEC-GC Interface

The continuous sample separations on the gel column followed by the GC analysis of selected fractions were achieved by the operation of two 6-port valves and a 34-port valve (All from Valco Instrument Company) as illustrated in Figure 2. Sample injection into the LC was performed by a 6-port valve (V_1) with a 2 ml sample loop and fitted with a syringe-needleport for variable sample size injection. The combined operation of another 6-port switching valve and the 34-port valve (V_3) with 16 sample loops (100 μl) enabled the linking of the liquid chromatograph with the autosampler of the gas chromatograph. The autosampler was modified to handle 100 μl samples directly from the fraction collection loops of V_3. When V_2 was turned clockwise, it kept V_3 in line of the LC effluent so that the fractions of separated sample could be collected and the autosampler was bypassed. V_2 at its counterclockwise position kept V_3 in line with the autosampler for sample injection but it bypassed the LC stream. Generally, 0.1 μl samples were used for the GC analysis. Sometimes the stream from the capillary column was split (50/50) for the simultaneous monitoring by the FID and TSD. The real time monitoring of the GC was possible on both Varian and IBM systems and the raw chromatographic data were stored on the 8" floppy disks. The fraction collections and sample injections into the GC, as well as the data collection, were performed by the integrated system composed of a Varian Automation System (VISTA 401) and the IBM microcomputer (CS 9000). For each sample injected into the SEC column, up to 16 fractions were collected and analyzed by the GC using appropriate gas chromatographic programs stored in the memory without any manual interaction.

In addition to the use of the LC-GC interface (Figure 2), 1 ml fractions were manually collected and analyzed by GC using the autosampler. The fractions were also evaporated using a slow stream of nitrogen and analyzed each fraction by GC-MS using

a SGE on-column injector.

RESULTS & DISCUSSION

SEC of Wyodak Recycle Solvent

Figure 3 shows the SEC separation of Wyodak recycle solvent. The separation pattern of various chemical species and chemical groups are assigned based on reported[4-15] as well as unreported studies. When valves V_2 and V_3 (Figure 2) are engaged, the SEC effluents are collected in the sample loops of V_3 at specific intervals. The refractive index detector output shows the effect of such fraction collections as negative peaks (Figure 4).

GC Analysis of SEC Fractions of Wyodak Recycle Solvent

Sixteen SEC fractions of 100 μl each were collected from the Wyodak recycle solvent (Figure 4) at 0.5 min intervals. Each fraction was analyzed by injecting 0.1 μl into the GC, which used the flame ionization detector (FID). The first three fractions and the last fraction showed the GC of the solvent; so the GC of those fractions are not included in Figure 5. The first GC (Figure 5.1) corresponds to the GC of fraction #4 and the last GC (Figure 5.12) is that of fraction #15. By increasing the GC oven temperature the larger alkanes in fraction #2 and #3 can be detected. A shorter column enhances the FID response as these heavy alkanes accumulate on the column probably due to irreversible adsorption or decomposition.

Identification of Species in SEC Fractions of Wyodak Recycle Solvent

Figure 5.1 shows the GC of fraction #4. It shows alkanes ranging from C_{25} to C_{30}. It is quite possible that the fraction may contain higher alkanes which are not detected due to the GC-oven temperature limit. The peaks are identified from the MS fragmentation pattern. Fraction #5 is collected after a 0.5 minute interval and its GC (Figure 5.2) shows alkanes ranging from C_{19} to C_{30}. This fraction has lower alkanes (C_{19}-C_{24}) in larger proportions in addition to smaller amounts of alkanes (C_{25}-C_{30}) which were detected earlier in fraction #4.

When SEC columns are overloaded the peaks tail to longer retention time or volume. In the case of other modes of chromatography, such as gas chromatography, the overloading causes a shift in the retention time toward lower values, and peaks skew toward lower retention times. A "cascading effect" occurs due to the decreasing number of active sites seen by the sample as the number of the same sample molecules, which temporarily block the active sites, increases. The reverse phenomenon is true in the case of SEC where a larger sample size causes peak spreading and the sample to elute over a slightly longer retention time period.

The peak due to C_{27} is larger relatively to other alkanes in Figure 5.1 and 5.2. Our experience with fossil fuels indicates that the straight chain alkanes (n-alkanes) have a normal distribution over a wide molecular weight range. Even in other reported works on hydrocarbon fuels an unusual enhancement of a particular straight chain alkane is not observed. The alkane fractions always contain branched alkanes such as pristane, phytane, and hopane, and some of them are called biological markers. It is quite possible that the C_{27} peak could be due to some branched alkanes co-eluting with n-C_{27}.

The GC of fraction #6 is shown in Figure 5.3, which contains mostly alkanes in the range of C_{15}-C_{24} and small amounts of C_{14} and C_{25}-C_{29}. The fraction #6 was collected 0.5 minute after fraction #5 and one minute after fraction #4. If fraction

#5 had not been collected, the GC of fraction #4 and #6 which were one minute apart could have been used to qualitatively, but not necessarily qualitatively, determine all of the species. Fraction #5 has species from both fractions #4 and #6. The peak width of species eluting at these retention times is about one minute. Hence SEC fraction collection at one min (one ml) intervals would have contained all the species with less overlapping and analysis time could have been reduced to half. A short peak immediately after C_{17} is pristane (trimethylhexadecane). The short peaks that appear between the n-alkane peaks appear to be isoalkanes or branched alkanes. The baseline appears to be shifted slightly upward compared to the baseline of the GC's in Figure 5.1 and 5.2. This is probably due to a large number of possible isomers of phenolic species. GC of fraction #7 (Figure 5.4) has alkanes as small as C_{12}. The ratio of peak heights of pristane to C_{17} increases in the GC of this fraction compared to previous fractions as expected from its shorter linear molecular size. The smaller peaks between n-alkane peaks are alkylated phenols and branched alkanes.

Fraction #8 (Figure 5.5) is mostly alkylated phenols and indanols with a trace amount of smaller alkanes. The baseline shift is due to the co-elution of several large phenolic species in many isomeric forms. Fraction #9 (Figure 5.6) does not contain any alkanes. The ratio of the o-cresols to m-, p-cresols increases from fraction #8 to #9. Both m-cresol and p-cresol are structurally longer than o-cresol. Some long aromatic species such as biphenyls also appear in this fraction. Compared to fraction #8, the phenols in fraction #9 are of shorter size while the peaks appearing at long GC retention times are aromatics. It is safe to say that phenols appear before 16 minutes of GC retention time followed by aromatics after 16 minutes. The GC of fraction #10 is shown in Figure 5.7. Light phenols including xylanols and cresols present in this fraction are separated on the GC before a retention time of 8 minutes. The species appearing after 8 minutes are aromatics, mostly with alkyl side chains.

Fraction #11, whose GC is in Figure 5.8, contains phenol, which appears at 3 minutes. Phenol is the only phenolic in Fraction 11. Almost all possible isomers of one and two ring aromatics with alkyl side chains (propyl or shorter) are detected in this fraction. Since the number of species are higher, co-elutions of two or more components at one GC retention time is observed. The mass spectral fragmentation pattern can be used to assign the molecular formula and general structural nature. The identification of isomers is very difficult in a number of cases. The NBS Mass Spectral Data Base has only a fraction of the needed standard reference spectra to identify the species in this fraction. Most of the identification has been assigned based on the fragmentation patterns and boiling points derived from the GC retention times. Fraction #12 as shown in Figure 5.9 has overlapping from two types of aromatics - alkylated aromatics and polycyclic aromatics. Fraction #13 contains aromatics with slight alkylation and the ring numbers increase as shown in Figure 5.10. Both fractions #14 and #15 (Figure 5.11, 5.12) contain only multi-ring aromatics with few alkyl side chains. One exception to the rule that SEC separates species in decreasing order of linear molecular size is that condensed ring aromatics tend to remain in the column longer. Some polycyclic aromatics such as pyrene and coronene are eluted from the gel column only after napthalene although they are much larger. More pyrene is in Fraction #15 than in Fraction #14 but the reverse is true for anthracene which appears before naphthalene.

Effect of Solvent-Solute Interaction on SEC

The separation of chemical species by size exclusion chromatography is more reproducible than any other types of chromatography. Once the SEC columns, the mobile phase (most often a pure solvent like THF or toluene), and the flow rate are selected, the retention volume (or retention time assuming the flow rate does not change) is primarily a function of linear molecular size, which can be obtained from the valence bond structure if the compound is known.

Effect of Gel-Solute Interaction on SEC

If the molecules have a tendency to interact with the packing material of the column, molecules may elute at longer retention volume. In the case of PL gel columns which are packed with a gel formed by the co-polymerization of styrene and divinyl benzene, the aromatic species have a tendency to stay on the column slightly longer than expected from their linear molecular sizes. The SEC elution pattern shows that the aromatics appear to be smaller than similar structured cycloalkanes. Among similar aromatics such as benzene, naphthalene, and anthracene, the elution volume is in the decreasing order of linear molecular sizes (i.e. anthracene is followed by naphthalene and then benzene elutes last). In the case of polycyclic aromatics where three or more rings are attached to a single ring as in pyrene and coronene, the elution time increases as the number of rings increases. Pyrene has a retention time longer than that of anthracene. Coronene is eluted only after pyrene. The additional alkyl side-chain causes the molecules to elute sooner, as expected from the resulting linear size increase due to alkyl side-chains.

Probable Molecular Structure Based on SEC

Although the mechanism of SEC separation is controlled by linear molecular size as well as other parameters, the separation pattern is very reproducible. Considering all the molecular parameters responsible for the size exclusion chromatographic separation pattern and the known separation patterns of a number of compounds, it is possible to predict the retention volume of a compound of known structure. Based on the same principle the retention volume gives information on the structure of the molecule.

The role of size exclusion chromatography is the separation of rather complex coal liquids into simpler fractions. The retention volume can be used to help identify the chemical structure where GC-MS is unable to identify its possible structure. For example biphenyl and dihydroacenaphthene have the same molecular formula as well as similar mass spectral fragmentation patterns. Coal liquids contain both species. The one which appears first (lower SEC retention volume) is biphenyl (GC ret. time ≈ 17 min. in Figure 5.6). Dihydroacenaphthene appears later at longer SEC retention volume and is identified in Figure 5.12 at GC retention time of 13 minutes. The former has a longer structure compared to the latter.

Sample Spreading

This phenomenon is quite apparent from Figure 2.5. Since the 100 μl fractions are collected at 0.5 μl volume intervals and the species have about 1 μl peak width, each species is detected in two or more consecutive fractions. The fractions at the lower retention volumes spread less compared to those at the higher retention volumes, as illustrated by examining the spreading of $C_{25}H_{52}$ and phenanthrene. The component n-$C_{25}H_{52}$ is detected in three SEC fractions with a maximum concentration in the second fraction (Figure 5.1, 5.2, 5.3). Phenanthrene is detected in the last five fractions (Figures 5.8, 5.9, 5.10, 5.11, 5.12). The examination of any parti-

cular species shows that they are spread over three or more fractions and the range of spreading (a measure of peak width) increases with retention volume.

It is quite evident that the analysis of small fractions at retention volume intervals of 0.5 ml or even 1 ml does not miss any major or minor species. Almost all species at detectable levels are identified.

Quantitative Analysis by SEC-GC-MS

The quantitative estimation of species by SEC-GC-MS technique requires a mathematical solution. Two types of approaches for the quantitative estimation can be envisioned. One is for the estimation of one or more selected species of interest. The second approach is based on grouping of various species in coal liquids into a few chemical lumps and estimating the quantity of these lumps by using the data derived from the analysis technique.

When a particular component eluting at a certain retention volume is to be estimated, this approach can be outlined as follows. Since SEC is extremely reproducible, the peak shape, peak width and peak height are dependent on the amount of the species in the sample volume injected, sample volume and retention time. From these factors the SEC peaks can be simulated or elution pattern of any species within the separation range can be plotted as a function of mass vs. retention volume. The analysis data supplies the concentration of this particular species over two or more 0.5 ml intervals. A match-up computer program has to be developed so that it can pick up the peak shape and concentration based on three or four data points at known intervals.

The second approach towards quantitative analysis is based on dividing the coal liquid into distinct fractions containing similar chemical species as is illustrated in Figure 3. This type of chemical lumping gives more useful information on coal liquefaction reactions and on kinetic models of coal liquefaction processes.

It is a fact that coal liquids are composed of thousands or maybe millions of chemical compounds. Classifying them into a few meaningful groups of compounds can be a suitable procedure to evaluate coal liquid composition. Currently at least two types of classification approaches have been used. One is based on physical separation by appropriate combination of physical and chemical methods. The second approach is based on estimating functional groups or functionalities in a coal liquid by sophisticated instrumentation such as solid state NMR and FTIR. By the first methodology coal liquid is separated into fractions such as oils (pentane soluble) asphaltenes (pentane insolubles but benzene solubles) and preasphaltenes (pyridene soluble but insoluble in benzene and pentane) where no clean separation or estimation is achieved. By the second type of methodology more cumulative data is achieved on functional groups. This methodology has the disadvantage of looking at a compound with more than one functional group. The amount of each group is estimated as separate moieties and computed separately. The alkyl chains attached to an aromatic ring, which also has phenolic groups, is very different from saturated hydrocarbons such as normal paraffins but they are classified together in this approach.

Overlapping of Species in SEC Fractions

When SEC-GC is used in its automated version for coal liquid analysis, 0.1 μl fractions of SEC effluents are analyzed by GC to produce simpler gas chromatograms. Some of these gas chromatograms, for example the GCs of longer alkanes, are composed of chemically similar components. The flame ionization detector (FID) response

factor, based on mass, is essentially the same for these larger alkanes. The total area counts of such gas chromatograms excluding solvent peak which represents t sample volume (0.1μl), multiplied by the response factor will give the mass o alkanes in the SEC fraction analyzed. Certain SEC fractions are composed of two or more different chemical species due to the overlapping effect of similar size species. For example, the low boiling point alkanes are mixed with the high boiling point phenols where the linear molecular sizes of the species are similar. The alkanes appear at low retention times whereas phenols appear at longer retention times (Figure 2.5.5). In these cases the area counts have to be lumped into two groups, one for alkanes and another one for phenols. Each of these area counts multiplied by the corresponding FID response factor indicate the amount of alkanes or phenols present in the 0.1μl SEC fractions. All of the sixteen or more GCs of selected SEC 0.1μl fractions of coal liquids or recycle solvents are individually analyzed for various "lumped chemical" species in the fractions. Coal liquid samples can be separated by distillation and estimated for the nonvolatile content. The SEC of nonvolatiles and volatiles are reconstructed to show both in the same SEC output. These data along with SEC-GC data are used to reconstruct the SEC of Wyodak coal-derived recycle solvent as shown in Figure 2.3.

SEC vs. Distillation

The chemical lumping pattern shown in Figure 2.3 is very similar to the plotting of distillation temperatures vs. composition, a technique commonly used in petroleum refining to simulate the composition of distillate as a function of temperature. Since SEC includes nonvolatiles, information on their size distribution is also shown. In each chemical lump the molecular weight decreases as SEC retention volume increases. The individual chemical lump has a SEC separation pattern similar to a distillation temperature vs. molecular weight plot, a technique used in petroleum refining to illustrate the composition of various distillation cuts.

Chemical Lumping

The species not been identified as one of the major chemical lumps such as alkanes, phenols and aromatics are lumped together as unidentified. However, the species in this lump include saturated and unsaturated cycloalkanes with or without side chains, which resemble the naphthenes, a petroleum refinery product group. A number of well known species in coal liquid are not mentioned in this lumping scheme, such as heterocyclic compounds with sulfur, nitrogen or oxygen as the heteroatom, and other heteroatom-containing species. Some of these compounds appear with aromatics (e.g. thiophenes, quinolines) and with phenols (e.g. aromatic amines), and most of them are lumped with the unidentified species lump.

One exception to the rule that SEC separates species in the decreasing order of linear molecular size, is that condensed ring aromatics appear to adhere to the column longer so that some polycyclic aromatics such as pyrene and coronene are eluted from the gel column only after naphthalene, although their molecular sizes are much larger. More pyrene is in Fraction #15 than in Fraction #14, but the reverse is true for anthracene.

Variability in the Distribution of Chemical Species in Low Rank Coal Conversion Product

Almost all the samples from most successful low-rank coal liquefaction experiments were analyzed by SEC-GC-MS technique and MS raw data were stored on about 200

5¼"-floppy disks. Although the liquefaction experients used mostly the conditions used in the pilot plant at the UNDERC, some experiments were conducted under different conditions and solvents including water under supercritical conditions. Initially the SEC-GC-MS data on the recycle solvents and anthracene oil were very carefully studied and GC peaks were identified and the components in various fractions were tabulated. Certain SEC fractions of the recycle solvents were analyzed by the GC-MS several times varying samples sizes to identify any minor components. Since the coal liquids contain many components, the mass spectral data of some compounds were not available in the library. A very careful evaluation of the MS fragmentation pattern was necessary to establish the identity of the compound. Identification of unknowns needed better MS fragmentation pattern and time. Once a compound was identified, the information was continously used for identifying trace amounts based on masses of the major fragments.

Distribution of Alkanes

One of the major results of SEC-GC-MS studies is the discovery of an orderly pattern, by which various isomers and homologs of similar chemical species exist in coal liquids. For example almost any direct coal liquefaction process produces very similar species, which differ from each other by size and extent of isomerization but with an orderly distribution pattern. Alkanes ranging from $C_{12}H_{26}$ and $C_{44}H_{80}$ are detected in almost any coal liquid. Most of these are straight chain alkanes showing an orderly continuous pattern. Neither is a particular n-alkane almost absent nor is it present in a disproportionate amount. Exceptions exist for some branched alkanes such as pristane, phytane, and hopane. These species are also called biomarkers and their concentration varies depending on the sample. The straight chain hydrocarbons, mainly the alkanes, are observed as sharp GC peaks in the GC of certain SEC fractions of lignite-derived liquids. The corresponding SEC-fractions of the anthracene oil show a "hump" in the GC. It appears that the pyrolytic conditions used in a coking oven are destroying or converting most of the straight-chain alkane species into numerous isomeric hydrocarbons. The MS fragmentation patterns of the GC "hump", are similar to that of alkanes.

Distribution of Phenols

Phenols are a major chemical lump present in coal liquids. Phenols have basically one or more aromatic ring structures with alkyl substituents. Methyl, ethyl and propyl are the most common alkyl substituents. The smallest species is the one with a hydroxyl group attached to a benzene ring. Addition of a methyl group produces three isomers - o-, m-, and p-cresols. It appears that all three are present in about the same proportion. The number of possible isomers increases as the possible number and size of alkyl substituents increases. It is expected that higher degree of alkylation can produce larger molecules in a larger number of isomeric forms, separation of which is rather difficult even by high resolution GC methods. This could be the reason why a shift in the GC baseline is observed for the SEC phenolic fractions rather than resolved peaks. Since these shifts are quite reproducible and real, it can be assumed that these "bumps" are due to a large number of components eluting continuously without resolution. Their SEC retention time suggests that they are probably phenols. The gas chromatographers who are used to fewer sharp peaks from capillary GC may prefer to resolve them. Sometimes derivatization techniques are used to obtain sharper well resolved peaks. As a matter of fact unresolved "bumps" are telling a story. Too many isomers of close molecular weight or boiling point are eluting without resolution at close retention times. Phenols do

show peak tailing in most GC separation conditions. But currently available capillary columns do not show tailing as a serious problem. Peak tailing is expected to decrease as the degree of alkylation increases. Peak tailing for cresol is less than that for phenol. It is much improved for xylenols. The derivatization of phenols prior to GC separation may produce fewer well-resolved peaks but at the expense of losing some components.

Distribution of Aromatics

The number of isomers of alkylated aromatics is enormous. Lower members of alkylated benzenes such as xylenes are well-resolved and detected by FID and MS. Increased alkylation causes an increase in the number of isomers. In the case of both alkylated phenols and aromatics various isomers exist in a continuous pattern. The less alkylation gives few well-resolved isomers. The more alkylation gives a large number of isomers but in smaller concentrations.

We have observed a striking similarity in the identity of chemical species found in different types of coal liquids such as anthracene oil (A04), recycle solvents and the lignite-derived liquids from our liquefaction experiments as they are separated by SEC-GC and identified by MS. The polycyclic aromatic species which are characteristic of coking oven products from coal, such as anthracene oil and creosote oil are found in all lignite-derived liquids from our liquefaction experiments, including the liquid obtained by the dissolution of lignite in water under super critical conditions. Their relative concentration was found to increase varying with the severity which is used to produce the coal liquid. Anthracene oil has the highest concentration of polycyclic aromatics and the lignite liquefied in supercritical water has the lowest. The hydroxy aromatics, also known as alkylated phenols, which are produced under lignite liquefaction experiments, are not major components in anthracene oil.

CONCLUSIONS

The coal conversion products are compounds of at least two types of species. "a" The species which are released from the coal matrix and stabilized by the coal liquefaction process. This type of species retains most of its original structural characteristics. Most of the alkanes and alkylated phenols belong to this group. "b" The species which are characteristic of high temperature reactions. The polycyclic aromatics such as phenanthrene and pyrenes are products of high temperature chemistry. Coke ovens and even wood burning fireplaces produce these products. The liquefaction environment can cause additions of alkyl side chains to these species although higher temperature causes the dealkylation of these products. Some of these species may be existing in coal but in lower concentrations.

The coal liquefaction process generates both types of compounds. Lower temperatures favor type "a" compounds while higher temperatures tend to produce more of type "b" compounds. The SEC-GC-MS analysis data on a number of coal liquids produced under varying conditions from different coals and liquefaction solvents indicate that liquefaction temperatures below 400°C produce very little type "b" compounds although they are not totally absent. The alkylated aromatics such as alkyl indans and benzenes appear to be generated from the original coal structure although these compounds could be catatytically generated at these temperatures even from simple starting materials such as CO and H_2. Several low temperature reactions products from coal support the existence of one or two ring aromatics with other substituents, especially in low rank coals.

ACKNOWLEDGEMENTS

The financial support of the U.S. Department of Energy, (project Number DE-AC18-83FC10601), Texas A&M University Center for Energy and Mineral Resources and Texas Engineering Experiment Station is gratefully acknowledged. The Energy Research Center at University of North Dakota furnished samples for the study.

REFERENCES

1. Hendrickson, J.G., "Molecular Size Analysis Using Gel Permeation Chromatography", *Anal. Chem.*, 1968, *40*, 49.
2. Majors, R.E.J., "Recent Advances In HPLC Packing and Columns", *Chromatog. Sci.*, 1980, *18*, 488.
3. Cazes, J. and D.R. Gaskill, "Gel-permeation Chromatographic Observation of Solvent-solute Interaction of Low-molecular Weight Compounds", *Sep. Sci.*, 1969 4, 15.
4. Krishen, A. and R.G. Tucker, "Gel-permeation Chromatography of Low Molecular Weight Materials With High Efficiency Columns", *Anal. Chem.*, 1977 *49*, 898.
5. Philip, C.V., Anthony, R.G., "Dissolution of Texas Lignite in Tetralin", *Fuel Processing Technology*, 1980, *3*, p. 285.
6. Zingaro, R.A., Philip, C.V., Anthony, R.G., Vindiola, A., "Liquid Sulphur Dioxide - A Reagent for the Separation of Coal Liquids", *Fuel Processing Technology*, 1981, *4*, 169.
7. Philip, C.V., Zingaro, R.A., Anthony, R.G., "Liquid Sulfur Dioxide - as an Agent for Upgrading Coal Liquid", "Upgrading of Coal Liquids," Ed. Sullivan, R.F., *ACS Symposium Series No. 156*, 1981;p.239.
8. Philip, C.V., Anthony, R.G., "Chemistry of Texas Lignite Liquefaction in a Hydrogen-donor Solvent System", *Fuel*, 1982, *61*, 351.
9. Philip, C.V., Anthony, R.G., "Separation of Coal-derived Liquids by Gel Permeation Chromatography", *Fuel*, 1982, *61*, 357.
10. Philip, C.V. and Anthony, R.G., "Analysis of Petroleum Crude and Distillates by Gel Permeation Chromatography (GPC)", "Size Exclusion Chromatography", Ed. Prouder, T., *ACS Symp. Series*, 1984, *245*, 257.
11. Philip, C.V., Anthony, R.G. and Cui, Z.D., "Structure and Reactivity of Texas Lignite", "Chemistry of Low-Rank Coals, Ed. Schobert, H.H., *ACS Symp. Series*, 1984, *264*, 287.
12. Philip, C.V., Bullin, J.A. and Anthony, R.G., "GPC Characterization for Assessing Compatibility Problems with Heavy Fuel Oils", *Fuel Processing Technology*, 1984, *9*, 189.
13. Sheu, Y.H.E., Philip, C.V., Anthony, R.G. and Soltes, E.J., "Separation of Functionalities in Pyrolytic Tas by Gel Permeation Chromatography", *Chromatographic Science*, 1984, *22*, 497.
14. Philip, C.V. and Anthony, R.G. "Separation of Coal Liquids by Size Exclusion Chromatography - Gas Chromatography (SEC-GC)", *Am. Chem. Soc. Div. Fuel Chem. Preprints*, 1985, *30*, (1), 147.
15. Philip, C.V. and Anthony, R.G. "Characterization of chemical Species in Coal Liquids Using Automated Size Exclusion Chromatography - Gas Chromatography (SEC-GC)", *Am. Chem. Soc. Div. Fuel. Chem. Preprints*, 1985, *30* (4), 58.

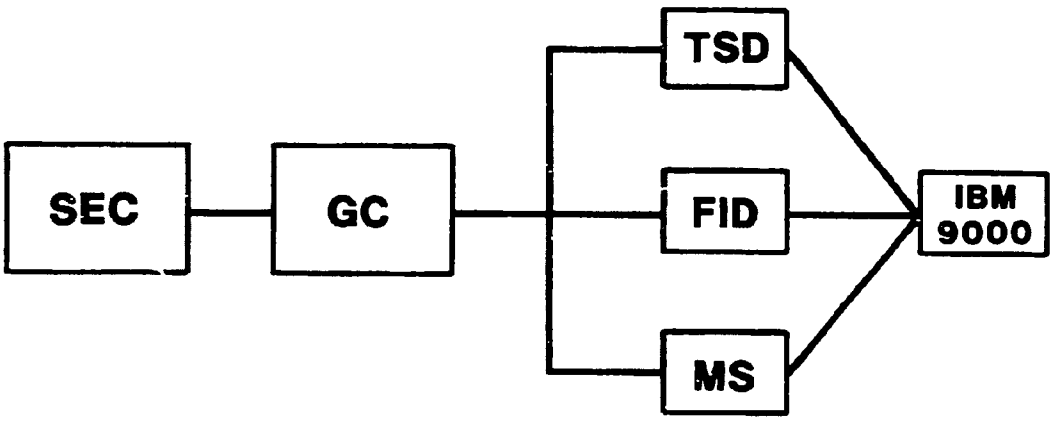

Figure 1. SEC-GC-MS instrumentation.

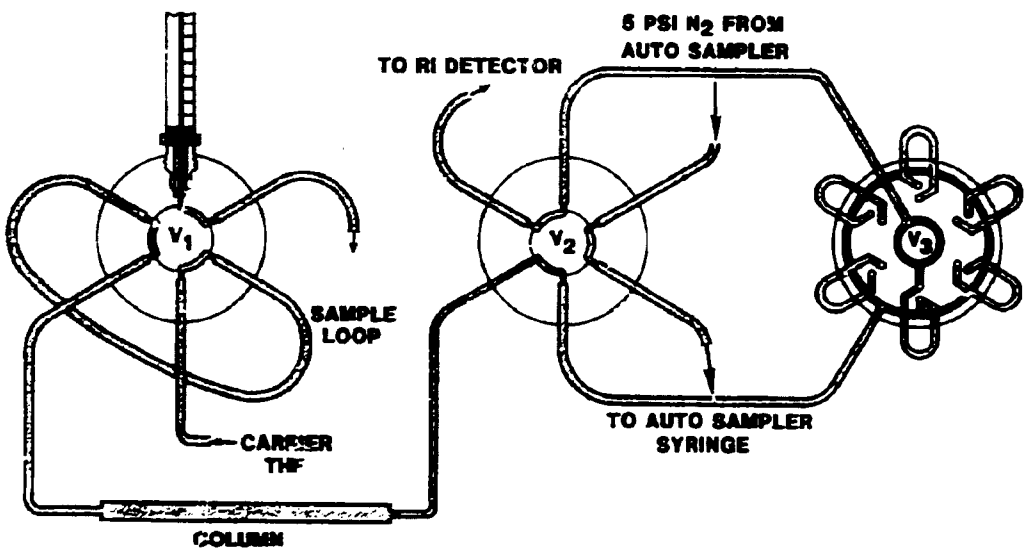

Figure 2. SEC-GC interface Note: V_3 has sixteen sample loops instead of six shown.

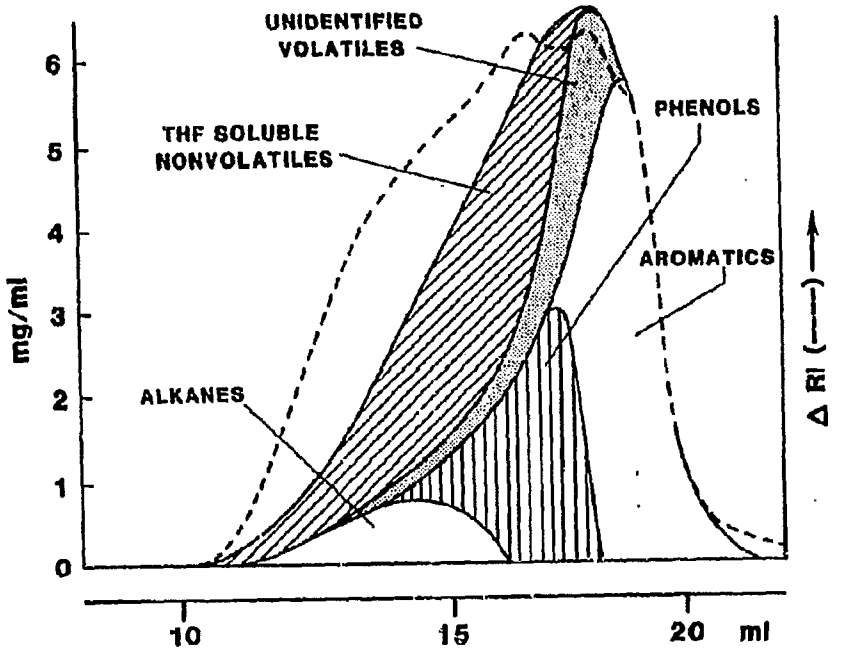

Figure 3. SEC of Wyodak recycle solvent.

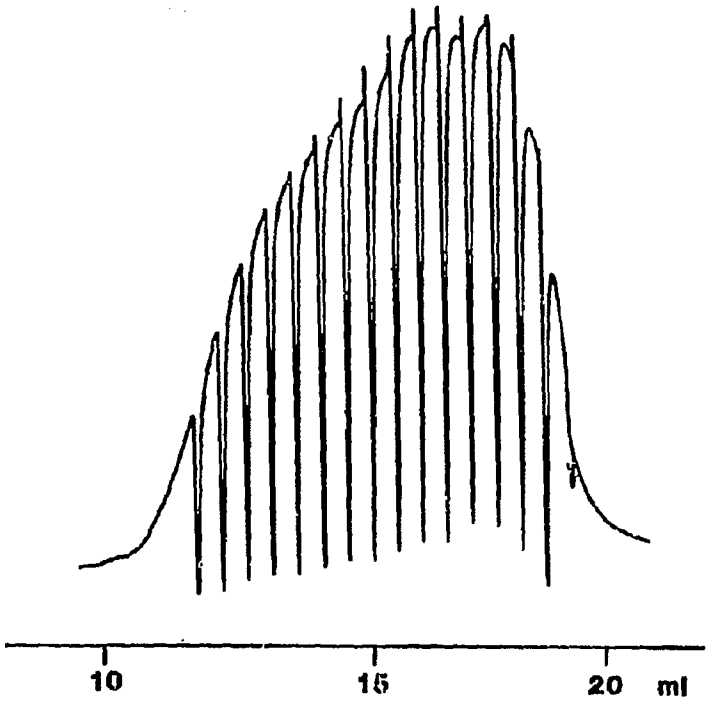

Figure 4. 100 µl fractions collected by SEC-GC interface (on-line).

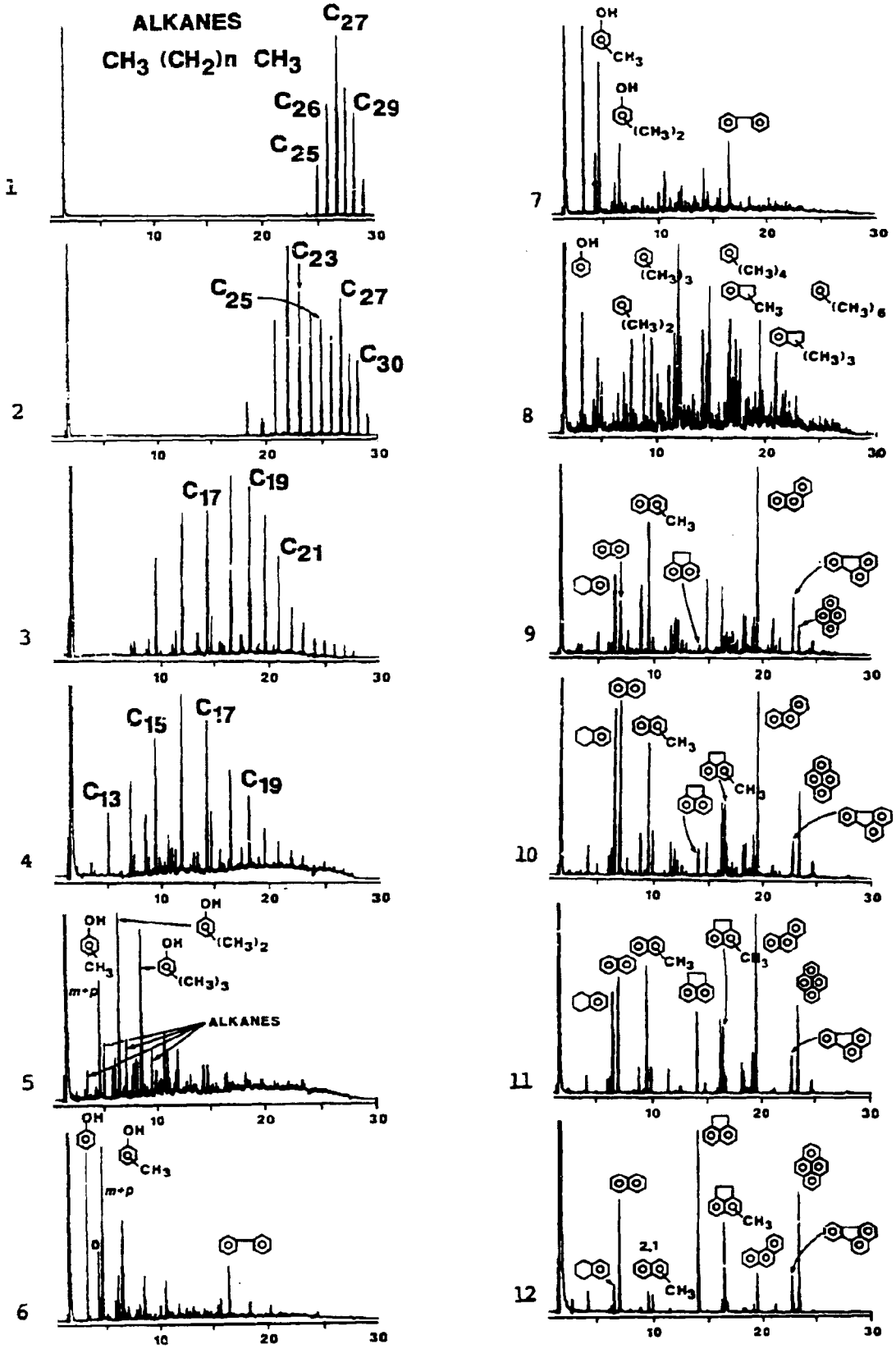

Figure 5. SEC-GC-MS of Wyodak re-cycle solvent.

CATALYTIC STEAM GASIFICATION OF LIGNITE CHAR

by

J.R. Kim, T.W. Kwon, S.D. Kim and W.H. Park*
Department of Chemical Engineering
*Division of Chemical Engineering and Polymer Technology
Korea Advanced Institute of Science and Technology
Seoul, 131 Korea

ABSTRACT

Reaction kinetics of catalytic steam gasification of Australian lignite chars having mean particle size of 0.3mm have been studied in a 5.5 cm-ID x 100 cm high thermobalance reactor.

The sample char has been prepared from the pyrolyzing the Australian lignite ($\%C^{daf}$= 75.7) at 700°C under the atmospheric pressure in a muffle furnace. Three different catalysts (K_2CO_3, Na_2CO_3, Li_2CO_3) and its mixture [$(Na, K)_2CO_3$] were impregnated into the chars in order to determine the effects of catalyst type and amount of catalyst loading (1-5 wt. %) at different reaction temperatures (700-800°C) on the rate of steam gasification. The mass conversion of the char has been determined by the ratio of the gasified carbon to the initial carbon content in the char.

The non-catalytic steam gasification reactions have been well represented by the unreacted shrinking core model in which chemical reaction is the rate controlling step. The reaction orders with respect to carbon were found to be 2/3 in the case of non-catalytic and Li_2CO_3-catalytic reactions. Whereas, the reaction with K_2CO_3 catalyst revealed a zeroth reaction order. In the cases of Na_2CO_3 and mixed $(Na,K)_2CO_3$ catalytic steam gasification reactions, the reaction order was found to be zero and the reaction rate constant can not be described as an unique value. The reaction rate increased with the reaction temperature and the amount of catalyst loading.

Under the same experimental conditions with 3 wt% catalyst loading, the catalytic activities were found to be ranked as Na_2CO_3> mixed $(Na,K)_2CO_3$> K_2CO_3> Li_2CO_3.

Reactivity enhancement factors for the mixed $(Na,K)_2CO_3$ catalysts were found to be the arithmetic mean values of the both Na_2CO_3 and K_2CO_3 catalysts. Activation energies and frequency factors of the catalytic reactions were smaller than those of the comparable non-catalytic steam gasification reactions which may give an evidence of the compensate effect in the reaction.

INTRODUCTION

Numerous investigations have been focused on the role of catalysts in the coal gasification reactions in order to enhance the reactivity under the low reaction temperature.

For the production of methane in a coal gasifier, the following reaction is considered because of its thermoneutral characteristics [1]:

$$2C + 2H_2O = CH_4 + CO_2 \quad (1)$$

The overall reaction is a combination of the exothermic water-gas shift and methanation reactions and the endothermic carbon gasification reaction. These three reactions are slow in the absence of catalyst, however,

the rates may be increased up to a certain level by increasing reaction pressure. But, equilibrium conversion is reduced with increasing pressure. The rate of carbon gasification with steam increases sharply with increase in temperature, however, increasing temperature severely limits the equilibrium production of methane. Therefore, the solution would be to operate the gasifier at an intermediate temperature around 1000 K with minimum equilibrium problems and to utilize catalysts to accelerate reaction rates. In the Exxon gasifier, K_2CO_3 as a catalyst has been employed for methane production as shown in reaction (1).

It has been known that the alkali, alkaline earth, and transition metals inherently present in the mineral matters of the raw coal or artificially added by physical mixing or impregnation are most effective catalysts. Active catalysts appear to participate in the gasification reaction by undergoing chemical or electronic interactions or both with the carbonaceous substrate [2], however, the details of these interactions are not yet clearly understood. Therefore, a number of studies have been carried out in order to determine the effects of catalysts on the gasification rate and the reaction mechanisms.

In this study, reaction kinetics of catalytic steam gasification of Australian lignite char have been investigated in a 5.5 cm-ID x 1 m high thermobalance reactor.

EXPERIMENTAL

The char samples used in char-steam gasification have been prepared by heating an Australian lignite ($\%C^{daf}$ = 75.7%) to 700°C at a heating rate of 6°C/min and charred at 700°C for 2 h. The proximate and ash analysis of the char sample are shown in Table 1.

Table 1. Analysis of char sample

Proximate analysis (dry basis, wt.%)		Ash analysis (wt.%)					
V.M.*	7.3	SiO_2	14.1	CaO	8.19	P_2O_5	0.04
ash	2.9	Al_2O_3	11.79	MgO	13.91	SO_3	10.30
F.C.**	89.8	Fe_2O_3	27.38	Na_2O	3.91	residue	9.26
		TiO_2	0.45	K_2O	0.67		

*V.M.: volatile matter, **F.C.: fixed carbon

Impregnated char sample was prepared from the char having particle size of −45 + 70 mesh by soaking it into the aqueous solution of alkali metal carbonate (Li_2CO_3, Na_2CO_3, and K_2CO_3) and consequent drying process.

Char gasification has been carried out in a 5.5 cm-ID x 1.0 m high stainless steel thermobalance [3] in which a sample of char was placed in a stainless steel wire mesh basket by means of a winch assembly for suspension of the sample which was connected to a electronic balance (Chyo model PD2-300W). The reactor was heated to a desirable reaction temperature under a stream of nitrogen. The initial weight loss may come from the evolution of moisture and the residual volatile matter present in the sample. When the system reached an isothermal steady state, a stream of superheated steam was instantaneously admitted to the reactor at a mass flow rate of 4 g/min. Fractional conversion of char sample was followed by recording the weight loss of the sample with time.

In this study, the effects of catalyst type (Li_2CO_3, Na_2CO_3, K_2CO_3, and mixed $(Na,K)_2CO_3$) and the amount of catalyst loading (0 - 5 wt.%) at

different reaction temperature (700 - 800°C) on the rate of steam gasification have been determined.

RESULTS AND DISCUSSION

1. Reaction Order and Activation Energy

The carbon conversion in steam gasification reaction, X, is defined as:

$$X = (W_o - W)/(W_o - W_\infty) \quad (2)$$

where W_o is the initial weight of char, W_∞ is the weight of ash in the sample char measured by complete ignition of the sample residue, and W is the sample weight at a given time.

For non-catalytic steam gasification of the lignite char, the fractions of converted carbon from 700 to 800°C are shown in Fig. 1. The time required for 50% conversion were found to be 140, 42, and 19 min at the temperature of 700, 750, and 800°C, respectively. It can be seen that the conversion rate is primarily affected by the reaction temperature.

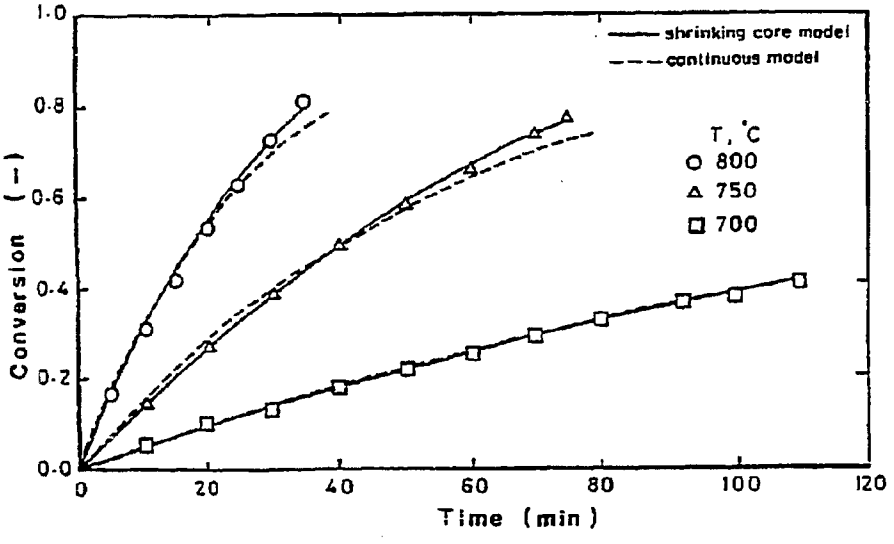

Fig. 1. Carbon conversion with time for non-catalytic steam gasification

The reaction rate, r, is defined as:

$$r = dX/dt = K(1 - X)^n \quad (3)$$

where K, t, and n are the reaction rate constant, time, and order of reaction, respectively.

Equation (3) is consistent with the volumetric reaction model [4] when n is unity and the unreacted shrinking-core model in the chemical reaction control regime [5] in which n is 2/3. It can be seen both models fit the experimental data well at low temperature, and the predicted values from the volumetric reaction model exhibited larger deviation than those from the shrinking-core model at the higher conversions and at higher temperatures.

The order of non-catalytic steam gasification reaction of the lignite char has been well represented by the unreacted shrinking-core model in which chemical reaction is the rate controlling step. The activation energy under the non-catalytic reaction was found to be 176.5 kJ/mol from the Arrhenius plot.

Fractional conversion of carbon in the non-catalytic and catalytic steam gasification of Australian lignite char with time at 750°C are shown in Fig. 2 in which straight line passing the origin was obtained up to 80% conversion for K_2CO_3 catalytic gasification reaction.

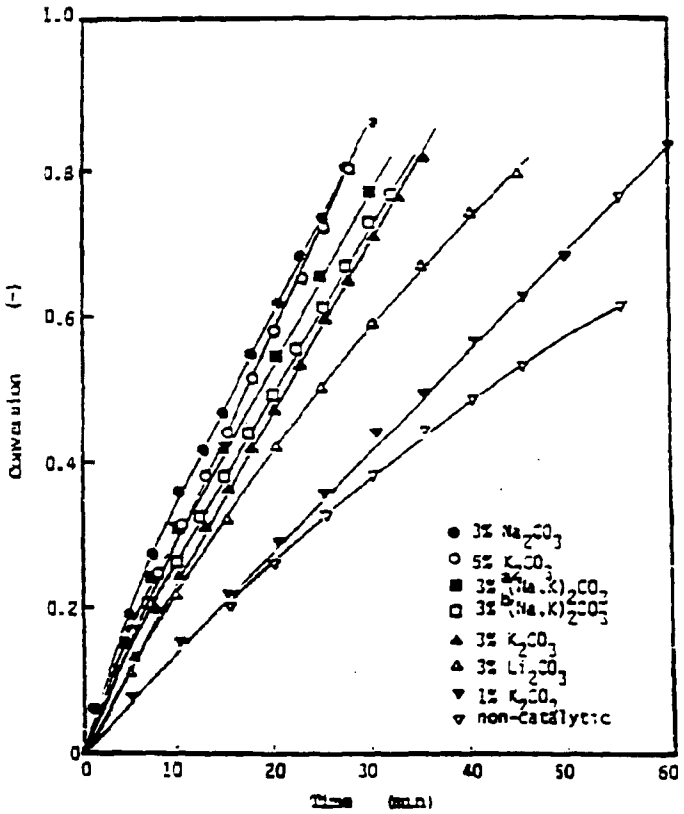

Fig. 2. Relation between X and t for non-catalytic and catalytic steam gasification at 750°C.
[a: mole ratio Na/K = 2; b: mole ratio Na/K = 1]

It can be seen that the reaction rate is irrelevant to the conversion and the order of reaction, n in Eq. (3) is zero as reported by Huhn et al. [6] and Miura et al. [7]. However, Juntgen and van Heek [8] and Kayembe and Pulsifer [9] have reported that n is 2/3 and 1.0, respectively.

Catalytic gasification using Na_2CO_3 exhibited uniquely high value of initial reactivity followed by constant reactivity with time. Thus a plot of conversion versus time for Na_2CO_3 gasification was combination of two straight lines having different slopes and the inflection point of conversion was found to vary with temperature. The reaction orders were found to be zero in Na_2CO_3 catalytic gasification and 2/3 in Li_2CO_3 catalytic gasification in the same manner of the non-catalytic gasification condition.

The existence of different n values for the type of catalysts can be explained by differences in the accessibility of the catalyzed carbon

atoms and mineral matters which may deactivate the amount of active catalyst by side reactions. The reaction order would be a function of the accessibility and the activity of the catalyzed carbon atoms during the course of conversion which is related to their mobility. The mobility of catalyst depends on the melting or boiling points, thus, it can be affected by the reaction temperature. With this regard, Juntgen and van Heek [8] reported that the reaction order is zero for the high-mobility catalyst and larger than zero order for the low-mobility catalyst.

2. Relative Catalytic Activities of Alkali Metal Carbonates

Relative catalytic activities of alkali metal carbonates vary with the physical and chemical properties of substrate carbon, amount of catalyst loading, and gasifying agent. In the catalytic steam gasification of the lignite char adding Li_2CO_3, Na_2CO_3, or K_2CO_3, the catalytic activities were found to be ranked as Na> K> Li under the same experimental conditions with 3 wt.% catalyst loading as shown in Fig. 2.

Relative activities of catalysts were found to vary with temperature. Activities of Li_2CO_3 increased noticeably with reaction temperature than comparable K_2CO_3, and the initial gasification reaction rate of the char with Li_2CO_3 at 800°C surpassed that of K_2CO_3 catalytic reaction. Relative activities of Na_2CO_3 was found to be lower at the higher temperature (750 - 800°C) than that of K_2CO_3 which may result from the higher deactivation of Na_2CO_3 at higher temperature than that of K_2CO_3.

The effectiveness of the catalysts is related to their mobility on the surface and the latter depends on the boiling point relative to the reaction temperature [8]. Since the boiling points of Li (1330°C) is much higher than K (760°C), K has larger activity than Li at lower temperature below the boiling point of K. Thus, activity of Li would be higher than K at high temperature may be due to the higher relative mobility of Li at the given higher temperature.

3. Reaction Characteristics of Mixed Catalysts

The steam gasification rate of the lignite char with the mixed catalyst of $(Na,K)_2CO_3$ is shown in Fig. 2. The catalytic activities and the reaction characteristics of the mixed catalyst exhibited the medium values of each single catalyst which is similar values of the previous study of coke-CO_2 gasification with mixed catalyst [11].

Considering the reaction characteristics with each catalyst of Na_2CO_3 and K_2CO_3, the high initial reactivity at large mole ratio of Na to K (2:1) is similar to the behavior of Na_2CO_3 catalyst, while the constant reactivity over the entire conversion range at smaller mole ratio of Na to K (1:1) is similar to the behavior of K_2CO_3 catalyst used.

Reactivity of the mixed catalyst steam gasification is defined as the initial reaction rate in terms of the mass ratio of each component of the mixed catalyst at the different reaction temperature as shown in Fig. 3.

As can be seen from the figure, the reactivity values of the mixed catalyst gasification were found to be the arithmetic mean values of both Na_2CO_3 and K_2CO_3 catalysts. This result can be interpreted by the vapor cycle reaction mechanism [2] which consists of reduction of alkali metal carbonate to alkali metal followed by the same oxidation cycle in both Na_2CO_3 and K_2CO_3 catalysts.

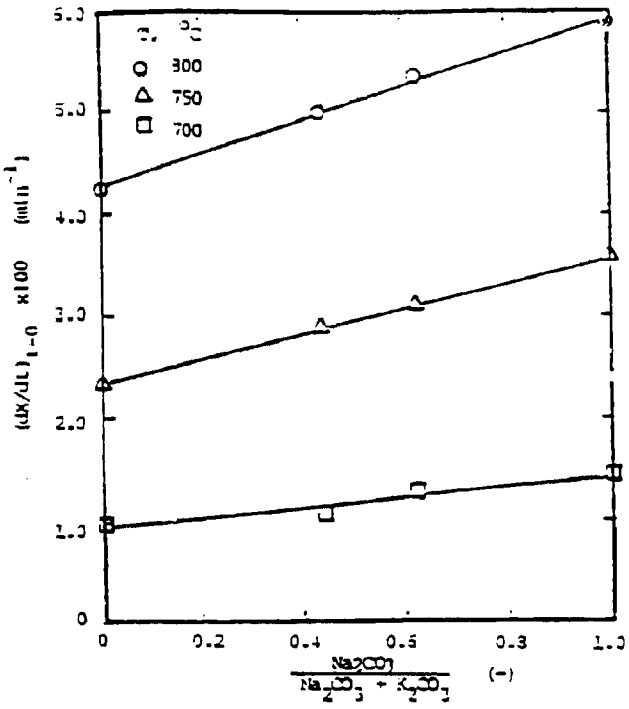

Fig. 3. Initial gasification rate of K_2CO_3, Na_2CO_3 and $(Na,K)CO_3$ mixed catalysts at various reaction temperature

4. Effect of Catalyst Loading on the Reaction Rate

As shown in Fig. 2, time required for 50% conversion were found to be 42, 30, 20 and 16 min for 0, 1, 3, and 5 wt.% K_2CO_3 loading, respectively. It may indicate the positive catalytic effect on the reaction rate, however, the initial reaction rate did not increase at low concentration of catalyst (1 wt.%). Apparent reaction rate constant in terms of K_2CO_3 loading, C_k, at various temperature are shown in Fig. 4 in which the rate constant increased linearly with K_2CO_3 loading as:

$$K = K_1 + K_2 C_k \tag{4}$$

where K_1 is the intercept of the straight line represented as Arrhenius equation;

$$K_1 = A \exp(-E_o/RT) \tag{5}$$

where A and E_o have been obtained from the experimental data and their resulting values are 9.15×10^6 min^{-1} and 175.9 kJ/mol, respectively. These values are consistent with those of non-catalytic steam gasification condition.

Activation energies obtained from the Arrhenius plot are shown in Fig. 5. As can be seen, the activation energies are 176.5, 148.0, 127.5 and 119.0 kJ/mol for 0, 1, 3 and 5 wt.% K_2CO_3 loading, respectively.

Relation between activation energy and K_2CO_3 loading is shown in Fig. 6 with the following expression as:

$$E = E^o + \beta \exp(-\gamma C_k) \tag{6}$$

where β and γ are the constants which were obtained from the exper-

imental data of the present and previous studies [6,10,12,13] using the non-linear regression. The resulting values exhibited three different patterns in proportion to β and γ values (Table 2).

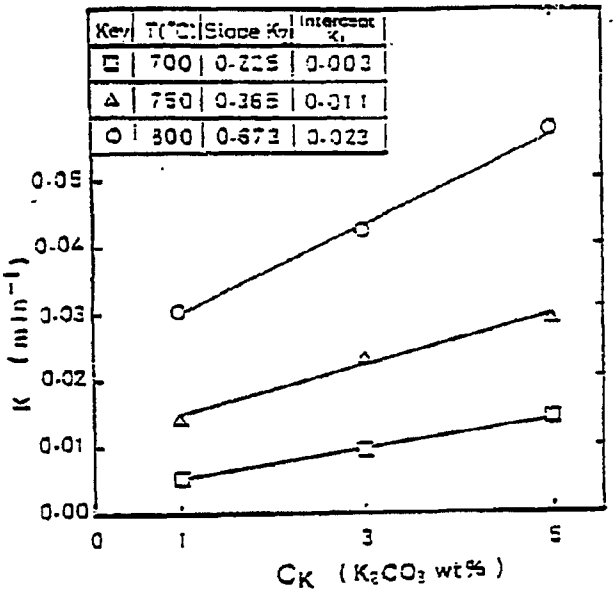

Fig. 4. Effect of catalyst loading and reaction temperature on gasification rate

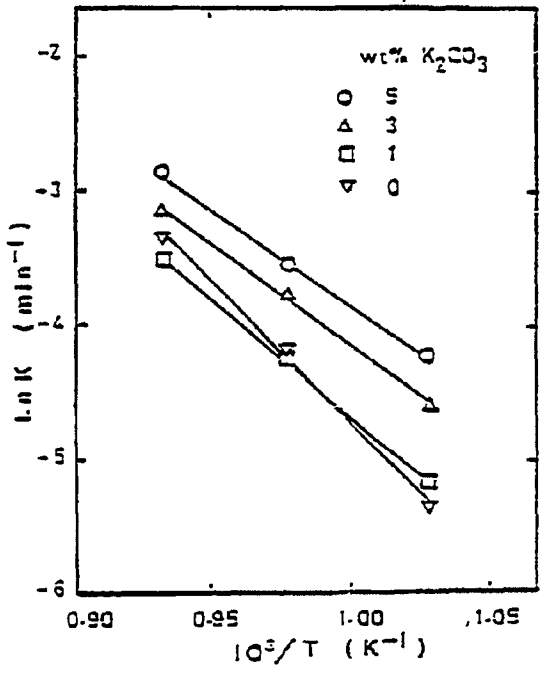

Fig. 5. Arrhenius plots for non-catalytic and catalytic char-H_2O reactions

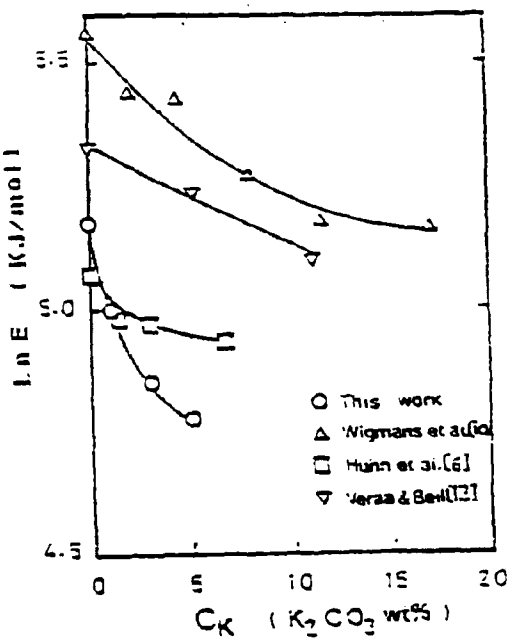

Fig. 6. Relation between the activation energy and the amount of K_2CO_3 loading

Table 2. Comparison of the constants of Eq. (6) with the literature values

Authors	Material	P_{H_2O}(KPa)	% K_2CO_3	E_o(KJ/mol)	E^o	β	γ
This work	lignite char	100	0 - 5	176.5	117.6	58.6	0.6
Wigmans et al.[10]	active carbon	2.6(in He)	0 - 17.1	260	144.5	120.0	0.1
Veraa and Bell [13]	sub-bituminous coal	50 (in He)	0 - 11.1	205.6	150	50.0	0.1
Chin et al.[12]	active carbon	85 (in Ar)	0 - 10.7	148	148	0	-
Huhn et al.[6]	coke	100	0 - 6.7	159	142	17.3	2.1

When the beta, β , is small, the activation energy, E, is almost constant and the value is identical to the non-catalytic gasification with the variation of catalyst loading [12]. Whereas, β and γ are large, the activation energy, E, decreased at the lower catalytic loading and it did not vary with the additional loading of K_2CO_3 as the data of Huhn et al. [6]. In addition, when β is large and γ is small, the activation energy decreased continuously with C_K as reported by Wigmans et al. [10] and Veraa and Bell [13]. The results of present study can be classified in this category having the resulting values of E^o, β and γ are 117.6, 58.6 and 0.6, respectively.

5. Compensation Effect

When catalytic reaction having the compensation effect, the frequency factor, A, and activation energy, E, change in the same direction with catalyst and tend to compensate each other in the Arrhenius equation.

Therefore, the rate constant, K, would be restricted [14].

These effects have been reported previously for the catalytic gasification of carbon with O_2 and CO_2 [15] and H_2O [16].

For the reactions, Arrhenius equation is defined as:

$$K = A \exp(-E/RT) \tag{7}$$

which is related to the following equation,

$$\log A = jE + \log K_o \tag{8}$$

in which A changes with the variation of E at the different experimental conditions.

Combining equations (7) and (8), the following equation can be derived.

$$K = K_o \exp[E(2.30j - 1/RT)] \tag{9}$$

The isokinetic temperature, T_s, the temperature at which all the reaction with a given gasification agent proceed at the same reaction rate, is derived as:

$$T_s = 1/(2.30\ jR) \tag{10}$$

where j and R are the slope of the empirical equation (8) and the gas constant, respectively.

The resulting values from Eq. (8) are plotted in Fig. 7 in which the

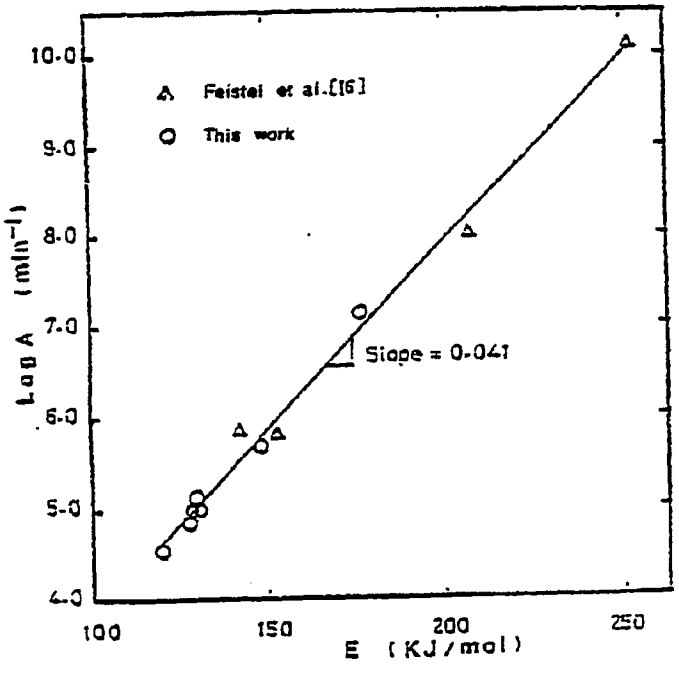

Fig. 7. Plot of log A versus E

experimental data of Feistel et al. [16] on the gasification of three different chars under the steam pressure of 1-10 atm are also included. The isokinetic temperature for steam gasification of the present study resulted in 1275 K. In addition, the isokinetic temperature for the CO_2 gasification of graphite was 1250 K as reported by Kawana [17] and Biederman [18].

ACKNOWLEDGEMENT

We wish to acknowledge a grant-in-aid for research from the Korea Science and Engineering Foundation.

REFERENCES

1. Walker, P.L., Jr., Matsumoto, S., Hanzawa, T., Miura, T., and Ismail, I.M.K., Fuel. 62, 140 (1983)
2. McKee, D.W., Fuel, 62, 170 (1983)
3. Kwon, T.W., Kim, S.D. and Fung, D.P.C., submitted to Fuel for pub. (1987)
4. Wen, C.Y., Ind. Eng. Chem., 60, 34 (1968)
5. Fung, D.P.C. and Kim, S.D., Fuel, 62, 1337 (1983)
6. Huhn, F., Klein, J. and Juntgen, H., Fuel, 62, 196 (1983)
7. Miura, K., Aimi, M. and Naito, T., Fuel, 65, 407 (1986)
8. Juntgen, H. and van Heek, K.H., Erdol und Kohle, 38, 22 (1985)
9. Kayembe, N. and Pulsifer, A.H., Fuel, 55, 211 (1976)
10. Wigmans, T., Elfring, R. and Moulijn, J.A., Carbon, 21, 1 (1983)
11. Adjorlolo, A.A. and Rao, Y.K., Carbon, 22, 173 (1984)
12. Chin, G., Kimura, S., Tone, S. and Otake, T., Int. Chem. Eng., 24, 246 (1984)
13. Veraa, M.J. and Bell, A.T., Fuel, 57, 194 (1978)
14. Thomas, J.M. and Thomas, W.J., "Introduction to the Principles of Heterogeneous Catalysis", Academic Press, London (1967)
15. Walker, P.L.,Jr., Shelef, M. and Anderson, R.A., "Chemistry and Physics of Carbon", Vol. 4, 287, Marcel Dekker, New York (1968)
16. Feistel, P.P., van Heek, K.H. and Juntgen, H., Carbon, 14, 363 (1976)
17. Kawana, Y., Bull. Chem. Soc., Japan, 27, 574 (1954)
18. Biederman, D.L., Ph.D. Thesis, Penn. State Univ., (1965)

LABORATORY SIMULATION OF POSTBURN UCG CONTAMINANT PRODUCTION

J. E. Boysen
C. G. Mones
R. R. Glaser

ABSTRACT

Previous field tests have demonstrated the technical feasibility and confirmed the commercial economic potential of underground coal gasification (UCG). However, contamination of groundwater is a major environmental concern that may delay or prevent commercialization of UCG. When UCG recovery operations are terminated, energy is stored in the adjacent masses of rock and coal ash, and this energy is transferred into the coal seam. Coal continues to be pyrolyzed as a result of the energy transferred and the products of this coal pyrolysis are believed to be the major source of groundwater contamination resulting from UCG.

A laboratory simulator was developed, and six simulations of UCG postburn coal pyrolysis have been completed. The simulations show that the products of coal pyrolysis are the source of most contaminants associated with UCG operations. Injection of water into the UCG cavity can limit postburn coal pyrolysis and reduce the production of contaminants by cooling the masses of rubble and coal ash in the cavity. However, if the injected water forms channels as it flows through the cavity, the cooling effect is localized and the benefit of the water injection in limiting postburn coal pyrolysis is greatly reduced. Also, water flow through the coal limits postburn pyrolysis and subsequent contaminant generation although steam generated in the hot portions of the coal limits the rate of water flow.

UCG field tests should be operated so that the flow of pyrolysis liquids and gases into the formation is prevented, and the natural influx of water into the cavity is allowed. This can be accomplished by minimizing gas leakage to the formation during gasification, venting the cavity when the gasification process is complete, and being sure water injection into the cavity does not cause the steam generated to create too much pressure in the cavity.

INTRODUCTION

Underground coal gasification (UCG) is a process for producing gas from coal without mining the coal. UCG field experiments in subbituminous coal deposits have successfully demonstrated the technical feasibility of producing gas from coal (Covell et al. 1980; Hill et al. 1980; Ahner 1982). Economic data indicate commercial potential for the process, but the uncertainty of the environmental impact resulting from the process may delay commercial development. The contamination of groundwater resulting from UCG is one of the key environmental concerns (Cooke and Oliver 1985).

The mechanism for groundwater contamination is believed to be as follows: when oxidant injection is stopped, combustion ceases, but large masses of coal ash and rock are at high temperatures. The energy in these masses is slowly dissipated by heat conduction to adjacent portions of the resource. This conductive heating pyrolyzes part of the adjacent coal

resource, and the resulting liquids and gases are not recovered after shutdown of the production operations. With time, the high temperatures in the formation decrease and coal pyrolysis stops. However, the pyrolysis products remain in the coal seam and soluble contaminants are transported further from the cavity by the natural flow of groundwater (Glaser and Owen 1986). The production of pyrolysis products following shutdown of UCG recovery operations and the resulting groundwater contamination have not been previously investigated.

The objectives of this research are

1) to simulate pyrolysis processes following shutdown of UCG recovery operations,

2) to estimate postburn contaminant generation (based on the thickness of the pyrolysis zone), and

3) to determine potential postburn operating procedures for reducing postburn pyrolysis product generation and migration resulting from the Rocky Mountain 1 field demonstration.

The initial series of six experiments is completed.

TECHNICAL DISCUSSION

General

Data from the excavation of UCG tests (Oliver 1986) were used to produce a simplified schematic of postburn in situ conditions. The upper diagram in Figure 1 illustrates a coal seam in which an area of coal that has been gasified. This area is partially filled with hot ash and rubble from thermally affected coal and collapsed overburden (rubble). At injection shutdown, both the rubble and the thin char layer surrounding the cavity are at high temperatures.

Conditions in the cavity area depend upon the geohydrologic environment of the site and the UCG operation history. This cavity may be wet or dry depending upon the nature of the overburden and the nature of the coal seam. The gasification operating pressure history may have inhibited or promoted water influx into the cavity. The source of water influx can be the coal seam or the overburden. In addition, the postburn pressure in the cavity can be high or near atmospheric pressure depending upon whether the process wells are shut in or open.

The simulation of postburn pyrolysis is achieved by considering a small element of coal and rubble at the cavity boundary. This element is depicted in Detail A of Figure 1. This cylindrical differential element is considered to be one-dimensional.

SIMULATION OF UCG POSTBURN PYROLYSIS

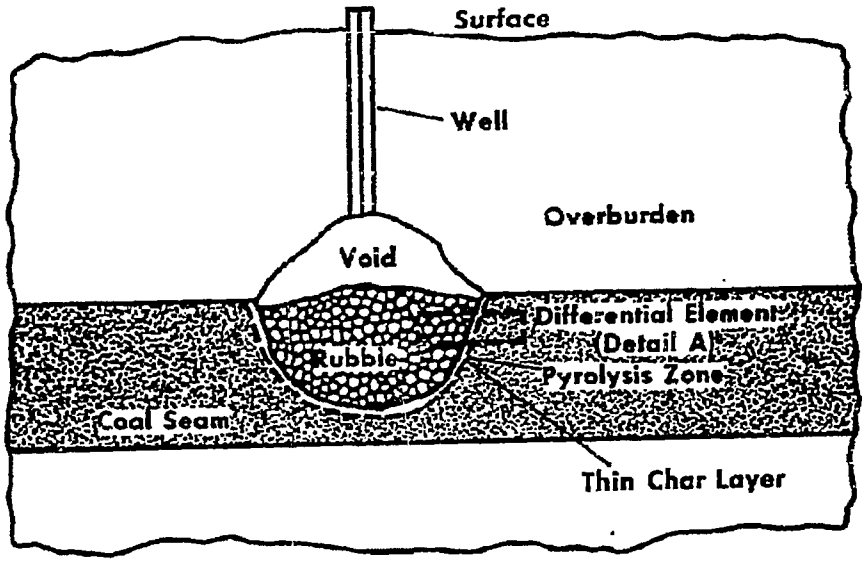

FIELD SITUATION

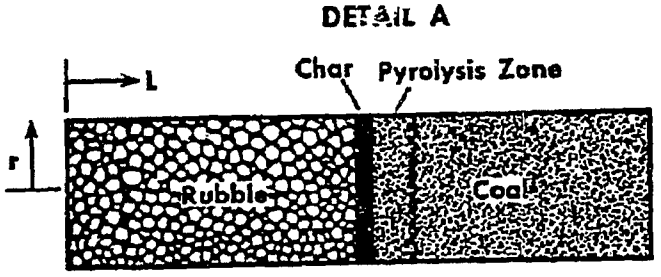

DIFFERENTIAL ELEMENT
FOR SIMULATION

Figure 1

Physical Simulation

Postburn coal pyrolysis was simulated in a laboratory reactor that is illustrated in Figure 2. Testing was conducted with Hanna coal samples taken parallel to the bedding plane. The samples used for testing were three inches in diameter and approximately one foot long. Each sample was placed in the reactor vessel as is illustrated in Figure 2. This sample configuration allows the simulation of a differential element on the cavity sidewall.

The coal face is heated with hot gas injected through port H and exhausted through ports B and C. A combustion zone develops because of the oxygen content in the injected hot gas. After combustion of the coal is achieved, the hot-gas injection is terminated and controlled cooling of the rubble zone simulates the heat transfer which would occur in the field. The rubble zone temperature is controlled by circulating hot gas through the tubing coil surrounding the outer circumference of the rubble zone. Ports H_I and H_O of Figure 2 are the coil inlet and outlet. Additional ports A and W are used to inject water into the coal and rubble zone, respectively. Thermocouples in the coal monitor the movement of the pyrolysis zone from the simulated cavity sidewall during cooldown.

The laboratory reactor is designed to test the range of water influx conditions that can be encountered in a UCG field test. Both influx rates and sources (locations) of water influx can be varied. In addition, the pressure in the rubble zone and at the outer boundary of the coal can be varied. The control of water influx from each source and control of pressure allows for the simulation of a variety of postburn conditions and potential operating procedures.

Experimental Procedure

The following experimental procedure for the physical simulations was developed during two shakedown tests. The simulation procedure is as follows:

1) The rubble boundary is heated to a predetermined temperature. A initial rubble boundary temperature of 1800°F (982°C) was selected to prevent damage to the laboratory reactor.

2) The coal is ignited with air to develop a char layer. Air is injected into the rubble until the coal core reaches a temperature in excess of 1800°F (982°C).

3) When the core reaches the desired temperature, the air injection is discontinued. The conditions are adjusted to match the selected simulation conditions and water injection.

4) The desired temperature versus time profile in the rubble zone is maintained during the physical simulation. The physical simulation lasts 24 hours or until the temperature at the coal face is less than 500°F (260°C).

CONTAMINANT CONTROL REACTOR

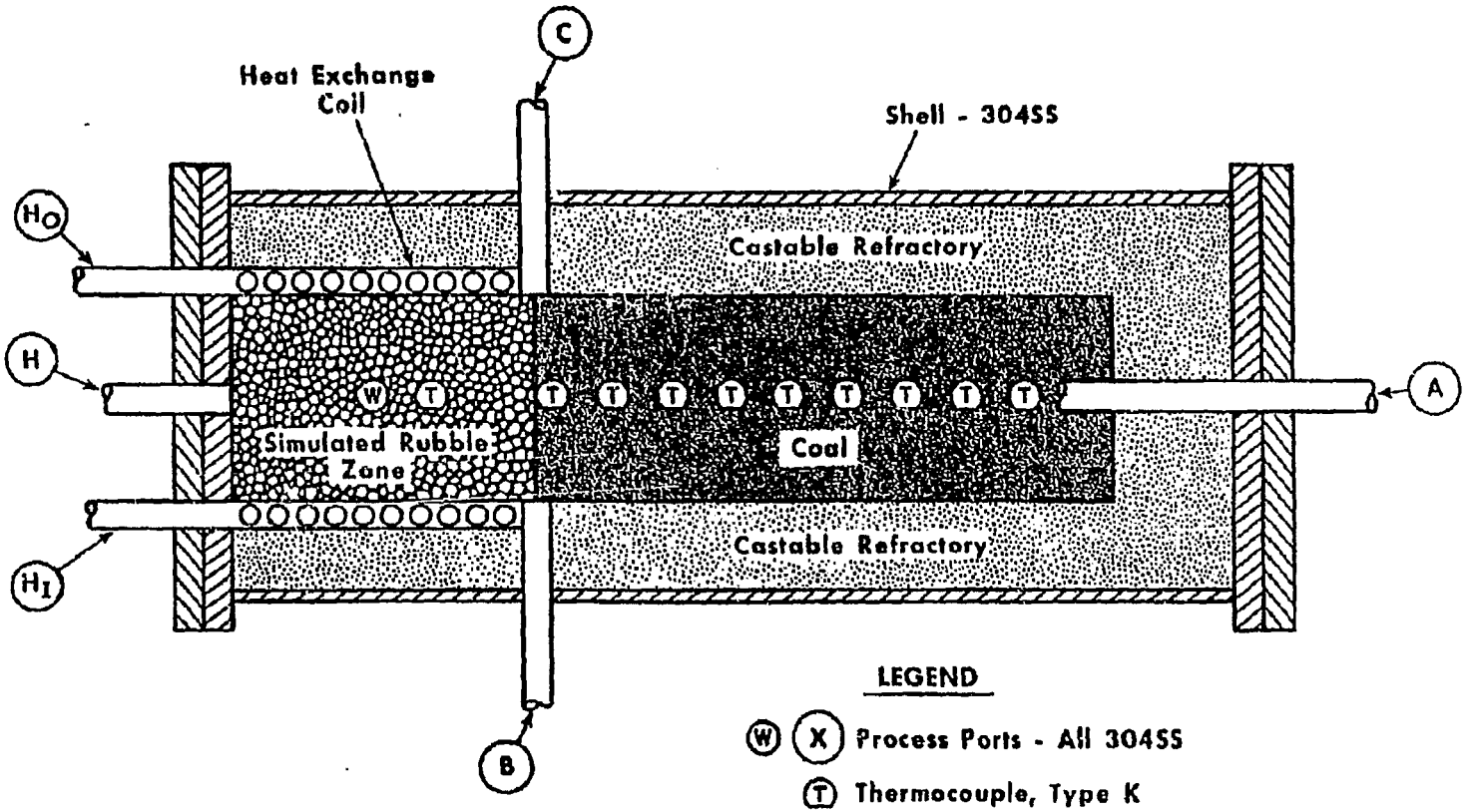

Figure 2

5) Coal samples are taken for analyses after the simulation reactor is shut down, cooled, and unloaded. Samples of liquids produced from the reactor are collected during the experiment. If water is injected during the experiment, samples of the injected water are taken during the water injection period. Also, hourly samples of the gases produced during the experiment are analyzed using gas chromatography.

The initial series of six physical simulations for UCG postburn coal pyrolysis was designed to consider the effects of three variables on postburn coal pyrolysis and the subsequent contaminant generation and migration. The three research variables are as follows:

1) Pressure gradient direction in the coal seam: pressure gradient direction is important in determining fluid transport in or out of the cavity.

2) Water influx rate through the coal seam: preliminary numerical model indications show the rate of water influx through the coal to be a key factor affecting the pyrolysis zone penetration. Water influx through the coal is also important in the containment of generated contaminants.

3) Water influx into the cavity: water influx into the cavity should result in lower cavity temperatures.

The experimental conditions for the six simulations are presented in Table 1.

Table 1. Postburn UCG Coal Pyrolysis Physical Simulation Experimental Conditions

Experiment No.	Rate of Water Injection	Test Conditions
3	0.1 cc/min	Cavity Water Injection Cavity Shut-in
4	1.0 cc/min	Cavity Water Injection Cavity Shut-in
5	1.0 cc/min	Cavity Water Injection Cavity Vented
6	4.0 cc/min	Water Injection Into Coal Seam Cavity Vented
7	0.16 cc/min	Water Injection Into Coal Seam Cavity Vented
8	1.60 cc/min	Water Injection Into Coal Seam Cavity Vented

Note: Experiments 1 and 2 were trial experiments (shakedown).

The specific questions to be answered from this series of simulations are

1) Can postburn coal pyrolysis be reduced by injecting water into the cavity and/or by inducing water influx through the coal seam?

2) What is the source of specific contaminant species (i.e. which contaminants come from the coal seam)?

3) Are gaseous and liquid pyrolysis products the main source of phenolic contamination or is the remaining pyrolyzed coal a significant source of contamination?

Results of Simulations

Pyrolysis Zone Penetration

Temperature profiles in the coal core are used to determine the maximum penetration depth of the pyrolysis zone into the coal core. The penetration of the pyrolysis zone for these six experiments are compared to determine the relative effectiveness of test conditions in limiting postburn pyrolysis. The temperature selected, 500°F (260°C), is the temperature at which significant pyrolysis of the coal begins.

Typical temperature profiles for the coal core are illustrated in Figure 3. The temperature profiles in the coal at three different times during experiment 3 are shown. The initial temperature profile at the time coal combustion is terminated is curve "1", the temperature profile at the time of maximum penetration of the 500°F (260°C) temperature zone is curve "2", and the final temperature profile when the face of the coal cools below 500°F (260°C) is curve "3". Also, listed on the figure are the test conditions for the experiment. Data for the maximum penetration of the pyrolysis zone (500°F/260°C) during the physical simulations are presented in Table 2.

Table 2. Experimental Pyrolysis Zone Penetration

Experiment No.	Maximum Penetration Depth
3	0.53"
4	0.38"
5	0.59"
6	0.21"
7	0.31"
8	0.28"

The data presented in Figure 4 illustrate the relationship between the rate of water injection through the coal and the pyrolysis zone penetration over the range of experimental conditions considered. The higher the rate of water injection through the coal, the less the pyrolysis zone penetration.

TEMPERATURE PROFILES OF COAL CORE FOR EXPERIMENT NO. 3

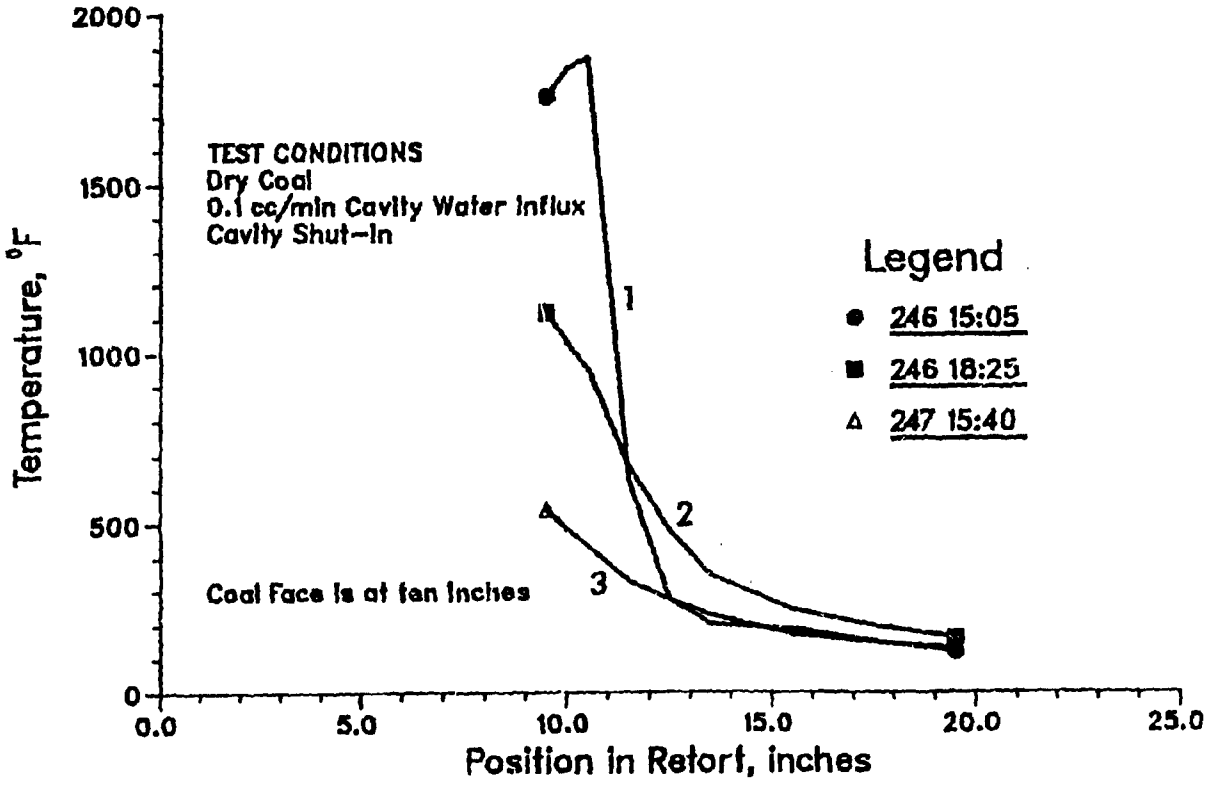

Figure 3
6 A2-8

When the cast coal core was removed from the reactor after these experiments, some valuable observations were made. In each test involving water injection through the coal core, substantial radial flow of water out of the coal core and through the refractory casting was observed in the portion of the core below steam temperatures. The previously measured permeability of the refractory at these temperatures is on the order of 0.1 millidarcies (md). This permeability is at least an order of magnitude less than that published for Hanna No. 1 coal (Hutchinson et al. 1977). This observation indicates that as steam is generated in the coal pores, the volume expansion creates a considerable impedence to water flow through the hot coal. Also, in experiment 6, which tested the highest water injection rate through the coal, the refractory around the coal core was fractured from the point where the coal core was at steam temperature out to the coal face. This phenomena may limit water influx through the coal seam in field conditions.

The data presented in Figure 5 illustrate the results of the cavity water injection tests. Comparing the two experiments in which the cavity was shut in indicates that higher water influx into the cavity will limit postburn pyrolysis. However, the test data for the case in which the cavity was vented (experiment 5) do not indicate a benefit from cavity water injection. The data indicate that there was little or no cooling of the rubble or coal face as a result of the injected water. In experiments 3 and 4, steam generated from the water injected into the cavity was forced to disperse and flow through the coal core. In experiment 5, the steam generated from the injected water took the path of least resistance and flowed out of the rubble zone cooling only a local region of rubble. Without significant cooling of the rubble zone or the coal face, the pyrolysis zone penetration was not reduced. In a field situation, channeling of water injected into a UCG cavity is possible, especially in cavities having a high-void volume, but over a long period of time cavity water injection should be beneficial in the cavity vent case also.

Contaminant Production and Migration

The data presented in Figure 6 illustrate the phenol concentration distribution in the coal core after experiment 3, and the maximum temperature profile achieved during the experiment. The data in this figure illustrate that as pyrolysis of the coal occurs, the concentration of the water soluble phenols bound to the coal increases until the coal is completely pyrolyzed. Charred regions of the coal core have low concentrations of water soluble phenols if the pyrolysis products generated in the core flow away from the char zone. If the pyrolysis products flow through the char zone as in experiment 5 (Figure 7), the char tends to reabsorb phenols.

The concentration of phenols found in the produced liquids is much greater than the concentration of phenols found on the thermally altered coal. Table 3 provides a listing of the measured phenol concentrations found in the produced liquids and injected water for the six experiments. The concentration of phenols in the produced liquids is in the range of mg/L as compared to the µg/kg range found in the coal samples. Also, the mass of phenols in the produced liquids are several orders of magnitude greater than the mass of water-soluble phenols remaining on the coal. The data listed in Table 4 illustrate this fact.

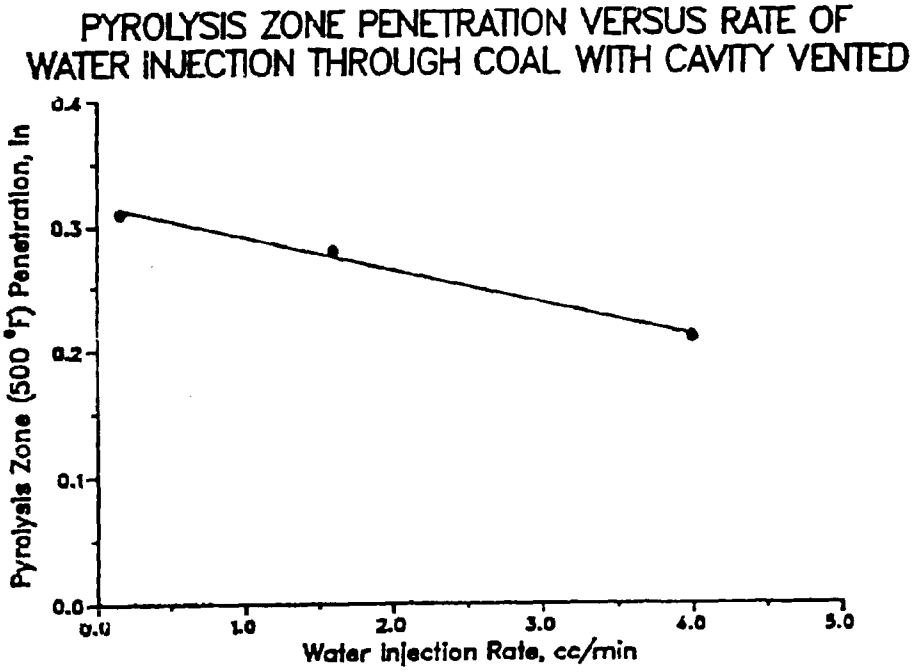

Figure 4

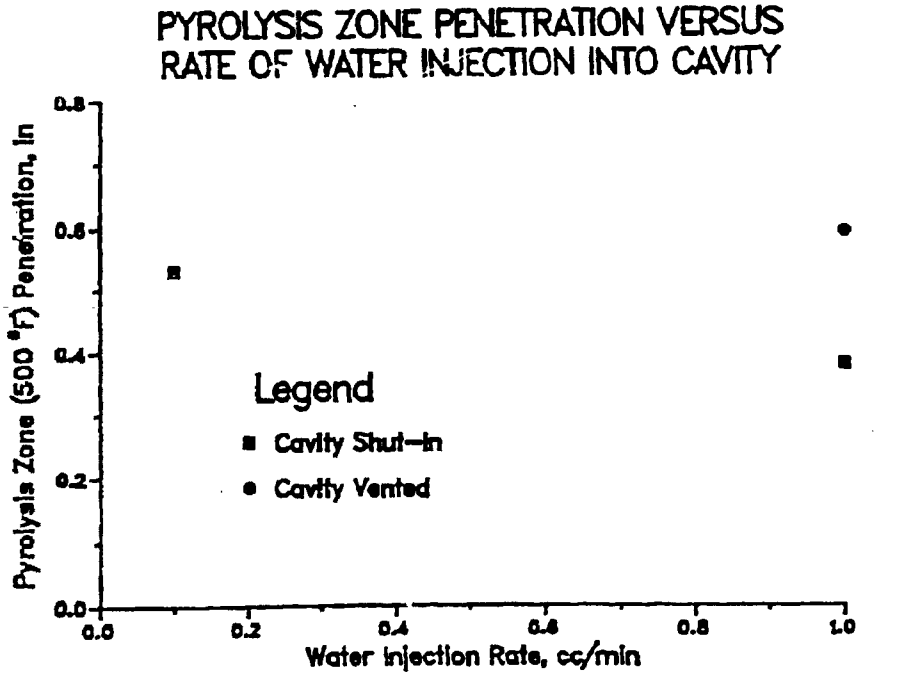

Figure 5

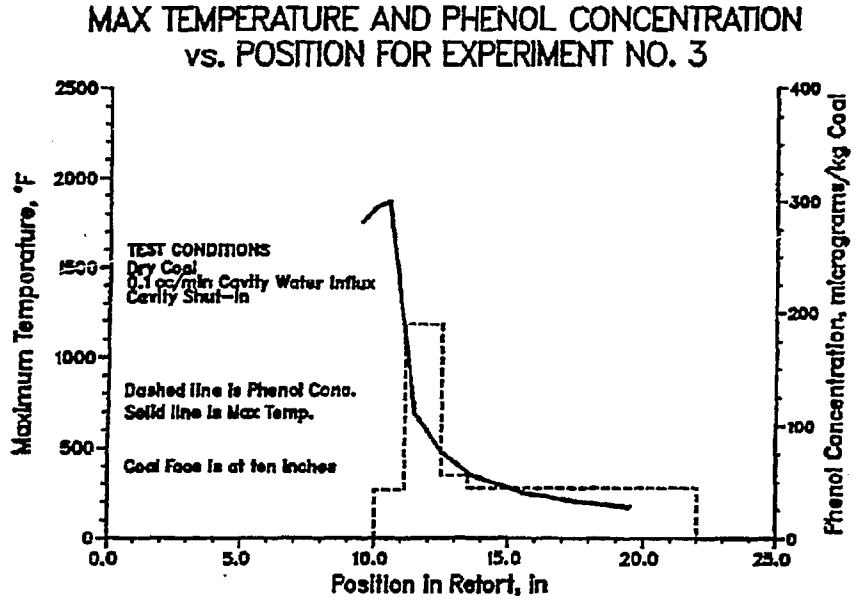

Figure 6

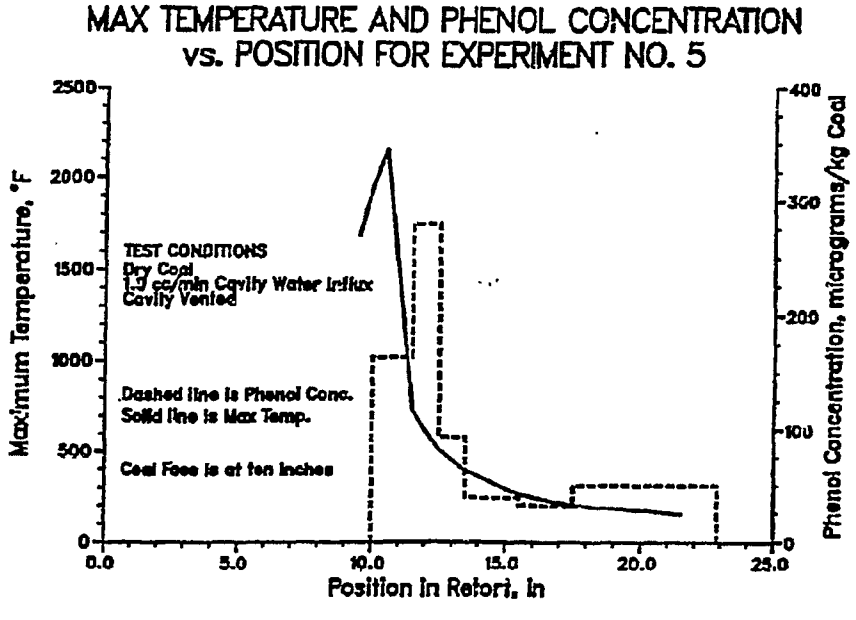

Figure 7

Table 3. Phenol Concentrations of the Liquids Produced During the Physical Simulations

Experiment No.	Injection Rate cc/min	Phenols Concentration In Injected Water µg/L	Phenols Concentration In Produced Liquid mg/L
3	0.1	*	650
4	1.0	*	---
5	1.0	*	210
6	4.0	*	51,6.1,2.1,2.5,2.3,(11)
7	0.16	*	1100
8	1.6	*	130,58,6.2

* Value less than the detection limit for the analytical procedure (<20 µg/L)

Table 4. Phenol Distribution in the Coal and Product Liquids

Experiment No.	Injection Rate cc/min	Phenol Distribution Residual Phenols on Coal (µg)	Phenol Distribution Phenols in Produced Liquid (µg)
3	0.1	106	40,000
4	1.0	116	------
5	1.0	118	77,000
6	4.0	43	25,000
7	0.16	73	61,000
8	1.6	77	34,000

The mass of other selected contaminant species found in the produced liquids per mass of coal pyrolyzed during the physical simulations was calculated from the concentration of the species found in the liquid produced, the volume of liquid produced, and the mass of coal pyrolyzed during the simulation. The results of these calculations are presented in Table 5. The variation of results is significant, but it is evident that these contaminant species originate from the coal seam, ar mobilized when coal is pyrolyzed, and migrate with the coal pyrolysis products.

Table 5. Other Contaminant Species Generated During Coal Pyrolysis

$$\text{Contaminant Species} = \frac{\text{Mass of Species in Produced Liquids}^*}{\text{Mass of Coal Pyrolyzed}}$$

	Lowest Value	Highest Value
Total Organic Carbon (mg/kg)	2900	4700
Sulfate (mg/kg)	300	4800
Ammonia (mg/kg)**	400	1600
Boron (µg/kg)	80	2800
Fluoride (mg/kg)	20	130
Barium (µg/kg)	90	8900
Arsenic (µg/kg)	Trace (<20)	700
Selenium (µg/kg)	Trace (<50)	120 (<360)
Lead (µg/kg)	70	4300

* Reported lowest and highest values based on comparison of results from experiments 3, 5, 6, 7, and 8. Values are presented to confirm contaminant species origin from coal pyrolysis.

** Values reported for ammonia represent the mass of nitrogen in the ammonia.

CONCLUSIONS AND RECOMMENDATIONS

The following conclusions are drawn from the results of the initial series of physical simulations.

1) Liquid and gaseous pyrolysis products are a major source of phenols in groundwater when compared to thermally altered coal. Phenols in produced liquids are at least an order of magnitude greater than those water soluble phenols remaining on the coal.

2) Most contaminant species associated with UCG operations are present in the pyrolysis products. Analyses of the produced liquids verify the presence of phenols, ammonia, sulfates, arsenic, boron, barium, fluoride, lead, and selenium.

3) Injection of water into the cavity can limit postburn pyrolysis, but only to the degree to which the cavity is cooled.

4) Water flow through the coal will limit postburn pyrolysis, but steam generation in the coal appears to limit the rate of water flow.

The conclusions drawn from the analyses of experimental results were used to formulate recommendations for operation of future UCG field tests. These recommendations are of particular value to the upcoming Rocky Mountain 1 UCG Field Demonstration jointly sponsored by the Gas Research Institute (GRI) and the United States Department of Energy (U.S. DOE). The following recommendations are made to minimize groundwater contamination and promote containment of contaminants near the UCG cavity.

1) The flow of pyrolysis liquids into the underground formation should be prevented. This can be accomplished by minimizing gas leakage to the formation during gasification and venting the cavity as soon as the gasification process is complete. Also, water injection into the cavity must not generate steam pressures greater than the hydrostatic pressure of the coal seam or connected aquifers.

2) Although preliminary indications show water influx from the coal seam is beneficial, it may be difficult to achieve an influx rate higher than the natural influx rate. Therefore, water injection wells surrounding the cavity are not expected to increase the water influx rate.

ACKNOWLEDGMENT

The authors express thanks and appreciation to the United States Department of Energy and the Gas Research Institute for funding of this work. Special thanks are given to the lead technicians for this project: Paul Paisley, Mark Lyon, and Ron Beckett. The data provided in this paper are a result of their conscientiousness and hard work.

DISCLAIMER

Mention of specific brand names or models of equipment is for information only and does not imply endorsement of any particular brand.

REFERENCES

Ahner, P. F. "Rawlins Tests 2 Data Analysis," 8th Underground Coal Conversion Symposium Proceedings, Keystone, CO, 1982.

Cooke, S. D., and R. L. Oliver. "Groundwater Quality at the Hanna Underground Coal Gasification Experimental Sites, Hanna, WY, Data Base and Summary," 1985, U.S. Department of Energy Technical Progress Report, in press.

Covell, J., et al. "Results of the Fourth Hanna Field Test," Sixth Underground Coal Conversion Symposium Proceedings, Shangri-la, OK, July 13-17, 1980.

Glaser, R. R., and T. E. Owen. "Postburn Generation, Control, and Recovery of Organic Compounds in Underground Coal Gasification," January 1986, prepared for the Gas Research Institute.

Hill, R. W., et al. "Results from the Third LLL Underground Coal Gasification Experiment at Hoe Creek," Sixth Underground Coal Conversion Symposium, Shangri-la, OK, July 13-17, 1980.

Hutchinson, H. L., et al. "Hydrologic Characterization for Hanna III," Third Annual Underground Coal Conversion Symposium Proceedings, Fallen Leaf Lake, CA, June 6-9, 1977.

Oliver, R. L. "Final Results of the Tono I UCG Cavity Excavation Project, Centralia, Washington," September 1986, report prepared for Lawrence Livermore National Laboratory.

Assessing Potential Benefits and Penalties of Cleaning Low-Rank Coals

Peter Suardini
Test Engineer
Kaiser Engineers, Inc.
Coal Cleaning Test Facility
P.O. Drawer H
Homer City, PA 15748

David J. Akers
Test Engineer
Science Applications International Corp.
Coal Cleaning Test Facility
P.O. Box 10
Homer City, PA 15748

Chuck Hancock
Technical Specialist
T U Electric
400 N. Olive St., LB. 81
Dallas, TX 75201

ABSTRACT

Approximately 70 percent of the eastern bituminous coal burned to generate electricity is physically cleaned in some manner prior to combustion. Therefore, a substantial amount of coal cleaning plant operating data and coal cleaning-related reserve information is available for most eastern bituminous coal seams. In contrast, only four percent of low-rank, western coal is presently being cleaned, and limited information is available assessing the response of this coal to physical cleaning. This paper outlines the general advantages and disadvantages of coal cleaning for existing low-rank coal mining and power plant operations. It also discusses procedures for evaluating the cleaning characteristics of low-rank coals. Results from cleaning investigations on three low-rank coals, one Robinson Seam subbituminous from Montana and two Hilcox Formation lignites from Texas, are used as examples.

INTRODUCTION

Low-rank coal deposits (subbituminous and lignite) often occur in shallowly buried seams, allowing the use of relatively inexpensive surface mining techniques. The low cost of these low-rank coals, coupled with the proximity of some of the reserves to areas of high population growth, are two reasons why domestic electric utility use of low-rank coal increased from 110M tons in 1977 to 267M tons in 1985 (1). In this same time period, utility use of eastern bituminous coal increased only five percent (from 380M to 399M tons).

Unfortunately, this shift to low-rank coal has posed some special problems to coal mining companies and electric utilities, especially utilities switching from higher-rank, eastern bituminous coals. For example, the higher inherent moisture contents and lower heating values of the low-rank coals necessitate that additional tons be mined, transported, and fired to produce the same power plant output that fewer tons of higher-rank coals produce. These low heating values, coupled with potential heat transfer efficiency problems caused by ash slagging and fouling tendencies, require conservative pulverizer and boiler designs for new power plants, or expensive boiler and pulverizer redesigns for existing power plants that are switching to lower-rank coals. The erosiveness and abrasiveness of some high quartz content, low-rank coals can also result in excessive maintenance costs and availability losses due to pulverizer-surface, boiler-feed line, and convection-tube deterioration or wear.

Although most western, low-rank coal mining operations do not clean the coal (2), physical coal cleaning is one commercially available technology with the potential for reducing many of the problems associated with burning low-rank coal. Physical coal cleaning is a sorting process based on one or more physical properties (usually particle size and particle density) used to remove undesirable species (such as ash- and sulfur-bearing mineral matter) from coal.

Figure 1 outlines the general advantages and disadvantages of coal cleaning for existing surface mining and power plant operations. The magnitude and in some cases the direction of these changes is dependent upon a number of factors, including:

- Characteristics of the coal reserve
- Mining logistics
- Cleaning plant design and operation
- Transportation distance and cost
- Power plant design
- Environmental issues

These factors and their interrelationships are site-specific, making it necessary to consider each case separately and on a system-wide basis in order to assess the feasibility of cleaning a given reserve. Figure 1 and the following discussion should therefore be used only as a guide to coal-cleaning considerations and not a listing of specific cause and effect relationships.

Coal Cleaning Plant Considerations

Cleaning plant capital and operating costs are dependent on factors such as the required capacity (tons per hour), complexity of the design and equipment selected for the cleaning plant, refuse disposal system, and local labor rates.

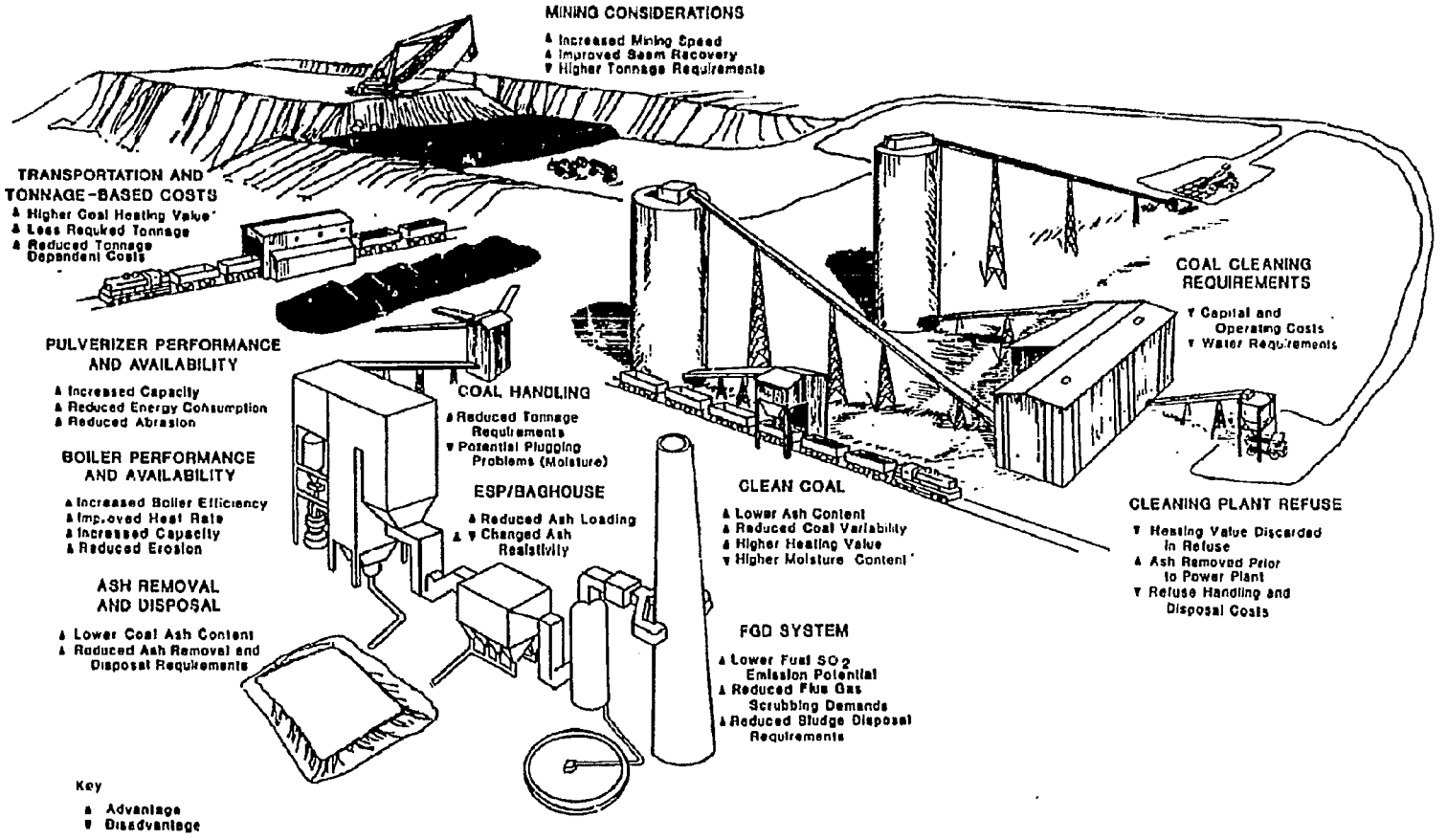

Figure 1
POTENTIAL EFFECTS OF COAL CLEANING
ON EXISTING SURFACE MINE AND POWER PLANT OPERATIONS

An EPRI study (3) assessing the cost impacts of coal cleaning for various regional coal sources suggests that coal-cleaning plants should have capital costs ranging from $4.00 to $12.00 per ton of annual plant capacity and operating and maintenance costs ranging from $0.40 to $2.00 per ton of raw coal processed. Water requirements for water-based, coal-cleaning processes may also be a concern in arid regions. Closed-water-loop cleaning plants can operate with water consumptions less than ten gallons per ton of coal processed. However, the solids dewatering and water reclamation systems required to minimize water usage increase cleaning-plant capital and operating costs.

The costs associated with a cleaning plant must be recovered through savings in the mining operation, reductions in tonnage-dependent costs, and/or benefits associated with coal quality improvement at the power plant.

Mining Considerations

Addition of a coal-cleaning plant has four primary effects on an existing mining operation. The first is that it creates a coal-quality buffer between the mine and the power plant. Equipment operators do not have to be as meticulous in segregating the coal seam from other sediments because the coal-cleaning plant is available downstream to make that separation. This can promote less coal rejection in the mining phase and increase overall mining speed. Secondly, coal cleaning can increase coal heating value and improve boiler heat rate, which reduces the tonnage required to achieve the same power plant output. This not only affects raw-coal tonnage requirements, but reduces other tonnage-dependent costs (considered later in this discussion).

Thirdly, coal cleaning affects the life of the reserve. In some cases reserve life is extended because of improved coal recovery during mining and/or the use of portions of the reserve too low in quality to be marketed raw. In other cases, reserve life is shortened because of heating value lost in the refuse from the cleaning operation.

The final effect of coal cleaning on mining operations relates to mine production rate. Heating value that is lost in the refuse from the cleaning operation must be replaced by mining additional tons to maintain the same energy output from the mine. The energy lost to refuse may be offset to some degree by improved boiler performance (heat rate) at the power plant. However, if mining production rate (tons per day) must be increased when a cleaning plant is constructed, the capability of the existing mining operation to produce this additional tonnage as well as the cost impact of increasing production rate must be considered.

Transportation and Other Tonnage-Dependent Considerations

Higher coal heating values and any subsequent improvement in boiler heat rate resulting from coal cleaning decrease the tonnage required to achieve the same power plant output, thereby reducing tonnage-dependent costs such as transportation, and coal handling and loading costs. These cost savings can be substantial, especially in cases where the coal is transported long distances and significant heating value increases result from cleaning. For example, if the coal source feeding a power plant is upgraded from 7,000 Btu/lb to 8,000 Btu/lb by cleaning, transportation costs required to provide a given power-plant output (GW/yr) could be reduced by approximately 12.5 percent without any

improvement in heat rate. If an improvement in heat rate is realized, the potential savings become greater.

One point that should be emphasized is that clean-coal moisture content is a controllable variable dependent upon a number of factors, including inherent moisture content, coal size consist, cleaning-plant design, mining methods, and climate. In many cases, concerns over tonnage-dependent costs and coal-handling problems stemming from increased clean-coal moisture contents have necessitated that more elaborate physical dewatering equipment (i.e., high rpm horizontal centrifuges) or thermal drying equipment be used in the cleaning plant. In essence, the potential for reducing tonnage-dependent operating costs and improving power plant performance dictates the amount of cleaning plant capital and operating costs dedicated to minimizing the moisture content of the clean coal product.

Power Plant Considerations

Figure 1 lists a number of potential power-plant benefits resulting from cleaning, including improved pulverizer and boiler performance and availability, and reduced demands on ash- and SO_2-removal systems. The relative changes in ash- and SO_2-removal system demands can be assessed fairly accurately from heating value increases, ash reductions, and SO_2 emission potential reductions accompanying cleaning. However, because of variations that can occur in ash characteristics and composition, the effects of coal cleaning on pulverizer and boiler performance and availability are more difficult to quantify.

For instance, with certain coals, cleaning increases the proportion of basic constituents in the ash and reduces ash fusion temperatures. This may promote more tenacious ash slagging and fouling characteristics, which can to varying degrees counteract the favorable effect that reduced ash loading has on pulverized-coal-fired boiler performance. In such a case, the improvements in boiler efficiency and capacity resulting from cleaning may not be as pronounced as expected. Coal cleaning can also change coal mineral-matter distribution, fly-ash composition, and fly-ash resistivity, thereby affecting coal abrasiveness and erosiveness, fly-ash erosiveness, and electrostatic precipitator (ESP) performance.

BACKGROUND

The preceding discussion outlines the general advantages and disadvantages of coal cleaning, and points out the necessity of conducting individual case studies for each coal reserve. The overall feasibility of cleaning a given reserve can only be determined by weighing the cost benefits resulting from cleaning against the cost penalties.

For the last six years, the Electric Power Research Institute (EPRI) has been investigating the cleaning characteristics of prominent domestic coal seams to assess the changes in coal quality and power-plant benefits associated with physical-coal cleaning. The coal-cleaning phase of this research has been performed primarily at EPRI's Coal Cleaning Test Facility (CCTF) near Homer City, Pennsylvania: a demonstration facility equipped with commercial-scale, coal-cleaning equipment. Some of the CCTF-produced clean coals and parent raw coals are subjected to comparative bench- and pilot-scale combustion testing

through EPRI's Availability and Life Extension Program. This combustion testing is designed to quantify the improvements in power-plant performance achieved by cleaning and gain a better understanding of coal-quality parameters that dictate various aspects of combustion performance (i.e., slagging and fouling).

The remainder of this paper discusses general methods for evaluating the feasibility of cleaning a given low-rank coal reserve. Results from CCTF coal-cleaning investigations on three low-rank coals, one Robinson Seam subbituminous from Montana and two Wilcox Formation lignites from Texas, serve as examples (4, 5).

COAL CLEANING FEASIBILITY EVALUATION

The first step in any coal-cleaning evaluation involves collecting information about the coal reserve. If the reserve is not being mined, the only sources of samples are from drilling, channel samples taken along outcrops, and coal removed from test pits. These three sampling methods can provide valuable information about changes in coal characteristics throughout the reserve and are valuable in mine planning as well as evaluating coal cleaning. Unfortunately, the size consist of samples extracted in this manner (especially by drilling and channel sampling) may bear little relationship to run-of-mine samples. If the reserve is being mined, an empirical relationship between these samples and run-of-mine samples can be developed. If not, engineering judgment based on past experience with similar coals must be used.

A special advantage of an existing mine is that enough coal is available to allow commercial-scale cleaning tests. The ideal method of evaluating any reserve involves extensive core drilling to assess the overall characteristics of the reserve, including coal variability, commercial-scale cleaning tests to develop reliable plant design and clean-coal quality and cost information, and pilot- or commercial-scale combustion tests to assess the impact of clean coal quality on boiler performance. This entire procedure is rarely followed because of time and cost constraints. Rather than assume the availability of some specific level of test data, the following discussion covers most of the commonly utilized test procedures for making this evaluation.

Size Analyses

One of the most important analyses required to evaluate the cleaning potential and desired cleaning-plant design for a given run-of-mine coal is the distribution of weight, heating value, and impurities concentration (ash, sulfur, pyrite, quartz, etc.) in the various size fractions of the coal. This information is obtained by laboratory screening procedures developed for the testing and evaluation of coals.

Tables 1 through 3 list the size analyses for three low-rank, run-of-mine coal samples tested at the CCTF. All analyses are on a dry basis because a wet-screening procedure is required to obtain efficient screening.

The "Direct" columns in Tables 1 through 3 list the weight proportion, ash content, sulfur content, and heating value in each size fraction. The "Proportions of Total (%)" columns list the proportion of the raw-coal's ash, sulfur, and energy in each size fraction.

Table 1

RAW-COAL QUALITY BY SIZE
Robinson Seam Subbituminous
Absaloka Mine
Big Horn County, MT

Size			Direct (Dry Basis)				Proportion of Total (%)		
Passing	×	Retained	Proportion of Coal (Wt %)	Ash (Wt %)	Total Sulfur (Wt %)	Heating Value (Btu/lb)	Ash	Sulfur	Energy
+2-in	×	3/4-in	14.9	11.1	0.57	11,289	16.0	9.8	14.9
3/4-in	×	3/8-in	15.2	9.0	0.85	11,638	13.3	13.6	15.7
3/8-in	×	28M	48.7	8.6	0.91	11,512	40.6	46.9	49.6
28M	×	100M	15.1	11.6	1.41	10,893	16.9	22.6	14.6
100M	×	200M	3.3	14.7	1.43	10,445	4.5	5.0	3.1
200M	×	0	2.8	32.0	0.96	8,394	8.7	2.9	2.1

Table 2

RAW-COAL QUALITY BY SIZE
Wilcox Formation Lignite
Big Brown Mine
Freestone County, TX

Size			Direct (Dry Basis)				Proportion of Total (%)		
Passing	×	Retained	Proportion of Coal (Wt %)	Ash (Wt %)	Total Sulfur (Wt %)	Heating Value (Btu/lb)	Ash	Sulfur	Energy
6-in	×	1 1/2-in	14.5	11.5	0.93	11,121	9.9	14.2	18.4
1 1/2-in	×	3/4-in	16.9	12.6	1.10	10,917	11.0	17.2	18.5
3/4-in	×	3/8-in	18.2	13.9	1.24	10,684	13.1	20.9	19.5
3/8-in	×	28M	33.4	15.5	1.22	10,470	26.9	37.7	35.2
28M	×	100M	5.1	21.3	1.17	9,279	5.6	5.5	4.8
100M	×	200M	1.2	36.3	0.98	7,543	2.3	1.1	0.9
200M	×	0	8.7	69.2	0.43	3,058	31.3	3.4	2.7

Table 3

RAW-COAL QUALITY BY SIZE
Wilcox Formation Lignite
Winfield North Mine
Titus County, TX

Size			Direct (Dry Basis)				Proportion of Total (%)		
Passing	×	Retained	Proportion of Coal (Wt %)	Ash (Wt %)	Total Sulfur (Wt %)	Heating Value (Btu/lb)	Ash	Sulfur	Energy
6-in	×	1 1/2-in	13.5	21.4	0.68	9,723	9.0	13.4	16.0
1 1/2-in	×	3/4-in	9.9	21.4	0.70	9,735	6.6	10.1	11.8
3/4-in	×	3/8-in	14.8	22.5	0.68	9,533	10.4	14.7	17.2
3/8-in	×	28M	37.2	21.7	0.88	9,418	25.2	47.7	42.8
28M	×	100M	4.9	22.1	0.89	9,430	3.4	6.4	5.6
100M	×	200M	2.0	31.7	0.91	8,164	2.0	2.6	2.0
200M	×	0	17.7	78.2	0.20	2,131	43.4	5.1	4.6

One of the most significant characteristics of the size analyses in Tables 1 through 3 is that, for all three coals, the ash contents of the finest size fraction (200M x 0) are substantially higher than those of the coarser size fractions. For the two Wilcox Formation lignite samples (Big Brown Mine and Winfield North Mine), this high clay content fraction represents a significant weight proportion of the raw coal (8.7 and 17.7 percent, respectively). The "Proportion of Total (%)" columns show that 31.3 and 43.4 percent of the total ash is in the 200M x 0 size fraction, but this represents only 2.7 and 4.6 percent of the raw-coal's heating value (energy). Removal of the 200M x 0 size fraction during cleaning would therefore be a feasible approach to reducing ash content in the two lignites, without sacrificing a large proportion of the raw-coal's heating value.

For the Robinson Seam subbituminous sample, the 200M x 0 size fraction is only 2.8 weight percent of the raw coal and contains 2.1 percent of the raw-coal's energy. The ash content of this size fraction (32 percent) is lower than the two lignites, indicating a higher cleaning potential. The normal commercial method of cleaning this size range of bituminous coal is froth flotation. While CCTF work with Robinson Seam (6) did include a preliminary evaluation of the use of froth flotation to clean this coal, additional work in this area is needed before this technology is applied commercially to low-rank coals. The lack of commercially demonstrated technology, combined with the low proportion of the raw coal's energy value contained in the 200M x 0, indicate that it would be best to discard this fraction.

Another advantage of removing the 200M x 0 size fraction during cleaning is that moisture-content increases stemming from coal cleaning and potential coal-handling problems will not be as pronounced as in cases where the fines are recovered in the clean-coal product. This simplifies cleaning-plant design and results in lower cleaning-plant capital and operating costs than are required when the 200M x 0 coal must be separated, dewatered, and combined with the clean-coal product.

Lastly, Tables 1 through 3 illustrate that, for all three coal samples, the sulfur contents in the fine 200M x 0 size fractions are either equal to or lower than the remaining plus 200M raw coal. Although removal of the minus 200M size fraction will reduce ash contents and increase heating values for these three coals, it may not reduce sulfur content. The coarser size fractions would have to be cleaned to obtain any significant sulfur or SO_2 reductions.

Washability Analyses

Since conventional coal-cleaning processes are primarily based on differences in particle density as well as size, it is also important to determine the distribution of weight, heating value, and impurities concentrations (ash, sulfur, pyrite, quartz, etc.) in the various specific gravity fractions of raw coal samples. This specific gravity distribution, termed a washability analysis, is most useful when performed on the various size fractions of run-of-mine samples or the seam zones of drill cores and channel samples.

During CCTF investigations of the three low-rank coals, washability analyses were performed on the various size fractions of each run-of-mine sample. Figure 2 is a plot of ash loading (lb/MBtu) and SO_2 emission potential (lb/MBtu) versus energy recovery obtained from the plus 200M washability analyses. Ash and SO_2

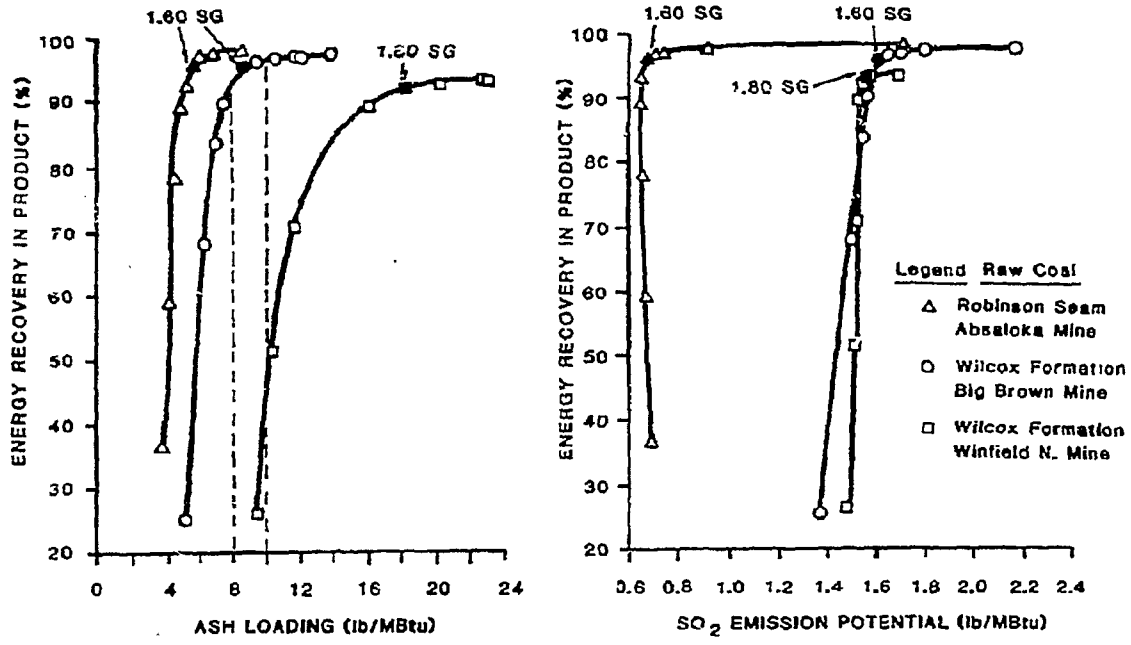

Figure 2

THEORETICAL ASH AND SO_2
VERSUS ENERGY RECOVERY RELATIONSHIPS
From +200M Raw Coal Washability Analysis

Table 4

COMPARISON OF RAW COAL HEAD ANALYSES
TO THEORETICAL CLEAN COAL PRODUCTS
From Raw Coal Washability Analyses
(As-Received Basis)

	Yield (Wt %)	Energy Recovery (%)	Moisture (Wt %)	Ash (Wt %)	Sulfur (Wt %)	Heating Value (Btu/lb)	SO_2 (lb/MBtu)	Ash (lb/MBtu)
ROBINSON SEAM SUBBITUMINOUS								
Raw Coal	100	100	22.3	6.2	0.72	8,761	1.64	9.4
Theoretical Clean Coal	94	96	24.3	5.2	0.30	8,960	0.68	5.8
BIG BROWN MINE LIGNITE								
Raw Coal	100	100	31.9	12.5	0.77	6,779	2.27	18.5
Theoretical Clean Coal	87	96	33.9	6.4	0.60	7,420	1.63	8.7
WINFIELD NORTH MINE LIGNITE								
Raw Coal	100	100	32.8	21.1	0.46	5,550	1.67	38.0
Theoretical Clean Coal	77	92	34.8	11.8	0.30	6,454	1.55	18.3

Notes: - Theoretical clean coal products do not contain the 200M x 0 size fraction. On plus 200M sizes, a perfect density separation at 1.60 specific gravity was assumed for Robinson Seam subbituminous and Big Brown Mine lignite, and a perfect separation at 1.80 specific gravity was assumed for Winfield North Mine lignite.

- As-received basis estimates are made assuming a 2.0 percentage point moisture increase upon cleaning for all three coals.

are shown because they are of interest at many power plants; however, other impurities, such as quartz or iron content, can be evaluated in the same manner. Quantities are listed on a lb/MBtu basis to orient the evaluation more toward boiler loading and because lb/MBtu quantities are independent of moisture content. The 200M x 0 size fraction washability results are not included in the plots because this size fraction would probably be discarded. Only the plus 200M size fraction would be subjected to any type of density separation. The energy recoveries in Figure 2 do not reach 100 percent because the portion of energy in the 200M x 0 size fraction has already been subtracted.

The main purpose of these impurities-versus-energy recovery curves (Figure 2) is to quantify the theoretical level of impurities reductions which can be achieved by upgrading the coal in density-based equipment, as well as the proportion of the raw-coal's energy which must be sacrificed to achieve these impurity reductions. From a coal-cleaning perspective, it is best to separate the coals at or near the specific gravity where these curves level off. For example, the Big Brown Mine lignite ash-versus-energy recovery curve levels off in the range of eight to ten lb/MBtu of ash (see Figure 2). Separations yielding a product containing less than eight lb/MBtu of ash would probably be undesirable because a small incremental ash reduction must be traded for a sharp drop in product energy recovery. Separations yielding a product with ash loading much above ten lb/MBtu may also be undesirable because a small increase in energy recovery must be traded for a large incremental increase in ash loading.

The changes in slope of the curves in Figure 2 suggest that it would probably be best to clean the Robinson Seam subbituminous and Big Brown Mine lignite samples at a specific gravity of approximately 1.60, and the Winfield North Mine lignite at a somewhat higher specific gravity (approximately 1.80). In certain cases, environmental or power-plant considerations can override the logic of using the washability analyses to estimate desired separating gravity and clean-coal quality. The actual separation gravity and cleaning approach at commercial operations is also affected by site-specific economic and contractual considerations.

Table 4 compares the raw-coal analyses to the laboratory clean-coal qualities and recoveries obtained at 1.60 and 1.80 specific gravities, respectively. The clean-coal analyses, normally reported on a dry basis, have been converted to as-received basis by assuming a 2.0 percentage point moisture increase when the coals are cleaned. These rather small moisture content increases seem reasonable because the difficult to dewater 200M x 0 size fraction will not be recovered in the clean-coal product.

The laboratory results in Table 4 suggest that the ash reductions and heating value increases achieved by cleaning the two lignites will be much more pronounced than for the Robinson Seam subbituminous. Therefore, the potential savings in transportation and other tonnage- or ash-quantity-dependent costs will be more dramatic for the lignites.

In contrast, the potential for SO_2 reduction is highest for the Robinson Seam subbituminous sample (from 1.64 to 0.68 lb/MBtu) because pyrite (FeS_2) is removed during cleaning. Sulfur dioxide reductions of this magnitude (61 percent) would bring the coal well into compliance with the 1971 New Source Performance Standards (NSPS) of 1.20 lb/MBtu, and could dramatically reduce

flue-gas scrubbing demands at power plants that must achieve the 70 to 90 percent SO_2 reduction restrictions in the 1979 NSPS legislation.

Table 4 also illustrates that at these reasonably high separation gravities (1.60 to 1.80), between 92 and 96 of the raw coal's energy was recovered in the laboratory clean-coal products. However, in commercial-scale cleaning processes, the yields and energy recoveries at these given clean-coal qualities should be substantially lower because of the inherent inefficiency of commercial-scale cleaning equipment.

CCTF Cleaning Results

The preceding section illustrates that a substantial amount of cleaning information can be obtained from relatively inexpensive laboratory analyses on run-of-mine coal samples. Drill core and channel samples can be analyzed in the same fashion, except that it may be more meaningful to separate these seam-only samples by the zones of the seam instead of by size. If other impurities such as quartz, pyrite, or Na_2O are causing specific problems at the power plant, their potential cleaning reduction can also be assessed by including them in the size and washability analyses.

If these preliminary laboratory results look promising and warrant further investigation, actual cleaning tests can then be performed to determine the true cleaning response of the coal and the performance of specific cleaning circuits. Such tests also provide bulk samples for comparative combustion testing.

For the two Wilcox Formation lignites and the Robinson Seam subbituminous samples, actual cleaning tests were performed using the 25 ton-per-hour, demonstration-scale circuits at the CCTF. The circuits utilized combinations of a heavy-media vessel to clean 6-in x 3/8-in coarse coal and a concentrating table or water-only cyclones to clean 3/4 or 3/8-in x 200M intermediate size coal. The fine 200M x 0 raw coal was discarded in all tests.

Table 5 lists the raw-coal qualities and resultant clean-coal qualities and cleaning-circuit performances for each coal. For moisture-dependent parameters, the information is given on both as-received and dry bases.

The actual cleaning results verify the observations made from the raw-coal size and washability analyses (Table 4); namely, that the most pronounced ash reductions and heating value increases were achieved for the two lignites, and the SO_2 reductions were most significant for the Robinson Seam subbituminous. The energy recoveries of 87 to 90 percent also illustrate that 10 to 13 percent of the raw coal's energy was sacrificed to achieve these coal-quality improvements.

As expected, the energy recoveries in Table 5 are substantially lower than for the laboratory-produced clean coals in Table 4 because of circuit inefficiency. The slightly lower separation gravities and clean-coal ash contents for the Robinson Seam subbituminous and Big Brown Mine lignite cleaning tests also contributed to the rather large differences between theoretical and actual performances for these two coals.

Table 5

ACTUAL COAL CLEANING PERFORMANCE RESULTS
From CCTF Cleaning Tests

	Absaloka Mine Robinson Seam Subbituminous		Big Brown Mine Wilcox Formation Lignite		Winfield North Mine Wilcox Formation Lignite	
Coal Size Cleaned	Crushed to 3/4-in x 0		Crushed to 3/8-in x 0		Crushed to 6-in x 0	
	As-Received Basis	Dry Basis	As-Received Basis	Dry Basis	As-Received Basis	Dry Basis
RAW COAL QUALITY						
Total Moisture (Wt %)	22.3	--	31.9	--	32.8	--
Ash (Wt %)	8.2	10.6	12.5	18.4	21.1	31.4
Volatile Matter (Wt %)	29.1	37.4	31.0	45.5	23.5	34.9
Fixed Carbon (Wt %)	40.4	52.0	24.6	36.1	22.6	33.7
Sulfur (Wt %)	0.72	0.93	0.77	1.13	0.46	0.69
Pyritic Sulfur (Wt %)	0.49	0.65	0.22	0.32	0.05	0.07
Heating Value (Btu/lb)	8,761	11,280	6,779	9,954	5,550	8,259
Ash (lb/MBtu)	9.4		18.5		38.0	
SO_2 (lb/MBtu)	1.64		2.27		1.67	
CLEAN COAL QUALITY						
Total Moisture (Wt %)	25.3**	--	34.6	--	33.2	--
Ash (Wt %)	4.7	6.3	6.0	9.1	13.0	19.4
Volatile Matter (Wt %)	28.2	37.7	30.8	47.1	30.3	45.3
Fixed Carbon (Wt %)	41.8	56.0	28.6	43.8	23.6	35.3
Sulfur (Wt %)	0.31	0.41	0.65	0.99	0.56	0.84
Pyritic Sulfur (Wt %)	0.09	0.12	0.08	0.12	0.03	0.04
Heating Value (Btu/lb)	8,950	11,981	7,437	11,369	6,596	9,874
Ash (lb/MBtu)	5.3		8.0		19.6	
SO_2 (lb/MBtu)	0.68		1.74		1.70	
CLEANING PERFORMANCE*						
Yield (Wt %)	85	83	87	84	75	75
Energy Recovery (%)	87		90		89	

* Yields and energy recoveries were determined from individual CCTF flowsheet tests during which feed coal quality was slightly different from raw coal quality listed above.

** Inadequate coal dewatering equipment was used in this test, resulting in unrealistic moisture content increases for the clean coal. Therefore, a reasonable moisture content increase of 3.0 percent was assumed for the clean-coal product.

Combustion-Related Analyses

Table 6 compares combustion-related laboratory analyses for the raw coals and CCTF-produced clean coals. The information is grouped into coal analyses, ash fusion temperature analyses, and ash compositions. The information in Table 6 is oriented toward pulverized-coal-fired, dry-bottom boilers due to their applicability for low-rank coal combustion. For cyclone-fired, wet-bottom boilers, the arguments and considerations could be vastly different.

With the exception of ash fusion temperatures and compositions, all analyses in Table 6 are on an as-received basis. Hardgrove Grindability Indices are obtained from a laboratory procedure to determine how difficult a coal will be to pulverize. Lower Hardgrove Grindability Indices (HGIs) signify that more energy will be required to pulverize a given quantity of coal to minus 200M (the typical pulverized-coal-fired boiler feed size).

Robinson Seam Subbituminous. Although the ash reduction was not as pronounced for the Robinson Seam subbituminous coal as for the two lignite samples, the Robinson Seam's drop in ash content should still significantly reduce the abrasiveness and erosiveness of the coal. Cleaning reduced ash loading (lb/MBtu) by 44 percent, possibly promoting reductions of similar magnitude in ash handling and disposal requirements and convection-tube erosion.

The HGI for the Robinson Seam coal remained essentially unchanged with cleaning. This signifies that, on a weight basis, pulverizer energy requirement (kWh/ton) and capacity (tons/hrs) should be very similar for the raw and cleaned coals. However, on an equivalent heating value basis, pulverizer energy requirements (kWh/MBtu) and capacity (MBtu/hr) should be improved by approximately the same magnitude as heating value increases resulting from cleaning.

The ash fusion temperatures for the Robinson Seam clean coal are slightly higher than for the raw coal, perhaps due to the removal of pyrite (FeS_2) and subsequent reduction of Fe_2O_3 content in the ash. The slagging index (R_s') determined from ash fusion temperatures increased significantly for the clean coal, indicating lower ash slagging potential. Heat transfer efficiency in the combustion zone of a pulverized-coal boiler should improve when burning this cleaned coal due to the combined effects of reduced ash loading and less tenacious ash slagging tendencies.

In contrast, the Na_2O content in the ash and resultant fouling index (R_f') increased when the Robinson Seam subbituminous coal was cleaned. Both the raw and clean coal fall within the low-to-medium fouling range, indicating that convection-tube fouling may not be a lead-limiting problem. However, the increased Na_2O concentration in the clean-coal ash may counteract the positive effects that reduced ash loading has on convection-tube, heat transfer efficiency.

Wilcox Formation Lignites. The raw lignite samples have much higher ash loadings (18.5 and 38.0 lb/MBtu) than the Robinson Seam subbituminous coal, and greater potential for ash removal and heating value enhancement with cleaning. Table 6 also illustrates that the quartz contents of the lignites, particularly the Winfield North Mine lignite, decreased with cleaning. The reductions in power plant ash disposal requirements, coal abrasiveness, and fly-ash

Table 6

COMBUSTION-RELATED COAL AND ASH ANALYSES COMPARISONS From CCTF Raw and Clean Coal Products (As-Received Basis, Except Ash Analyses)

	Absaloka Mine Robinson Seam Subbituminous		Big Brown Mine Milcox Formation Lignite		Winfield North Mine Milcox Formation Lignite	
	Raw Coal	Clean Coal	Raw Coal	Clean Coal	Raw Coal	Clean Coal
Yield (Wt %)	100	85	100	87	100	75
Energy Recovery (%)	100	87	100	90	100	89
Total Moisture (Wt %)	22.3	25.3	31.9	34.6	32.8	33.2
COAL ANALYSIS						
Ash (lb/MBtu)	9.4	5.3	18.5	8.0	38.3	19.6
SO_2 (lb/MBtu)	1.65	0.68	2.27	1.74	1.67	1.70
Moisture (lb/MBtu)	25.4	28.3	47.8	46.5	59.1	50.3
Heating Value (Btu/lb)	8,761	8,950	6,779	7,437	5,550	6,596
Hardgrove Grindability Index at Given Residual Moisture (HGI @ Wt %)	62 @ 1.93	62 @ NA	48 @ 12.8	46 @ 13.3	73 @ 22.0	57 @ 22.0
Quartz Content						
Wt % in Coal	NA	NA	NA	NA	7.2	3.9
RQV/MBtu	NA	NA	101,000	94,000	NA	NA
ASH FUSIBILITY (°F) (Reducing/Oxidizing)						
Initial Deformation	1,966/2,080	2,107/NA	2,030/2,050	2,010/2,030	2,320/2,360	2,220/2,300
Softening	2,089/2,161	2,118/NA	2,120/2,120	2,050/2,060	2,370/2,430	2,290/2,350
Hemispherical	2,097/2,177	2,122/NA	2,260/2,280	2,100/2,110	2,300/2,380	2,300/2,370
Fluid	2,110/2,223	2,126/NA	2,310/2,320	2,110/2,120	2,390/2,440	2,400/2,440
ASH COMPOSITION (Wt % Oxide in Ash)						
SiO_2	35.9	34.3	54.5	39.8	66.1	58.7
Al_2O_3	12.6	14.9	15.9	13.8	16.7	12.6
Fe_2O_3	7.4	3.7	5.5	7.3	2.6	3.2
CaO	17.6	25.4	11.3	18.0	5.2	9.9
MgO	0.8	1.2	1.9	2.8	1.1	1.1
Na_2O	2.1	2.9	0.5	0.6	0.4	0.7
K_2O	0.6	0.4	0.7	0.4	1.1	0.8
TiO_2	1.6	1.7	1.1	1.7	1.1	1.2
MnO_2	0.1	0.2	NA	NA	0.0	0.1
P_2O_5	0.0	0.2	NA	NA	0.0	0.0
SO_3	15.2	12.4	8.9	15.7	5.1	7.6
Total	106.2	102.6	100.0	99.9	101.4	100.0
Slagging Index (R_s')*	2,008	>2,110	2,080	2,030	2,360	2,250
Classification	Severe	High	Severe	Severe	Medium	High
Fouling Index (R_f')**	2.1	2.9	0.5	0.6	0.4	0.7
Classification	Low to Medium	Low to Medium	Low to Medium	Low to Medium	Low to Medium	Low to Medium

Note:
- NA - Not Available
- RQV - Relative Quartz Value
- Ash fusibility and ash composition for Big Brown Mine coals were taken from Combustion Engineering's as-fired fuel analysis.

* Slagging Index (R_s') = $\frac{\text{Max. Hemispherical Temp.} + 4 * \text{Min. Initial Deformation Temp.}}{5}$

Classification	Slagging Index (R_s')
Low	greater than 2,450
Medium	between 2,250 and 2,450
High	between 2,100 and 2,250
Severe	less than 2,100

** Fouling Index (R_f') = Na_2O in Ash (Wt %)

Classification	Fouling Index (R_f')
Low to Medium	less than 3.0
High	between 3.0 and 6.0
Severe	greater than 6.0

erosiveness stemming from these coal quality improvements will undoubtedly lead to benefits in pulverizer and boiler performance and availability.

In contrast, the ash fusion temperature and ash composition analyses in Table 6 illustrate one area of concern when cleaning the two lignites. Namely, for both lignite samples cleaning increased the proportion of basic constituents, such as Fe_2O_3, CaO, MgO, and Na_2O, in the ash, and reduced ash fusion temperatures. The conventional indices indicate that the slagging and fouling tendencies of the ash would be adversely affected by cleaning, which may have a negative impact on pulverized-coal-fired boiler performance.

Pilot-Scale Combustion Results. As part of another EPRI project (RP-2425), the Big Brown Mine raw and clean lignites listed in Table 6 were subjected to comparative bench- and pilot-scale combustion tests at Combustion Engineering's Fireside Performance Test Facility in Windsor, Connecticut. The combustion testing was designed to simulate full-scale, pulverized-coal-fired boiler performance and to reduce the level of uncertainty associated with predicting the impact of coal quality on boiler performance from laboratory tests alone.

The results from this project have not yet been issued as an EPRI report, but the preliminary data seem to verify many of the trends predicted by the analyses in Table 6; namely, that the main power-plant improvements resulting from cleaning the Big Brown Mine lignite will be reduced coal abrasiveness and erosiveness, decreased fly-ash erosiveness, and lower ash handling and disposal requirements and costs. In the tests, normalized erosion rates for an experimental convection-tube were reduced by approximately 50 percent when burning clean lignite. Coal abrasiveness and required grinding energy were also substantially lower for the clean coal, leading Combustion Engineering's staff to predict improvements in both pulverizer capacity and availability.

The main surprise in the pilot-scale combustion results for the Big Brown Mine lignite was that the increase in basic constituents and reduced ash fusibility temperatures for the clean coal did not seem to have any significant adverse effects on slagging and fouling tendencies in the pilot-scale furnace. Slag deposits produced from the cleaned lignite were generally thinner and more sintered in nature than those produced from the raw lignite. Fouling deposits were cleanable by sootblowers up to flue-gas temperatures of 2,330°F for the cleaned lignite, whereas deposits were cleanable up to flue-gas temperatures of only 2,220°F for the raw lignite.

The discrepancy between the pilot-scale slagging and fouling results and the tendencies predicted by the standard ASTM based indices illustrates the importance of comparative combustion studies to evaluate coal cleaning feasibility. Obtaining a better understanding of the reasons for these discrepancies is one of the goals of the continuing research of EPRI's Availability and Life Extension Program. A more complete evaluation of the pilot-scale combustion results for the Big Brown Mine raw and cleaned lignite is also included in the Biennial Lignite Symposium Proceedings (7). The paper, entitled "The Effects of Coal Cleanings on the Combustion Performance Characteristics of Big Brown Lignite," summarizes the pilot-scale combustion investigation results and predicts some of the economic implications of cleaning the feed to Texas Utilities Big Brown Power Station.

CONCLUSIONS

Assessment of the potential of physical coal cleaning to improve the combustion performance of low-rank coals requires evaluation of the entire system, from coal mining through power generation. While this evaluation can be performed using only laboratory data, commercial-scale cleaning tests and commercial- or pilot-scale combustion tests reduce the level of uncertainty inherent in using laboratory-scale data to predict commercial-scale performance.

The three low-rank, coal-cleaning investigations performed to date at the CCTF have all shown significant improvements in coal quality with cleaning, and acceptable energy recoveries in the clean-coal product (87 to 90 percent). At reasonably high separation gravities (1.60 to 1.80), the small proportion of ± 0.10 specific gravity material (2.0 to 3.0 percent) facilitates the use of relatively inexpensive to operate, water-based, coal-cleaning equipment (such as jigs, water-only cyclones, or concentrating tables). The ability to reject the fine 200M x 0 raw coal without losing an excessive amount of energy promotes lower clean-coal moisture content and less potential for coal-handling problems. Fines rejection may also eliminate the need for elaborate physical- or thermal-dewatering circuits in the cleaning plant.

The main differences in the cleaning results for the three low-rank coals are the potential power-plant benefits resulting from cleaning. The two lignite samples had more dramatic ash reductions and heating value improvements than the Robinson Seam subbituminous sample, indicating greater potential improvements in pulverizer and boiler availability and greater reductions in tonnage-dependent costs. In contrast, the Robinson Seam subbituminous had more pronounced SO_2 reductions, indicating greater potential reduction in flue-gas scrubbing costs.

EPRI is continuing its investigations into the potential benefits and applications of coal cleaning for low-rank coal reserves. One goal of this research is to provide information for EPRI-member utilities experiencing coal-quality-related problems or performing the type of evaluation discussed in this paper. Anyone interested in CCTF activities can obtain more information by contacting Clark Harrison, EPRI Project Manager, Coal Cleaning Test Facility, P.O. Box 98, Homer City, Pennsylvania 15748, (412) 479-3503.

ACKNOWLEDGMENTS

The authors would like to acknowledge TU Electric and Central Illinois Light Company, who cosponsored the low-rank, coal-cleaning investigations, and Dr. Arun Mehta for managing the pilot-scale combustion tests through EPRI's Availability and Life Extension Program.

REFERENCES

1. Cost and Quality of Fuels for Electric Utility Plants, 1985. Energy Information Administration. Washington, DC. DOE/EIA-0191 (85). p. 17.

2. Coal Production, 1984. Energy Information Administration. Washington, DC. DOE/EIA-0118 (84). p. 119.

3. Folz, D. J., Goodman, P. O., and L. Sybert. "Impact of Coal Cleaning on Cost of New Coal-Fired Power Generation." Electric Power Research Institute. Palo Alto, California. CS-1622. March, 1981.

4. Placha, M. F. and J. R. Cavalet. "Subbituminous Coal Characterization at the EPRI Coal Cleaning Test Facility." American Power Conference, Chicago, Illinois. April 1984.

5. Akers, D. J. and C. D. Harrison. "Improving Power Plant Performance by Physically Cleaning Texas Lignite." American Mining Congress Convention. May 1986.

6. Parkinson, J. W., et al. Coal Cleaning Test Facility Campaign Report No. 2: Robinson Seam Subbituminous Coal. Electric Power Research Institute. Palo Alto, California. CS-4081. July, 1985.

7. Durant, J. F., et al. "The Effect of Coal Cleaning on the Combustion Performance Characteristics of Big Brown Lignite." Fourteenth Biennial Lignite Symposium. Dallas, Texas. May, 1987.

THERMAL TREATMENT OF LOW-RANK COAL AND ITS RELATIONSHIP TO FLOTATION RESPONSE

Y. Ye, R. Jin and J. D. Miller
Department of Metallurgy and Metallurgical Engineering
University of Utah
Salt Lake City, Utah 84112

ABSTRACT

The deleterious effect of oxidation processes on coal flotation is generally recognized by researchers in the field. The present study, however, demonstrates that properly controlled low-temperature heating can actually improve coal flotation and its separation from mineral matter especially for low-rank coals. With a lignite sample, low-temperature heating at 130°C for a given time under ambient atmosphere leads to a higher yield and greater ash rejection during subsequent bench-scale flotation experiments. By combining experimental results from Hallimond-tube and bench-scale flotation experiments, bubble attachment-time measurements, wetting phenomena, and FTIR spectroscopy, it is clear that thermal treatment under the above conditions, which involves dehydration and oxidation reactions, changes the coal sample to a more hydrophobic state. These new results provide further evidence of the complexities involved in the analysis of coal surface chemistry as related to flotation phenomena.

INTRODUCTION

It is well known that generally coals with higher ranks possess a natural flotability whereas lower-rank coals have a more hydrophilic character. The flotation response of coals has long been known to vary with carbon content and ash content (1,2). Because of the hydrophilic character of low-rank coals, they are difficult to float even at a high dosage of oily collectors such as kerosene. It is not uncommon that several tens of pounds of fuel oil are required to float sub-bituminous coal or lignite (3,4). Further, at such a high oily collector level, particle aggregation phenomena is so severe that substantial separation of coal particles from mineral matter is difficult to achieve. Thus, a new and effective way to clean coals of lower rank by froth flotation is desired in order to establish technology to better utilize the vast resource of low-rank coals.

Poor flotability of low-rank coals is attributed to the higher content of oxygen-containing groups, such as carboxyl and hydroxyl groups (4-7). When a fresh coal surface is exposed to the atmosphere, oxidation starts and oxygen containing groups are formed at the coal surface. This oxidation phenomena has been reported by many authors to result in a decrease of the hydrophobicity and hence a decrease in the flotability of such coals. Fuerstenau et al. (8) further suggested that the oxygen functional groups control not only the thermodynamics but also the kinetics of coal flotation.

With the study of coal oxidation in solution by a variety of oxidants such as HNO_3, $K_2Cr_2O_7/HNO_3$, $KMnO_4/OH^-$, BUOOH/AIBN, $NaOCl/OH^-$, etc. (9-11), it has been observed that a polymeric amorphous and polydispersed product can be formed, which is often identified as humic acid. The major functional group of the humic acid is known to be the carboxyl group (12). Other constituents such as phenolic, alcoholic, carbonyl, and methoxyl groups are also present in humic acid in significant amounts (13). Yarzab et al. (6) have suggested that the humic acids thus formed are similar in structure to low-rank coal. As the oxidation of the coal suspension proceeds further, water-soluble acids are formed with the color of the solution changing from rusty-brown towards yellow-green and finally disappearing. From the foregoing brief review, a basis for the poor flotability of low-rank coals is established and the importance of oxidation phenomena in the technology of coal flotation is evident.

Nevertheless, in contrast to the decrease in hydrophobicity and flotability of coals by extensive oxidation as reported by many researchers, a few researchers have indicated that modestly controlled thermal treatment actually increases the flotability for certain types of coals. For example, in 7 out of 10 samples, continuous flotation using a kerosene/pine oil reagent showed that dehydration and oxidation by heating at 100°C can result in a higher flotation yield than that obtained in conventional control experiments (14). When tracing the literature back to 1954, experimental data from Sun (5) also show an increase in bench-scale flotation recovery for anthracite and lignite with a modest thermal treatment (Figure 1).

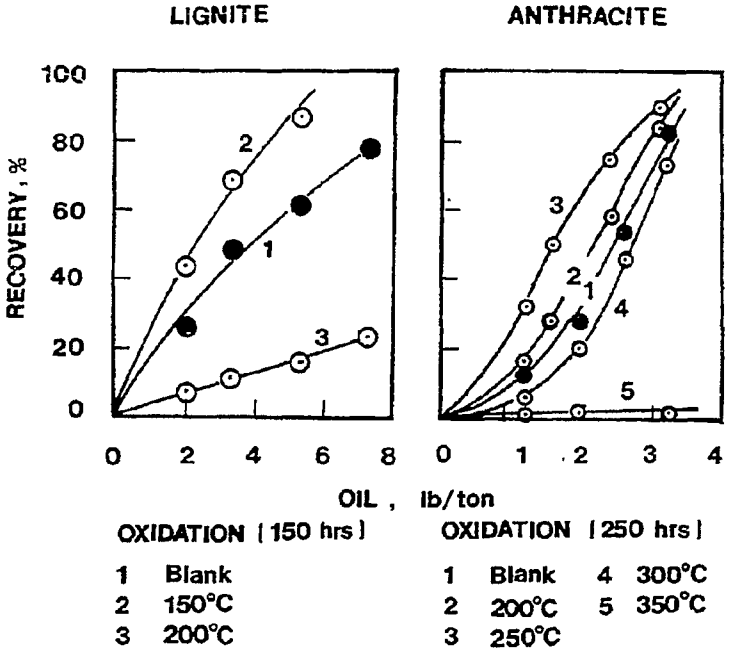

Fig. 1 Flotation recovery of lignite and anthracite coals from bench-scale flotation test as a function of thermal treatment (5).

Further experiments carried out in this present study substantiate these findings. It is confirmed that modest low-temperature heating does increase the hydrophobicity of low-rank coals, at least for the coals investigated. Of the six coal samples investigated (anthracite, low-volatile bituminous, medium-volatile bituminous, high-volatile bituminous, sub-bituminous and lignite), significant improvement in coal hydrophobicity in terms of bubble attachment times and flotation recovery is observed for both sub-bituminous coal and lignite after a modest thermal treatment under an ambient atmosphere. Examination of the coal using a DIGILAB FTS-40 FTIR spectrometer reveals a notable change in the FTIR spectra of lignite after low-temperature heating. Research is still in progress and preliminary results are presented in this paper.

SAMPLES AND PREPARATION

Six coals of different rank were initially chosen for this study. Table 1 gives the characteristics of these samples. Samples used for bubble attachment-time measurements and Hallimond-tube flotation experiments were wet-ground in a porcelain ball mill with distilled water, screened to a size of 100x200 mesh and then air-dried. The samples used for bench-scale flotation were directly wet-ground in the porcelain ball mill with distilled water to 100% passing 100 mesh before being transferred to the flotation cell. The samples used for FTIR spectroscopic analysis were wet-ground in a porcelain mortar with distilled water to a size of minus 5 μm then vacuum dried and stored in a desiccator. Low-temperature heating of the samples was done at 130°C under an ambient atmosphere.

Table 1 Identification and Characteristics of Coal Samples

Rank	Mine/Plant Location	% Ash	% Sulfur
Anthracite	Panther Valley, PA	8.0	0.65
Low-Volatile Bituminous	Cambria #33, Cambria County, PA	6.6	1.04
Medium-Volatile Bituminous	Helvetia/Helen Homer City, PA	6.9	1.10
High-Volatile Bituminous	Valley Camp of Utah Helper, UT	7.0	0.80
Sub-Bituminous	Clovis Point Mine Gillet, WY	11.0	0.56
Lignite	Big Brown Mine Freestone County, TX	27.9	1.08

HYDROPHOBIC CHARACTERIZATION BY BUBBLE ATTACHMENT-TIME MEASUREMENTS

In general, the hydrophobic character of coal can be studied by contact angle measurements, with either the captive-bubble method developed by Wark and Cox in 1934 (15) or the sessile-drop method introduced by Fox and Zisman in 1950 (16). Because of the heterogeneous character of coal, other methods have been developed to describe the hydrophobic/hydrophilic balance of coals, including wettability by surface tension measurements (17), immersion-time measurement (7,18), salt flotation experiments (19), bubble attachment time (20), etc. The bubble attachment-time measurement was chosen for the present study because no wetting agent was used in the flotation experiments.

Measurements of bubble attachment time were carried out with an electronic induction timer (product of Virginia Coal and Mineral Services, Inc.). A captive bubble (approximately 2 mm) held on a bubble tube was pushed by an electromechanical power driver so that the tip of the bubble was kept in contact with a bed of particles for a given time (contact time). After the bubble, together with the tube, returned to its original position, the bubble was observed through a microscope to determine whether attachment of particles at the bubble surface had occurred within that given contact time. The experiment was repeated to obtain ten observations at different positions of the particle bed, and the number of observations which resulted in attachment was counted. Afterwards, the contact time was then changed by adjusting the pulse frequency, and experiments at this new contact time were repeated. Finally, the contact time at which 50% of the observations resulted in attachment was taken as the bubble attachment time. Further, the contact times from the electronic induction timer were calibrated with an SP2000 high-speed video system (Spin Physics). The attachment time measured in the present study is quite accurate.

The bubble attachment time is defined as the time required for the disjoining water film between the solid and gas phases to drain to such a thickness that rupture of the water film takes place. The actual attachment of the particle on the bubble is established after the rupture of the water film. This parameter is a kinetic criterion and is determined by the surface chemistry features of the bubble and particle and can be altered by flotation reagents. Highly hydrophobic particles possess short bubble-attachment times, while hydrophilic particles require long contact times in order to establish attachment.

The bubble attachment time for the different coal ranks are contrasted in Figure 2. The low rank coals are generally the most hydrophilic as revealed from this data showing bubble attachment times as much as 10 times greater than the higher rank coal, the low-volatile bituminous coal. If these coals are subjected to low-temperature heating, some interesting results are obtained. The measured bubble attachment times as a function of low-temperature heating time for all six coal types are given in Figure 3. It was observed that a significant decrease in bubble attachment time is achieved for both the sub-bituminous coal and the lignite after heating at 130°C for a period of time. It can be realized that the low-temperature heating alters the surface character of both lignite and sub-bituminous coal. Based on the principles of bubble attachment phenomena, a decrease in attachment time implies that the coals have become more hydrophobic. A better flotation response for both lignite and sub-bituminous coal is expected after low-temperature heating.On

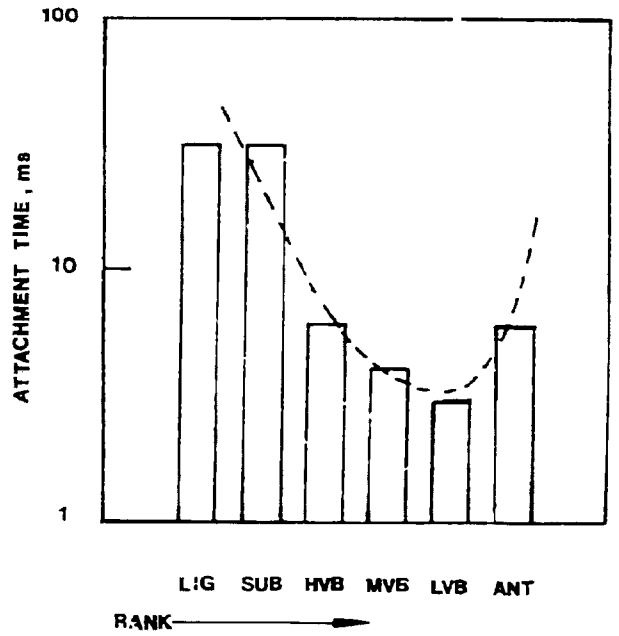

Fig. 2 Measured bubble attachment time for six coals of different rank (Particle size 100x200 mesh).

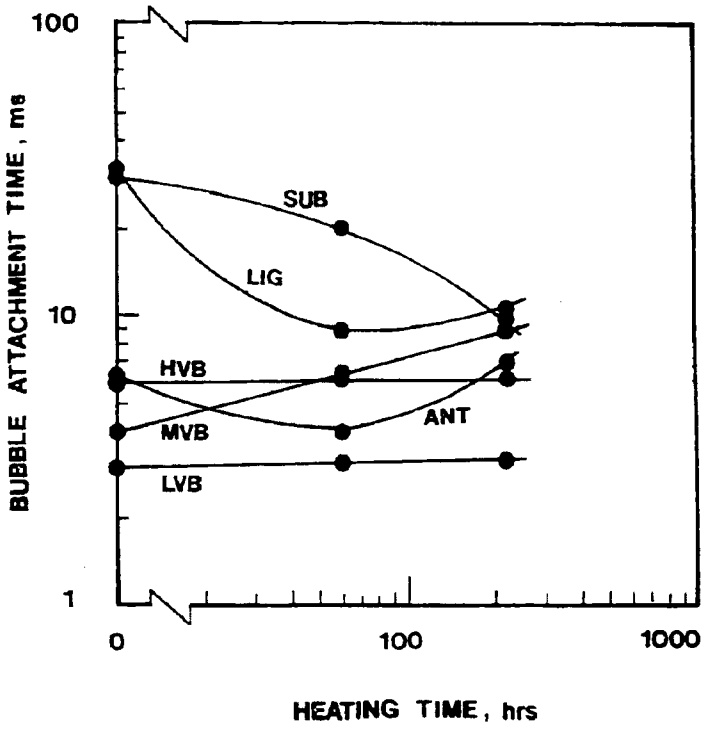

Fig. 3 Measured bubble attachment time of six coal samples as a function of heating time (Particle size 100x200 mesh).

the other hand, the thermal treatment has little effect on high- and low-volatile bituminous coals and actually increases the bubble attachment time for the medium-volatile bituminous coal. Bubble attachment time for anthracite coal is first decreased and then increases when the heating is extended beyond 60 hours.

HALLIMOND-TUBE AND BENCH-SCALE FLOTATION

The Hallimond-tube and bench-scale flotation tests were carried out with lignite, since the most significant change in bubble attachment time was observed in this case. The Hallimond-tube flotation experiments were done with 150 ml distilled water and 3 grams of coal, 50 ml/min air flow rate and pH 5.5 to 6.0. After the coal particles were heated at 130°C for a given time and cooled to room temperature, the sample was first transferred into a beaker containing 60 ml distilled water, then gently stirred for 5 minutes to wet the sample followed by 2-hour settering before the flotation process No flotation reagent was used for the Hallimond-tube flotation test. The experiments were designed for a slow flotation rate by using a low air flow rate and long flotation times so that indiscriminate transport of coal particles due to turbulence of bubble motion could be avoided and thus the true flotability of the coal particles was measured.

Experimental results from the Hallimond-tube flotation experiments are given in Table 2. Incredible improvement in flotation recovery was obtained with the low-temperature heating process. In fact, after two hours of Hallimond-tube flotation with no reagent addition, untreated lignite particles could not be recovered, whereas a recovery of 84% was achieved after low-temperature heating. Other results show that this recovery is sustained even after 65 hours of thermal treatment.

Table 2. Comparison of Flotation Yield for 100x200-Mesh Lignite Coal Particles with and without Thermal Treatment. Hallimond Tube (No Reagent)

Thermal Treatment Time (minutes)	Flotation Time (hours)	Yield (%)
0	2	0.3
3	2	27.0
5	2	55.4
10	2	55.3
50	2	83.9

Bench-scale flotation experiments were carried out with a 2-liter Galigher flotation machine at 5% solids, 4 ml/min air flow rate, 900 rpm, 1 kg/ton MIBC, and 10 kg/ton kerosene. Again, vigorous stirring was necessary to fully wet the thermally treated lignite particles before adding flotation reagents.

The improvement in lignite hydrophobicity by low-temperature heating is again evident from bench-scale flotation experiments, as shown in Table 3. With 10 minutes of flotation, lignite recovery is 18% without any thermal treatment and 69% with thermal treatment. It is noticed that the improvement in flotation recovery for bench-scale flotation experiments is less than that observed for Hallimond-tube experiments, probably because a high kerosene dosage was used for bench-scale flotation.

Table 3. Comparison of Flotation Yield and Ash Rejection for Minus 100-Mesh Lignite Coal Particles with and without Thermal Treatment. Bench Scale (1 kg/ton MIBC, 10 kg/ton kerosene)

Thermal Treatment Time	Flotation Time	Concentrate Product	
		Yield (%)	Ash Content (%)
0	5 minutes	16	12.5
0	10 minutes	18	13.1
65 hours	5 minutes	60	10.1
65 hours	10 minutes	69	13.4

Table 3 also gives the ash content in the lignite clean coal product from the bench-scale flotation with and without thermal treatment. Significant improvement in ash rejection at a high recovery with the heating process is evident from the data.

WETTING PHENOMENA

It has been observed from bubble attachment-time measurements and flotation experiments that low-temperature heating causes the lignite to become difficult to wet. Extended wetting and stirring had to be done after thermal treatment so that the coal particles would be wetted prior to Hallimond-tube flotation tests and bubble attachment-time measurements. In this regard, a natural wetting experiment was carried out in distilled water to observe the wetting kinetics of the lignite coal particles with and without low-temperature heating.

Immersion time and imbibition techniques have been shown to be successful to study the wettability of fine coal particles (7, 18, 21, 22). The imibibition technique was used to study the wetting phenomena of lignite with and without thermal treatment. The wetting test was carried out without addition of any wetting agents. In these experiments, 3 grams of coal (100x200 mesh) with and without low-temperature heating were placed on the surface of 80 ml distilled water in a 100-ml beaker. The system was not agitated. After a given time, the portion of particles which still remained at the air/water surface was collected, dried and weighed.

The experimental results from the wettability study are given in Figure 4. The effect of low-temperature heating upon the wetting of lignite is clearly shown from the figure. After thermal treatment, 60% of the particles still remain unwetted and float at the air/water surface even after 2.5 hours of wetting time, while almost 100% of the particles are wetted and immersed into the water in one minute without thermal treatment.

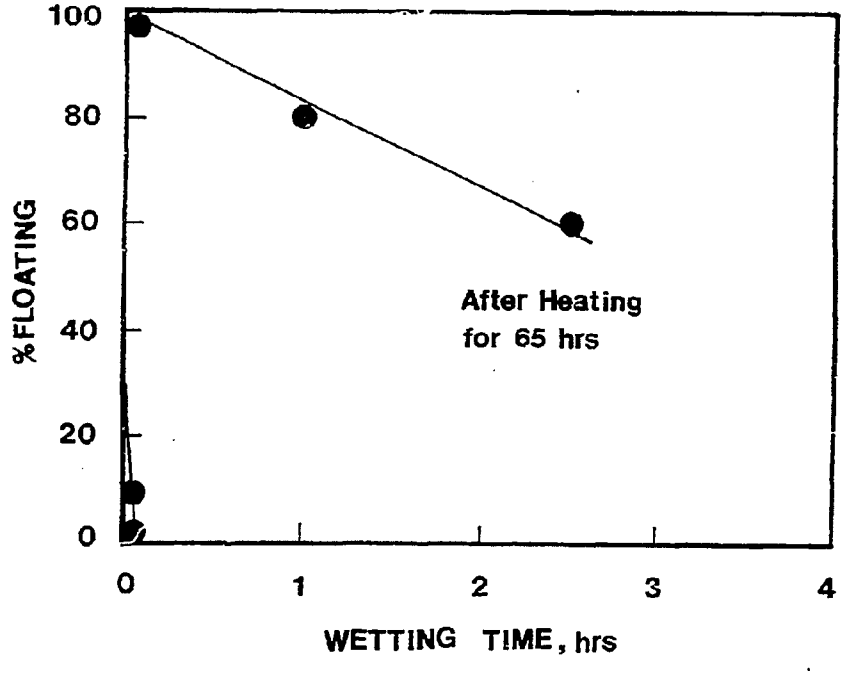

Fig. 4 Particle wetting versus time for lignite coal sample with and without low-temperature heating.

FTIR SPECTROSCOPY MEASUREMENTS

In order to understand the chemistry governing the low-temperature heating process and to monitor the hydrophobicity change of lignite during the course of low-temperature heating, FTIR spectroscopy measurements were carried out. The spectra were run on a DIGILAB FTS-40 FTIR Spectrometer equipped with an MCT detector. A diffuse reflectance technique with an environmentally controlled chamber was used for these measurements. All spectra were obtained with 700 scans at 2 cm^{-1} resolution, and the experiments were run against a KBr blank. The optical bench was purged with compressed dry air.

FTIR spectroscopy has been successfully used for the characterization of coal surfaces (20,23-25). In previous work it has been shown that coal hydrophobicity as determined by contact angle, bubble attachment time and flotation recovery can be characterized by an FTIR spectroscopic criterion which contrasts the abundance of surface hydrophilic groups (hydroxyl and carboxyl groups) with the abundance of surface hydrophobic groups (aliphatic and aromatic CH groups). Such a criterion was successful to show the rank-dependence of coal hydrophobicity. In the present work, however, it was observed that the value of absorption intensity of hydroxyl groups in low-rank coals, especially in the lignite sample used, decreased to zero after heating at 130°C for only a short time (See Figure 5). In addition, the aromatic hydrogen content in most low-rank coals is neglegible. It is difficult to detect this group by its absorption peak at 3030 cm^{-1}, especially after thermal treatment. In this regard, a revised index to describe the hydrophobic character of coals from FTIR spectra, which can be used for coals in both the natural state and after thermal treatment, was formulated:

$$\text{Hydrophilicity Index} = \frac{\Sigma\, K_i (HL)_i}{\Sigma\, K_j (HO)_j} \qquad (1)$$

where $(HL)_i$ is a measure of the abundance of the hydrophilic functional group i and $(HO)_j$ is a measure of the abundance of the hydrophobic functional group j at the coal surface respectively. K_i and K_j are corresponding coefficients and may be determined either theoretically or experimentally.

If we consider that the aliphatic and aromatic CH groups are the only hydrophobic functional groups and that the hydroxyl and carboxyl groups are the only hydrophilic groups, then the hydrophilicity index given by equation (1) can be simplified as:

$$\text{Hydrohpilicity Index} = \frac{(-COOM) + 2(-OH)}{(R\text{-}H) + (Ar\text{-}H)} \qquad (2)$$

where (-COOM), (-OH), (R-H), and (Ar-H) are the values of the absorption intensity as expressed by the Kubelka - Munk function (26,27) for carboxyl, hydroxyl, aliphatic CH, and aromatic CH groups. Because the hydroxyl group has dual functionality being able to act as both a hydrogen donor and hydrogen acceptor whereas the carboxyl group acts only as a hydrogen acceptor then the contribution to hydrophilic character from the hydroxyl group is expected to be twice that of the carboxyl group, a factor of 2 is used for the absorption intensity coefficient for the hydroxyl group whereas the coefficients for other functional groups at this time are assumed to be unity.

Using such a definition for the hydrophilicity index as given by equation (2), a rank-dependence of coal hydrophobicity for six samples is plotted in Figure 6. Comparing these results with measured bubble attachment times (Figure 2) and contact angles (Figure 7) for six coal samples, it is clear that this hydrophilicity index as determined from FTIR spectra presents a rather good measure of the hydrophobic/hydrophilic balance at a coal surface.

The hydrophilicity index as a function of lignite heating time is plotted in Figure 8. Two plateaus can be observed. The index drops quickly to the first plateau at an index value of 3.1. As heating at 130°C is extended and

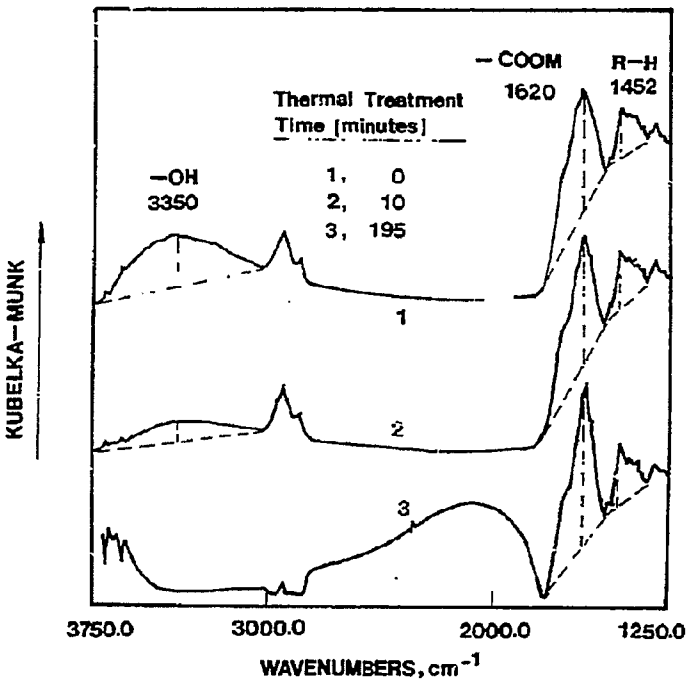

Fig. 5 FTIR spectra of lignite sample at different heating times.

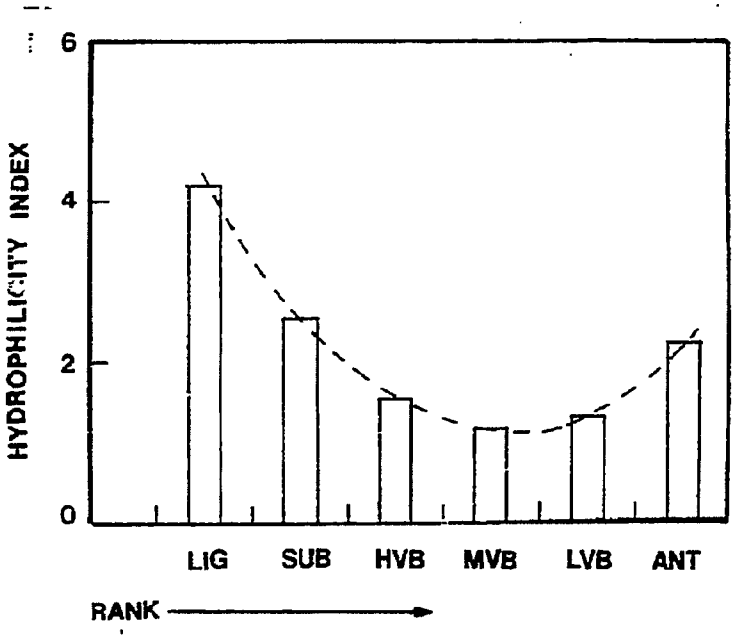

Fig. 6 Hydrophilicity index for six coals of different rank as determined from FTIR spectra.

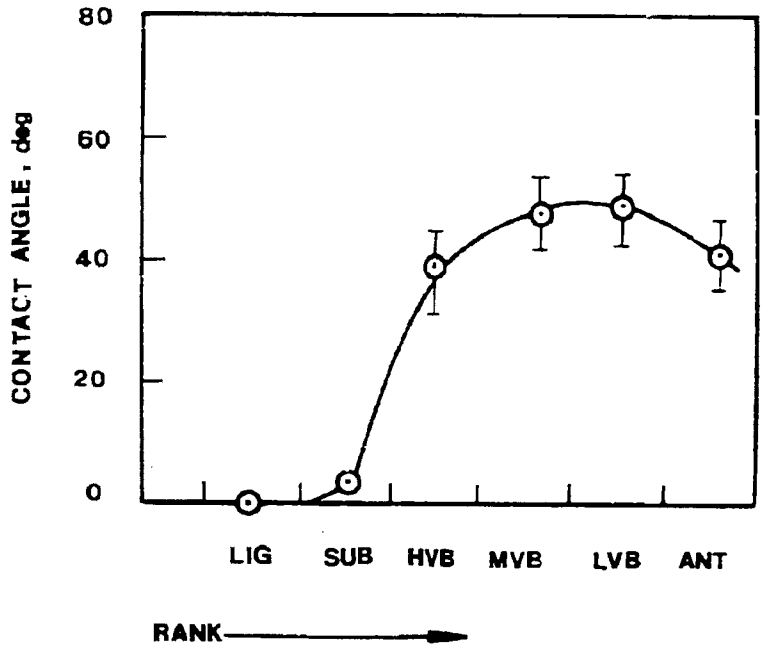

Fig. 7 Measured contact angles for six coals of different rank (20).

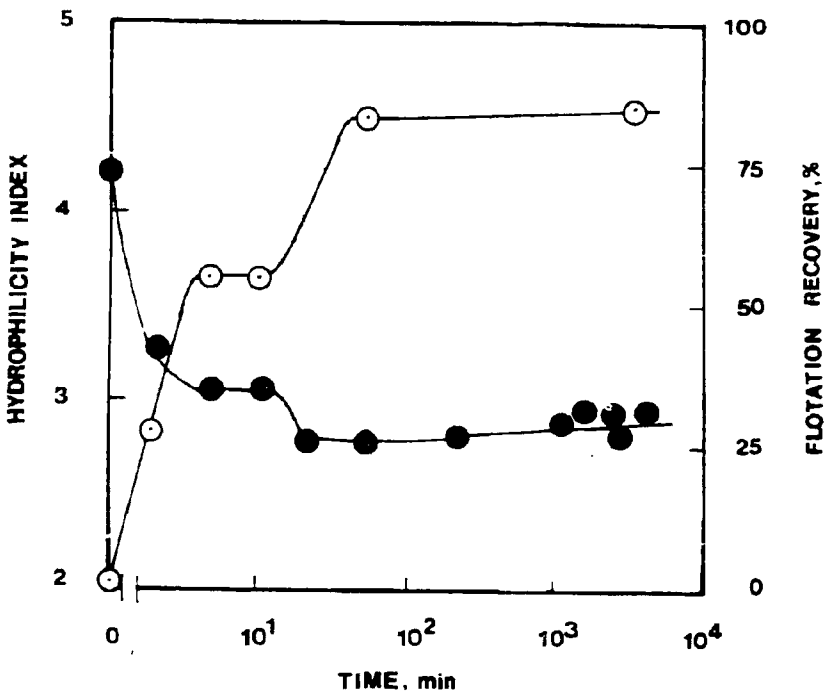

Fig. 8 Hydrophilicity index of lignite (●) determined from FTIR spectra and Hallimond-tube flotation recovery (⊙) as a function of heating time.

another plateau is found the index reaches a stable value of 2.8 within the heating time investigated. By combining the results from this figure together with those from bubble attachment-time measurements and flotation tests, it can be suggested that the hydrophilicity of the lignite coal decreases during thermal treatment at 130°C. At the same time, the OH groups disappear from the lignite surface as is evident from the spectra presented in Figure 5. More discussion follows in the next section.

Further, it has been found from these experiments that this new state of hydrophobicity created by low-temperature heating is not reversible. After low-temperature heating at 130°C for 65 hours, the hydrophilicity index given by Equation 2 remains essentially constant even when the heated coal sample has been placed in ambient air for up to 69 hours. These results are also shown by the data presented in Table 4.

Table 4 Hydrophilicity Index Determined from FTIR Spectra as a Function of Aging under Ambient Conditions after 65 hours Thermal Treatment at 130°C.

Aging Time (hrs)	0	2.8	13.5	25	69
Index Value	2.87	2.64	2.86	2.87	3.09

DISCUSSION

Although the effect of oxidation on the hydrophobicity of coals has been studied extensively before, and it has been shown in most reports that oxidation alters the coal toward a more hydrophilic state, the present study suggests that low-temperature heating can improve hydrophobicity for certain coal types, at least for the lignite sample studied in this work, if such heating is controlled at a modest temperature and for the proper time.

Low-temperature heating seems to involve two opposing phenomena which affect hydrophobic/hydrophilic balance at the coal surface. First, water molecules trapped in the pores of coal and adsorbed at the coal surface are removed during drying, and some carboxyl groups break up slowly with an increase in the heating time. These phenomena should alter the coal toward a more hydrophobic state. On the other hand, some hydrocarbon chains at the coal surface are slowly oxidized to yield new phenol and carboxyl groups, thus decreasing the hydrocarbon content, which will bring the coal toward a more hydrophilic state. Apparently, surface-chemistry features of the coals during the heating process are determined by the relative extent of these different reaction types. Most low-rank coals are high in moisture and carboxyl group content. An increase in hydrophobicity of the lignite after low-temperature heating seems to be attributed to the first reaction type, especially since the heating temperature was held at 130°C. The increase in hydrophobicity will facilitate the flotation separation of coal particles from mineral matter. Such is the case as shown in Table 3.

Change of the surface chemistry features of coal during thermal treatment should be determined by coal type and heating temperature. In Figure 1, heating at 150°C for 150 hours causes a greater flotability for that particular lignite sample but heating at 200°C for 150 hours is adverse to the flotation. On the other hand, in the case of anthracite, a greater flotability can be achieved even when the heating temperature is increased from 200°C to 250°C for 250 hours (Figure 1). For the medium-volatile coal sample used in this study, 130°C heating for any time period can only alter the coal sample toward a more hydrophilic state (Figure 3). However, in a previous study with another medium-volatile bituminous coal sample (28), it was observed that heating at 150°C for 8 hours actually decreases the carboxyl group content. The increase of carboxyl group content due to oxidation became significant only when the temperature of heating was increased to 200°C.

Further, for a given coal type which can be made more hydrophobic by thermal treatment, the proper heating temperature seems to be related to the time. In an early study on pneumatic transport of finely ground lignite by air, it was observed that even partially combusted lignite particles at 450°C for one minute exhibited a high hydrophobicity and were very difficult to wet by water (29).

In Figure 8, it can be noticed that the hydrophilicity Index for lignite decreases with an increase of heating time, then reaches a plateau value. Afterwards, it drops again and then reaches another plateau value. The first plateau of the hydrophilicity index occurs at a time from 5 to 10 minutes. Flotation yield from Hallimond-tube flotation follows the opposite pattern. It is suggested that the first plateau be attributed to the dehydration reaction, while the drop to the second plateau corresponds to decomposition of hydroxyl and carboxyl groups.

As can be noticed from Table 4, change in the coal surface-chemistry features of the lignite by low-temperature heating is irreversible. This phenomenon has also been observed by other authors (30,31) and indicates that a substantial structural change occurs at the surface of the lignite during low-temperature heating. In fact, from study of a sub-bituminous coal by in-situ FTIR difference spectoscopy, Gethner (31) has observed changes of the coal both with respect to internal hydrogen-bonding interactions and variations in carboxyl group frequencies even at 100°C for vacuum drying. On this basis it was suggested that the standard drying procedures in any particular laboratory might unknowingly change the coal structure and/or surface chemistry.

ACKNOWLEDGEMENT

The authors gratefully acknowledge the financial support provided from the DOE Grant No. DE-FG22-85PC80530 which made this study possible.

REFERENCES

1. R. M. Horsley and H. G. Smith, Fuel, Vol. 30, p. 54, 1951.
2. D. J. Brown, Froth Flotation, D. W. Fuerstenau ed., AIME, New York, p. 518, 1960.
3. F. F. Aplan, "Estimating the Flotability of Western Coal," Gold, Silver, Uraniam and Coal: Geology, Mining, Extraction and the Environment, M. C. Fuerstenau and B. K. Palmer ed., AIME, p. 380, 1983.
4. F. F. Aplan, Flotation, A. M. Gaudin Memorial Volume, M. C. Fuerstenau, ed., AIME, New York, p. 1235, 1976.
5. S. C. Sun, Trans AIME, Vol. 6, No. 4, p. 396, 1954.
6. R. R. Yarzab, Z. Abdel-Baset, and P. H. Given, Geochimica et Cosmochimica Acta, Vol. 43, p. 281, 1979.
7. D. W. Fuerstenau, G. C. C. Yang, and J. S. Laskowski, Coal Preparation, vol. 2, p. 1, 1986.
8. D. W. Fuerstenau, J. M. Rosenbaum, and J. S. Laskowski, Colloids and Surfaces, Vol. 8, p. 153, 1983.
9. P. H. Given, J. Bimer, and S. Raj, "Oxidative Study of the Structure of Vitrinites," Presentation at Fuel Division Chicago ACS Meeting, Aug. 1977.
10. R. E. Winans, R. Hayatsu, R. G. Scott, L. P. Moore, and M. H. Studier, "Examinations and Comparison of Structure, Lignite, Bituminous, and Anthracite Coal," Presentation at SRI Coal Chemistry Workshop, Menlo Park, California, Aug. 1976.
11. S. K. Chakrabartty and N. Berkowitz, Fuel, Vol. 53, p. 240, 1974.
12. H. C. Howard, Chemistry of Coal Utilization, H. H. Lowry ed., John Wiley and Sons, New York, Vol. 1, p. 346, 1945.
13. C. R. Kinney and P. M. Kerschner, Fuel, Vol. 31, p. 414,. 1952.
14. J. B. Gaule, W. H. Eddy, and R. Q. Shotts, U. S. Bureau of Mines, R. I. 6620, 1965.
15. W. I. Wark and A. B. Cox, Trans AIME, Vol. 112, p. 189, 1934.
16. H. W. Fox and W. A. Zisman, J. of Coll. Sci., Vol. 5/6, p. 514, 1950.
17. J. O. Glanville and J. P. Wightman, Fuel, Vol. 59, p. 557, 1980.
18. S. Chander, Seminar, University of Utah, November, 1986.
19. J. S. Laskowski and J. Iskra, Trans IMM, Vol. 79, p. C6, 1970.
20. R. Jin, Y. Ye, J. D. Miller, and J. S. Hu, "Characterization of Coal Hydrophobicity by Contact Angle, Bubble Attachment Time and FTIR Spectroscopy," 116th AIME annual meeting, Preprint No. 87-146, Denver, Colorado, 1987.
21. D. W. Fuerstenau and M. C. Williams, Colloids and Surfaces, Vol. 22, p. 87, 1987.
22. A. Marmur, W. Chen and G. Zografi, J. Coll. and Inter. Sci. Vol. 113, p. 114, 1986.
23. S. J. Yuh and E. E. Wolf, Fuel, Vol. 62, p. 252, 1983.
24. S. J. Yuh and E. E. Wolf, Fuel, Vol. 63, p. 1605, 1984.
25. P. C. Painter, M. Starsinic, E. Squires, and A. A. Davis, Fuel, Vol. 62, p. 742, 1983.
26. P. Kubelka and F. Z. Munk, Tech. Phys., Vol. 12, p. 593, 1931.
27. P. Kubelka, J. Opt. Soc. Am., Vol. 38, p. 448, 1948.
28. J. D. Miller, J. S. Laskowski and S. S. Chang, Colloids and Surfaces, Vol. 8, p. 145, 1983.
29. Y. Ye et al., "Utilization of Fine-Ground Lignite in Blast Furnace -- Feasibility Study Report," Kunming Institute of Technology, China, 1982.
30. D. N. Baria and A. R. Hansan, Energy Progress, Vol. 6 (1), p. 53, 1986.
31. J. S. Gethner, Applied Spectroscopy, Vol. 39, p. 765, 1985.